Infiltration Swales

Quantitative performance on an urban catchment scale

Hendrik Richard Geerling

Master of Science Thesis

TU Delft Delft University of Technology
Gemeente Utrecht
Deltares Enabling Delta Life
Blue Green Dream

Photo cover: Castellumknoop infiltration swale.

Note: This document has been designed for full color double-sided printing

INFILTRATION SWALES

Master of Science Thesis

For the degree of Master of Science in Civil Engineering at
Delft University of Technology

Hendrik Richard Geerling

August 13, 2014

Student number:	1267361	
Thesis committee:	Prof. dr. ir. N. C. van de Giesen	TU Delft
	Dr. ir. F. H. M. van de Ven	TU Delft/Deltares
	Dr. ir. J. G. Langeveld	TU Delft
	Ing. M. Rijsdijk	Gemeente Utrecht

Faculty of Civil Engineering and Geosciences (CITG) · Delft University of Technology

This research has been made possible by:

Gemeente Utrecht
Blue Green Dream project
Deltares

This thesis was written using LaTeX.

"Measurements are wrong until you can prove that it is reasonable to assume that they are correct"

KEYWORDS: infiltration swale, Sustainable Urban Drainage System, MODFLOW, MetaSwap, initial moisture conditions, Infoworks, Urban catchment scale

SUMMARY

Worldwide urban areas are getting larger. Existing rural areas will eventually be replaced by impervious areas like roofs or roads. This increasing urbanization influences the hydrology of the urban area and therefore the stress on urban drainage systems. More runoff will be generated as less water is 'lost' to the environment. Also the magnitude of peaks and the pollutant loading is increased.

The study performed for this thesis focuses on the quantitative performance of infiltration swales. Infiltration swales (swales) are designated green areas where the infiltration of precipitation into the ground is encouraged. Roads and other impervious areas are disconnected from the drainage system and runoff is dealt with at the source rather than transporting it over large distances. Also infiltration facilities reduce the volume of runoff instead of spreading the volume over time as is done in detention ponds.

The research objective for this study is defined as the assessment of the quantitative performance of infiltration swales on a urban catchment scale. The first three research questions defined concern the individual swale performance and focus on different weather circumstances, the inflow characteristics of a swale and the initial soil moisture conditions. The last research question concerns the performance of infiltration swales on an urban catchment scale.

The first step in achieving the objective and answering the research questions was monitoring of an infiltration swale in Utrecht. The goal of the measurements was to get insight in the quantitative performance of the swale. Inflow and outflow was measured with v-notch discharge measurements. Groundwater levels were recorded with pressure divers in observation wells. Infiltrometer test were performed to measure the infiltration capacity of the top layer. Artificial inflow simulations were done in order to study the difference in inflow characteristics where lateral inflow was compared to head inflow.

The second step was to develop a model of an individual swale. A MetaSwap-Modflow model was developed in order to study the effects of the initial soil moisture conditions on the quantitative performance and provide input to the urban drainage model. An urban drainage model of the Schepenbuurt in Utrecht was used to study the performance of infiltration swales on an urban catchment scale.

Results of the measurements
In total 18 events (events 21-38) were observed for this study of which 7 are artificial inflow simulations (events 32-38). Events 1-20 are observed 4 years ago by Donkers (2010). The process of doing measurements was not ideal and (large) uncertainties were present in the observed data. Fourteen events were used for the analysis and a (large) mistrust in four of the events was reason to exclude them from the analysis. The large mistrust was based on the estimates for runoff coefficients (ratio between inflow volume and precipitation volume) , the consistency between the precipitation and inflow and large outflow surplus (more outflow than inflow) in the observations.

The precipitation observed is considered to be low to medium intensity storms, according to KNMI classification. The maximum storm that was simulated (artificial inflow simulation) had a return period of 6 months. This simulations showed that the swale is filled in less than 45 minutes. The storage of the swale is filled fairly quickly for this T=0.5 yr. storm.

In general, it can be concluded that the emptying time of the swale is a slow process. In the 5.5 weeks of the measuring period, the subsurface part of the swale did not become completely dry. The reaction of the swale to precipitation is fast. Groundwater levels in the swale rise fast while groundwater levels outside the swale show a less significant reaction to precipitation.

The volume reduction of a swale is highly variable and ranges between -50% and +100%. The negative volume reductions can be explained by the uncertainties in the inflow and outflow recordings as well as the precipitation that directly falls on the swale. The median volume reduction is 41%. The outflow of the swale is active quite shortly after the inflow started. In 75% of the events, the outflow delay is shorter than 30 minutes with a median value of 21 minutes.

The peak reduction of the swale is quite large. In 85% of the events more than 40% of the inflow peak is 'lost'. The median value for the peak reduction is 79%. The peak delay is shorter than one hour for more than 60% of the events. The median peak delay is equal to 40 minutes. The subsurface part of the swale is never completely dry. The part above surface level and the top 40 cm of the swale is empty within 24 hours after the inflow has started with a median value of 20 hours. A combination of a high initial groundwater level, high average inflow intensity and high total inflow volume seem to be ideal situations for overflow situations. The filling time of the swale (above and under surface level) in these cases is quite quick with a median time to overflow of 49 minutes.

In general, it is concluded that the performance of the swale has not decreased in 4 years. The volume reduction and peak reduction show similar results as 4 years ago. It can be concluded that the influence of possible occurred clogging of the top layer is small. The peak delay is even larger for this study. The median peak delay is more than two times bigger for this study. This is an improvement of the performance.

Inflow characteristics
For this swale, the lateral inflow seems to perform a little better or at least equal to the head inflow. Improvement in outflow delay and volume reduction is found. This increase in performance can be explained by the fact that less water is ponding at the head of the swale at the beginning of the event. The water is more divided over the swale and the drainage level will be reached not as fast as in case of a head inflow.

Results of the modeling exercise
The modeling exercise consisted of two parts. An individual swale model made with MetaSwap-Modflow was used to model the performance of a swale with different initial soil moisture condtions. The output of the swale model was also used for the second model, an urban drainage model in Infoworks. This model was used to determine the performance of swales on an urban catchment scale.

Initial soil moisture conditions
The MetaSwap-Modflow model was used to determine the effects of changing initial soil moisture conditions. Design storm bui08 (T=2 yr.) was used. The effects of the initial conditions on the maximum water level in the swale are small, in order of centimeters. The discharge of the drain is highly related to the heads. The peak in the drain discharge is also not influenced significantly by the initial soil moisture condition. The difference in maximum drain discharge between the scenario with high initial soil moisture conditions (startin heads at +0.20 m NAP) and deep initial conditions (starting heads at -0.40 m NAP) is about 3 m^3/day.

The total drained volume and the outflow delay seem to be influenced more by the initial soil moisture condition. The difference in volume reduction between a deep and high initial moisture conditions is about 10%. The difference in peak delay and outflow delay between the deep and high initial soil moisture conditions is larger than 3 hours .

Urban catchment scale
The Infoworks model was used to determine the performance of infiltration swales on an urban catchment scale. The model showed that using infiltration swales in urban planning is beneficial. The total volume that discharges on the surface water and the peak discharge is lowered. The peak reduction is between 4% (scenario with 10% of the area connected to a swale) and 88% (scenario with 90% of the area connected to a swale). The scenario with only swales and no conventional system performs a little less than the 90% scenario. This can be explained by the fact that the peak in outfall is caused by the areas with a swale. The 90% scenario has less area connected to a swale and thus is the peak smaller. The total volume reduction is between 5% and 62%.

The model also showed that it is effective on flood control. The flooding that occurred in the reference scenario (no swales and design storm bui08) was eliminated with an area percentage of infiltration swales of 30%.

SAMENVATTING

Wereldwijd neemt de urbanisatie toe. Bestaand landelijk gebied wordt meer en meer vervangen door bebouwing. Vegetatie wordt vervangen door wegen en daken. Als gevolg hiervan verandert de hydrologie van het gebied en daarmee ook de belasting op rioleringssystemen. Doordat minder water ' verloren' gaat aan de omgeving zal er meer water afstromen naar het rioleringsstelsel. Toenemende piekbelasting en vervuiling zullen een grote invloed hebben op het gebied.

Het rapport voor u is het resultaat van een studie naar de kwantitatieve prestaties van infiltratie geulen, in Nederlandse beleidsdocumenten vaak aangeduid als wadi. Wadi's zijn groene voorzieningen in het stedelijk gebied waarbij de infiltratie van hemelwater bevorderd wordt. De wadi kan tussen het afstromend oppervlak en het oppervlakte water geplaatst worden om afstromend water ter plekke te verwerken (infiltreren) in plaats van over grote afstand te vervoeren voordat het geloosd wordt op het oppervlakte water. Hierbij wordt, in tegenstelling tot oplossingen met berging, de volumebelasting op het rioleringsstelsel verkleind.

Het doel van de studie is de bepaling van de kwantitatieve prestaties van wadi's op een stedelijk gebied. De eerste drie onderzoeksvragen beschouwen de prestaties van individuele wadi's en zijn gericht op verschillende weersomstandigheden, de invloed van de instroom wijze en de initiële bodemvocht conditie (droog vs. natte wadi). De laatste onderzoeksvraag beschouwt de prestaties van wadi's op wijkniveau.

De eerste stap in het bereiken van het onderzoeksdoel is het bemeten en monitoren van een wadi in Utrecht. Het doel van de metingen was om inzicht te krijgen in de factoren die bijdragen aan de kwantitatieve prestaties van de wadi. Instroom en uitstroom debiet metingen zijn uitgevoerd met behulp van een 'v-notch'. Grondwater niveaus zijn bepaald met behulp van druksensoren in een zevental peilbuizen. De infiltratie capaciteit van de bovenste laag is bepaald doormiddel van dubbel-ring infiltratie testen. Kunstmatige instroomsimulaties (m.b.v een pomp) zijn bovendien uitgevoerd om inzicht te krijgen in de invloed van de manier waarop het water de wadi instroomt (kop vs. homogene instroom).

Het tweede gedeelte bestond uit het modelleren van een individuele wadi en het modelleren van wadi's op wijk niveau. Hiervoor is een Modflow-MetaSwap model (wadi model) en een rioleringmodel opgesteld. Het doel van het wadi model was het verkrijgen van inzicht in het effect van de verschillende initiële bodemvocht condities voor de start van een bui. Bovendien zijn de uitkomsten van het wadi model gebuikt als input voor het tweede model, het rioleringsmodel. Dit Infoworks model modelleert de prestaties van wadi's op wijk niveau.

Resultaten van de metingen
In totaal zijn 18 buien (events 21-38) gemeten waarvan 7 kunstmatige instroomsimulaties (events S1-S7) zijn. Events 1-20 zijn gemeten en beschreven door Donkers (2010). De metingen voor dit onderzoek zijn niet zonder slag of stoot verlopen en de onzekerheden in de resultaten worden als vrij groot beschouwd. In totaal zijn 14 events gebruikt omdat bij de metingen van vier buien dermate grote onzekerheden zijn geconstateerd dat deze buien niet zijn meegenomen in de analyse. De onzekerheden kwamen vooral aan het licht door de schattingen van de runoff coëfficiënten (ratio tussen instroom volume en regen volume), de consistentie tussen regenval en de instroom metingen en de grotere uitstroom dan instroom in sommige gevallen.

De buien die optraden gedurende de meetperiode zijn gekwalificeerd als kleine tot middelgrote buien, volgens de KNMI classificatie. De maximale bui die gesimuleerd is, had een herhalingstijd van 6 maanden. Bij deze simulatie bleek dat de berging van de wadi binnen 45 minuten gevuld was.

De metingen laten ook zien dat leeglopen van de wadi een langzaam proces is. In de 5,5 weken durende meetperiode is het gedeelte van de wadi onder het maaiveld niet één keer volledig leeg geweest. Echter, de reactie van de wadi op regenval is snel. Grondwaterstanden in de wadi lopen snel op terwijl de niveaus buiten de wadi een veel minder snelle reactie vertonen.

Volume reductie is heel erg variabel en de gemeten waarden lagen tussen -50% and +100%. De negatieve waarden kunnen verklaard worden door de regenval die direct op de wadi valt en de onzekerheden in de metingen. De mediaan van de metingen is 41%.

De uitstroom is redelijk snel actief nadat de instroom is begonnen. In 75% van de buien begint de uitstroom binnen 30 minuten nadat de instroom is begonnen te lopen.

De gemeten piekreductie is vrij hoog. In 85% van de buien is de piekreductie meer dan 40%. De mediaan is 79%. De piekvertraging, tijd tussen de piek in de instroom en uitstroom, is korter dan een uur in 60% van de buien. De mediaan ligt rond de 40 minuten. Zoals eerder vermeld was het gedeelte van de wadi onder het maaiveld nooit helemaal droog. De eerste 40 cm van de wadi onder het maaiveld was in alle gevallen binnen 24 uur leeg met een mediaan van 20 uur. Een combinatie van een hoge initiële grondwaterstand, een hoog gemiddeld instroomdebiet en instroomvolume zijn ideaal voor overstort situaties. Het vullen van de berging van de wadi (boven en onder het maaiveld) in het geval van overstorten gaat snel. De mediaan is 49 minuten.

Over het algemeen kan geconcludeerd worden dat er nauwelijks tot geen verslechtering is opgetreden in de prestaties van de wadi in vergelijking met 4 vier jaar geleden. De invloed van verstoppen van de toplaag is dus klein. De gemeten piekvertraging is zelfs groter dan 4 jaar geleden.

Instroom wijze
De bemeten wadi presteert iets beter maar zeker niet slechter in het geval van een homogene instroom in vergelijking met een kopinstroom. Uitstroomvertraging en volume reductie zijn beide groter voor een homogene instroom situatie. De verbeterde prestaties kunnen toe worden geschreven aan de betere verdeling van het water over de lengte richting van de wadi. Bij een kopinstroom hoopt het water zich op aan het begin van de wadi. Hierdoor wordt het drempelniveau van de drain in de wadi eerder bereikt en is de uitstroom van de wadi eerder actief.

Model resultaten
Twee modellen zijn ontwikkeld om de invloed van initiële bodemvocht condities en de prestaties van wadi's op wijkniveau te bepalen. Het MetaSwap-Modflow model is gebruikt om de invloed van de initiële condities te simuleren en de invloed op de resultaten te bepalen. De gemodelleerde drain debieten zijn ook gebruikt in het Infoworks model (rioleringsmodel) . Dit model modelleert de prestaties van wadi's op wijkniveau.

Initiele bodemvocht condities
Het MetaSwap-Modflow model is gebruikt om de invloed van initiële bodemvocht condities te bepalen. Hiervoor is ontwerpbui 8 (T=2 jaar) gebruikt. De invloed blijkt klein te zijn wat betreft de maximale waterstanden in de wadi en de piek debieten in de drain. Het verschil in waterstanden in de wadi bij de scenario's met een diepe en hoge stijghoogte is in de orde van centimeters. Terwijl het maximum debiet met een diepe initiële stijghoogte (-0,40 m NAP) slechts 3 m^3/dag hoger is dan in het geval van hoge stijghoogte (+0,20 m NAP).

Het totale drain volume en de uitstroomvertraging (tijdsverschil tussen start bui en het moment dat de drain actief begint te worden) worden meer beïnvloed door de initiële conditie. In totaal wordt er 10% meer water afgevoerd door de drain in de scenario met een hoge initiële stijghoogte in vergelijk met de diepe stijghoogte aan het begin van een bui. Het verschil in de uitstroomvertraging tussen de meest natte en de meest droge scenario is meer dan 3 uur.

Prestaties op wijkniveau
Het rioleringsmodel (Infoworks) is gebruikt om de prestaties van wadi's op wijk niveau te bepalen. De resultaten van het model met bui08 laten zien dat het toepassen van wadi's van toegevoegde waarde is voor het water systeem van een wijk. De totale impact op het oppervlakte water systeem in de vorm van totaal volume en piek belasting is lager in het geval dat er wadi's zijn aangelegd in een wijk. De piek reductie varieert tussen 4% (10% van het verhard oppervlak aangesloten op een wadi) en 88% (90% van het verhard oppervlak aangesloten op een wadi). De volume reductie op wijk niveau wijkt niet af van de volume reductie van een individuele wadi. De volume reductie ligt tussen de 5% en 62%.

Uit de resultaten van het model blijkt ook dat de wadi's effectief zijn bij het voorkomen van wateroverlast (water op straat). In de referentie situatie (bui08, geen wadi's) staat er water op straat. Door toepassen van wadi's op 30% van het verhard oppervlak blijkt er geen water meer op straat voor te komen.

PREFACE

This report is the final product of my research project in order to obtain the degree of Master of Science at Delft University of Technology.

The project was divided into 2 stages. The first stage was done at he municipality of Utrecht and covered the practical work of this thesis. Measurements were done at one of the infiltration swales in Leidscherijn Utrecht.

The second stage can be subdivided into 2 parts and includes the modeling activities of this thesis. The first part of the second stage included the creation of an infiltration swale model in MetaSwap-Modflow. This was done at Deltares in Utrecht. The second part was an urban drainage model in Infoworks with which the performance of infiltration swales on an urban catchment was modeled. The model was provided by the municipality of Utrecht.

This thesis gave me the opportunity to combine fieldwork with modeling. Valuable lessons on using equipment, performing measurements and analysis of measurement results were obtained. The whole modeling exercise was in particular interesting because I had to start from scratch using software I was not yet familiar with.

This research could not be achieved without the assistance of many people who I would like to thank. First of all I would like to thank my graduation committee Nick van de Giesen, Frans van de Ven, Jeroen Langeveld and Michiel Rijsdijk for their guidance, advice and feedback during this project. Furthermore I would like to thank my Deltares collegues and the collegues at the municipality of Utrecht for their help and support. I am also grateful to the municipality of Utrecht, Deltares and the Blue Green Dream project for providing financial and material support during this project.

Special thanks goes to my girlfriend Valerie Stowell. Not only for her feedback on my report but also for the support during the process of writing this report.

Last, but not least, I would like to thank my family and especially my parents. The support they gave me throughout my thesis and in all the years before that has been great. Also many thanks to my brother Martijn for his hospitality during my work in Utrecht.

I hope that this document is providing the reader an interesting insight in the functioning of an infiltration swale. Enjoy reading it!

Delft, August 2014

Hendrik Richard Geerling

CONTENTS

LIST OF FIGURES

LIST OF TABLES

1

INTRODUCTION

Worldwide urban areas are getting larger. Existing rural areas will be replaced by impervious areas like roofs or roads. The increasing urbanization influence the hydrology of the urban area and therefore the stress on urban drainage systems. More runoff will be generated as less water is 'lost' to the environment. Also the magnitude of peaks and the pollutant loading is increased Barber *et al.* (2003). A study in Helsingborg, Sweden on the effects of urbanisation and climate change estimated sewer overflow volumes to be doubled due to urbanization. Increases in volumes up to 450 % are estimated when climate change is also taken into account (Semadeni-Davies *et al.*, 2008).

In the past, urban drainage systems were designed on fast transport of runoff from impervious areas (Holman-Dodds *et al.*, 2003). But with increasing stress on these gray urban drainage systems, sustainable solutions like green roofs, permeable pavements and infiltration swales have become more popular as these solutions deal with the rainfall water in a more natural way. Also the intention to improve ecological conditions of surface waters (and stricter regulations) is a reason for increasing interest in sustainable urban drainage systems (SUDS) (Revitt *et al.*, 2003).

The study performed for this thesis focuses on the quantitative performance of infiltration swales. Infiltration swales (swales) are designated green areas where the infiltration of precipitation into the ground is encouraged. Roads and other impervious areas are disconnected from the drainage system and runoff is dealt with at the source rather than transporting it over large distances. Also, infiltration facilities reduce the volume of runoff instead of spreading the volume over time as is done in detention ponds (Brander *et al.*, 2004).

Figure 1.1 shows an impression of an infiltration swale with lateral inflow.

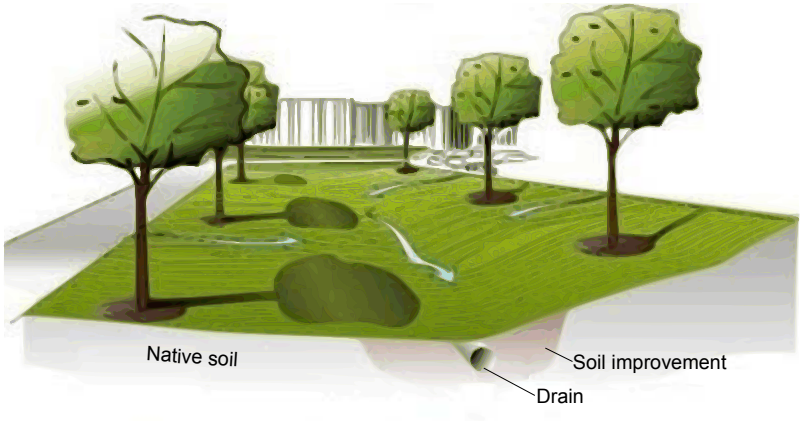

Source: WBDG (wbdg.org/resources/lidtech.php)

Figure 1.1: Artist impression of a typical infiltration swale

Boogaard *et al.* (2003) describes the four main tasks of infiltration swales:

1. infiltration
2. storage
3. drainage
4. first treatment of runoff

Swales have two main advantages with respect to conventional gray solutions. Because of the infiltrating capacity and the storage within a swale, the peak discharge to the drainage system or surface waters can be delayed and the volume of runoff can be decreased. Reducing the risks of flooding and recharge the groundwater resources (drainage). The second advantage is the onside first treatment of the runoff by the first layer of the swales. This reduces the polluting load on receiving surface waters and groundwater.

This study, in cooperation with the municipality of Utrecht (Gemeente Utrecht) and Deltares, will focus on the quantitative performance of infiltration swales. The work done for this project is the continuation of the work done by Donkers (2010). The same infiltration swale, Castellumknoop,was monitored for this study. The intention at the beginning was to study a second location in order to compare the results. The Cliviapad swale was chosen as a second site and the preparation was done. A v-notch weir was calibrated at the small flume at the Delft University of Technology. Unfortunately the installation of the weir in a manhole to measure the outflowing discharge was unsuccessful after several attempts. Also there was just a small amount of water available for inflow simulations and the surface water was far away. These two factors contributed to the decision to put the focus on only one infiltration swale. Then it was also planned to study frozen en non-frozen situation. The winter of 2013/2014 was very mild and problems with the measuring equipment made it impossible to consider this aspect as well.

The report in front of you has eight chapters. After this introduction, the research outline will be described followed by a literature review. The main part of this report consists of the description of measurement, inflow simulation and modeling. Separate chapters consider the results of the measurements and the modeling. The last chapter includes conclusions and recommendations.

2

RESEARCH OBJECTIVE AND QUESTIONS

This chapter deals with the objectives, questions and approach to this study. The research questions are defined in order to achieve the objective in a structural way.

2.1. RESEARCH OBJECTIVE

The research objective of this study is defined as:

'Assessment of the quantitative performance of infiltration swales on an urban catchment scale'

Assessment in this case is defined as the gathering of data and analysis of this data in order to get a better understanding of the quantitative performance of infiltration swales. The performance on a larger scale than only the individual swale will also be studied with a modeling exercise.

2.2. RESEARCH QUESTIONS

The main research questions to be answered will address the quantitative behavior of infiltration swales. The main research questions are:

I How do infiltration swales perform quantitatively under different weather circumstances?

II How do the inflow characteristics influence the quantitative performance of infiltration swales?

III What is the influence of the initial moisture conditions of the swale on the swale performance?

IV How do infiltration swales perform on an urban catchment scale?

In research question I, the quantitative performance will focus on the following indicators:

- Volume reduction
- Outflow delay
- Peak reduction
- Peak delay
- Emptying time of the swale
- Time to overflow

Different weather circumstances in this case include natural inflows (precipitation events during the monitoring period) and inflow simulation.

The inflow characteristics, as referred to in research question II, describe the way the water is entering the swale. For swales, both a head inflow and a lateral (overland) inflow are possible. Both these inflow characteristics will be considered in this study.

The initial moisture condition of the swale is the state in which the swale is at the beginning of an event. A dry swale will react differently to the same storm event than an already wet swale. The effects of the initial conditions will be studied.

The performance on an urban catchment scale will be determined based on the flow on the surface water system

2.3. APPROACH

The general approach in this thesis will be the monitoring and modeling of an individual infiltration swale. A swale is therefore monitored and the data is analyzed. The observed data is also used to validate a MetaSwap-Modflow model that has been developed for this study.

Artificial inflow simulation is the main tool used in this study to determine the quantitative performance of infiltration swales. The simulations provide data that make comparison of the performance of head vs. lateral inflow swales possible.

The developed model simulates the quantitative performance. The influence of changing initial conditions on the performance of the swale is modeled. The results of the swale model will be used as input to the urban drainage model. This will be an one-way coupling where the output of the swale model affects the sewer model but not vice versa.

.

3

LITERATURE REVIEW

This chapter concerns the literature review and theory. This review focuses on the quantitative performance of infiltration swales. The first part of the review consist of papers about the performance of individual swales. The second part will deal with the performance od infiltration swales on a neighborhood scale.

Individual swales
Researches including (Brander *et al.*, 2004), (Holman-Dodds *et al.*, 2003) and (Williams and Wise, 2006) studied the influence of development with and without infiltration facilities (not only swales). All these studies show that the runoff volume for potential development area is reduced due to infiltration. Brander *et al.* (2004) and Holman-Dodds *et al.* (2003) also conclude that infiltration practices are most effective for small storms.

This study is a continuation of the work performed by Donkers (2010). It was concluded that there was no clear relation between the inflow and discharge of the infiltration swale. Peak reduction was determined between 40-100 % for deep initial water levels and for shallow initial 40-89 %. Volume reduction ranged between 8-100 % (deep initial water levels) and 8-89% for shallow initial water levels. Peak delays ranged between 10-108 minutes.

Davis (2008) describes a two year monitoring project of two infiltration swales on the University of Maryland campus. In total, 41 full data runoff events were recorded and the analysis included mainly the peak flow reduction and peak delay. During 18 % of the events monitored no outflow was recorded and the swales were able to store the inflow. The mean values for the total volume reduction of the two swales were 48 % and 35 %. The volume reduction was defined as the percentage of inflow volume that was discharged after 24 hours. In more than 51 % and 61 % of the events the discharge ratio between inflow and outflow was 33%. Peak reductions that were monitored were in the range of 42 % and 51 %. Peak delay was defined as the ratio between the time elapsed to a peak of the inflow and the outflow. Mean values for both swales were 5.8 and 7.2.

Barber *et al.* (2003) performed a study on ecology ditches. The functioning principle of the ecology ditches is the same as for the infiltration swales considered in this study. The only difference is the compost top layer which should provide an increase in potential for evapotranspiration and improve the treatment performance. A decrease in peak reduction and peak delay was found for increasing storm size. The trend in the % peak reduction shows flatting for bigger rainfall events. Higher soil moisture contents explain the reduction in performance for larger storm sizes. Percentages of peak reduction range between 56 % and 69%. Peak delays were measured between 15 min and 60 min.

Longer storm durations cause lower peak reduction and increase the peak delay. The increase in the peak delay can be explained by the lower intensities of the longer rainfall events. Peak reduction percentages range from 50 % to 66 %. Peak delays range from 22 min to 27 min.

Peak reduction and peak delay for different storm distributions show similar results with increasing storm size. The performance flattens out to a minimum value with increasing storm sizes. The distribution, however, has a big effect on the total reduction and delay. For relative higher intensity events, the reduction in peak is much lower than for lower intensity storms. The distribution has almost no effects on the peak delays.

Initial water content conditions only have an influence on smaller storm sizes. Dry periods of 3h, 24h and 72h result in a similar initial condition of about 11 %. The minimum peak reduction and peak delay is almost not affected by the initial water content condition for larger storms.

Abida and Sabourin (2006) studied the quantitative performance of infiltration trenches in Canada. Inflow simulations were done by means of a fire hydrant and a hose. Total volume reduction was about 50 %. Also natural rainfall events were monitored at two infiltration swales in the City of Nepean, Ontario, Canada. It was shown that the seasonal average value of discharge from the swales was 7.5 % and 37.5 % of the seasonal value for precipitation.

Sabourin *et al.* (2008) found that peak reduction was in the range of 14 to 53 % compared to conventional storm water systems. Swales also perform better than conventional (gray) systems looking at the total volume reduction, which ranged from 14 to 27 % of the conventional system.

Urban catchment scale
No studies of the performance of infiltration swales on a urban catchment scale are known. Roldin *et al.* (2012a) describes the results of modeling soakaways in a urban catchment in Copenhagen, Denmark. Roldin *et al.* (2012b) describes ways to couple soakaway models with urban drainage and groundwater models. Since the soakaway shows similarity to the infiltration swale the methods of coupling models can also be used for swale modelling.

The first method that is mentioned is simply reducing the impervious area in the area of an soakaway in the rainfall-runoff of an urban drainage model also described in (Semadeni-Davies *et al.*, 2008). More complex coupling is the on-way and two-way coupling of the soakaway model and the urban drainage model. With one-way coupling the individual soakaway model is run seperately from the urban drainage model. The results are then used to use as input for the rainfall-runoff part of the sewer model. There is however no feedback from the sewer model to the soakaway model, hence one-way coupling. In the two-way coupling method the sewer model also affects the soakaway model and the effects of water flowing (back) from the pipe system to the soakaway can be modeled.

4

MEASUREMENTS AND INFLOW SIMULATIONS

The study site, the measurement set up and the inflow simulations will be discussed in this chapter.

4.1. STUDY SITE

Measurements were done at Castellumknoop swale in Utrecht, the Netherlands. The study site is located in Leidsche Rijn, a neighborhood of the city of Utrecht. The swale is located near the roundabout intersecting the Vicuslaan and Langerakbaan. Figure 4.1 shows the location of the swale. The right hand picture shows an overview of the swale with observation wells.

Figure 4.1: Castellumknoop infiltration swale

The Castellumknoop swale is designed to infiltrated water drained from the roads and roundabout near the swale. The intake of the swale is located at the head of the swale, located on the Langerakbaan side. The water that does not infiltrate into the ground is discharged onto surface water. The swale characteristics are summarized in table 4.1 (Donkers, 2010).

Table 4.1: Castellumknoop swale characteristics

Characteristic	
Inflow	head inflow
Outflow	on surface water overflow discharges on surface water as well
Level of the inflow	+0.70 m NAP
Level of the outflow (overflow)	+0.75 m NAP
Level of the drain	-0.20 m NAP
Level of the bottom of the trench	-0.20 m NAP
Drainage level	+0.35 m NAP
Drainage area	0.2 ha
Average surface level	+0.80 m NAP
Average surface water level	+0.15 - +0.45 m NAP
Storage above surface level	5.6 mm
Top layer thickness	20 cm
Side slope	1:3
Bottom width	1.35 m
Swale length	35 m
Drain diameter	125 mm

Six soil profile are available for the Castellumknoop swale. All profiles are located inside the swale. The vertical soil profile in the middle of the swale is shown in figure 4.2 and is considered to be representative of the soil profile of the entire swale.

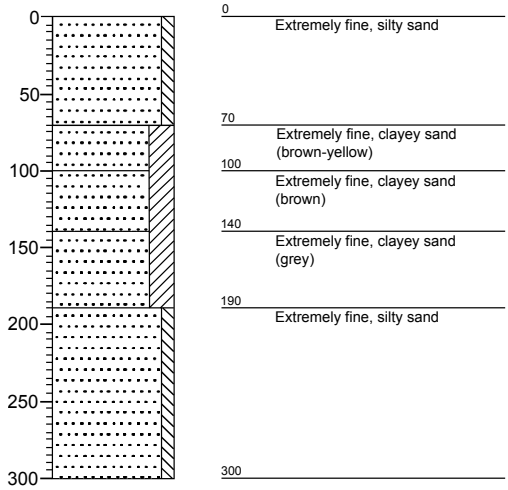

Figure 4.2: Soil profile Castellumknoop swale

The saturated hydraulic conductivity was determined in 2005 using the falling head test. The experiments were done at a depth of 0.5 m to 1.0 m below surface level. The resulting values are between 0.09 m/day and 0.36 m/day (Donkers, 2010).

4.2. MEASUREMENT SET UP

The measurement setup of this study includes the monitoring of inflow and outflow, groundwater levels, infiltration capacity and precipitation.

4.2.1. INFILTRATION

The infiltration capacity and the saturated hydraulic conductivity are determined.

Infiltration capacity
Double ring infiltrometer tests were done to determine the infiltration capacity of the top layer of the infiltration swales.

For this test two rings (outer and inner ring) will be pushed approximately 5 cm into the top layer of the swale. The outer ring has a diameter of 55 cm, the inner ring has a diameter of 32 cm. Water is added to both rings. An equal water level in the inner and outer ring should ensure vertical infiltration in the inner ring and prevents lateral flow. The principle is also shown in figure 4.3. The drop of the water level in the inner ring divided by the time step yields the infiltration capacity.

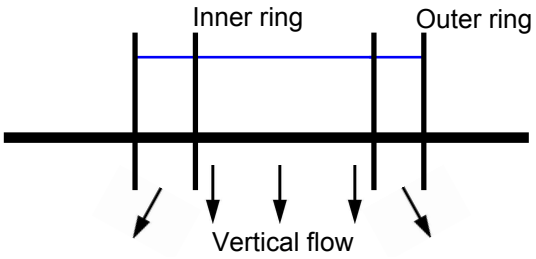

Figure 4.3: Double ring infiltrometer test principle

Saturated hydraulic conductivity
The saturated hydraulic conductivity was determined in the past by the municipality of Utrecht by means of a falling head test. Donkers (2010) also determined the conductivity based on the water balance and Darcy's law.

The latter method is also used for this study. In this method the period between the beginning of an event and the moment when the water level in the swale is at the same level as in the beginning is considered. It is assumed that the water balance in this period closes and that the storage is zero. The infiltrated volume is calculated by subtracting the outflow from the inflow volume and the average infiltration rate is found by dividing by the time of consideration. When considering the head difference between the aquifer and the swale, the hydraulic conductivity is the only unknown and can be calculated.

4.2.2. PRECIPITATION

Precipitation data is used to validate the inflow data of the swale and if necessary it is also used as an estimation of the inflow volume. The precipitation data is provided by the Municipality of Utrecht. The data is based on radar measurements (Hydronet) and the spatial resolution is 1x1 km. The Castellumknoop swale is located in raster cell 129A185. The center of this cell is about 400 m to the west of the swale.

4.2.3. INFLOW AND OUTFLOW

Discharges are measured by means of v-notch weirs. Two v-notch weirs (inflow and outflow) were installed for a previous study (Donkers, 2010). The overflow is measured by a RBC-flume. Head above the weir level are measured by means of pressure divers. For the inflow and outflow a Keller pressure diver was used. The overflow was measured by means of a mini diver. The locations of the divers are shown in figure 4.5.

The weir characteristics are shown in figure 4.4 and table 4.2. The weir at the outflow discharges on surface water.

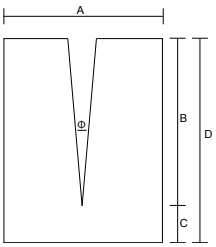

Figure 4.4: Dimension of the v-notch weir

Table 4.2: V-notch weir dimensions

	Inflow weir	Outflow weir	
Φ	30	10	°
A	300	180	mm
B	260	210	mm
C	40	90	mm
D	300	300	mm

The calibrated relation between the head above the weir and the discharge for both the inflow as the outflow is given in equation 4.1 and 4.2 (Donkers, 2010).

$$Q_{in} = 0.5509\ h^2 \tag{4.1}$$

$$Q_{out} = 0.2402\ h^2 \tag{4.2}$$

where:
Q_{in} = inflow [l/h]
Q_{out} = outflow (discharge of the drain) [l/h]
h = water level above the weir [mm]

The discharge of the overflow is given by equation 4.3 (Eijkelkamp, 2014):

$$Q_{overflow} = 7 * 10^{-7}\ h^3 + 6.26 * 10^{-4}\ h^2 + 1.569 * 10^{-2}\ h - 0.0665 \tag{4.3}$$

where:
$Q_{overflow}$ = overflow [l/s]
h = water level above the weir [mm]

4.2.4. GROUNDWATER LEVELS

Groundwater levels are measured by means of pressure divers in seven observation wells. Figure 4.5 shows the location of the observation wells. The figure is not on scale. The pressure divers for the groundwater levels are mini divers.

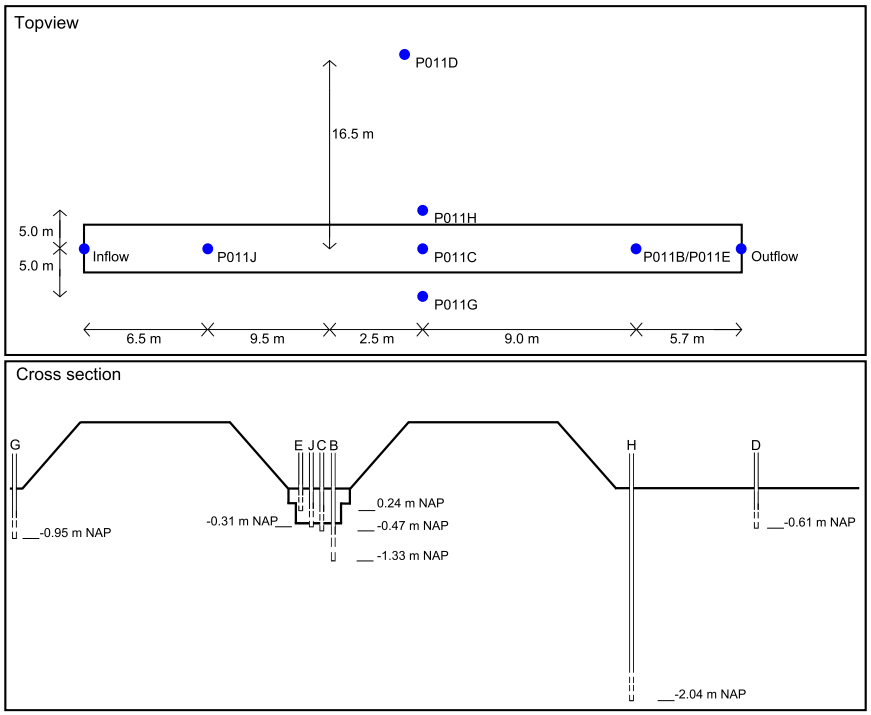

Figure 4.5: Location observation wells and discharge divers

An overview of the pressure divers are given in table 4.3. Divers P011B and P011E are situated in the same observation well.

Table 4.3: Installed divers Castellumknoop swale

Diver	Bottom filter [m NAP]	Sensor height [m NAP]	Surface level [m NAP]
P011F (inflow)	-	0.70	-
P011I (outflow)	-	0.35	-
P011A (overflow)	-	0.75	0.90
P011J	-0.31	-0.15	0.58
P011D	-0.61	-0.43	0.86
P011G	-0.95	-0.74	0.73
P011C	-0.47	-0.37	0.64
P011H	-2.04	-1.34	0.78
P011B	-1.33	-0.52	0.70
P011E	0.24	0.24	0.70

4.3. INFLOW SIMULATIONS

Inflow to the swale is simulated by pumping water from the surface water to the swale.

4.3.1. HEAD VS. LATERAL INFLOW

Storm event simulations are done with a head and a lateral inflow. The events that are simulated are described in paragraph 4.3.2. The main purpose of the simulations is to compare the performance of a swale with head inflow and lateral inflow.

Head inflow
Head inflow is simulated with a pump and one hose. The inflow is at the head of the swale, as shown in figure 4.6. The average discharge of the pump is measured by filling a barrel and recording the time to fill. The volume is measured by means of measuring cylinders.

Figure 4.6: Head inflow simulation with a pump

Lateral inflow
Lateral inflow simulations were done with a gutter (figure 4.7) installed in the longitudinal direction of the swale. The intention was to equally divide the water over the swale. As with the head inflow, the pump discharge for the lateral flow is measured with a barrel and a stopwatch.

4.3.2. SIMULATED EVENTS

In total, seven simulations were done. The simulated events were both done with a head inflow as well as a lateral inflow. In this way the differences and similarities could be identified.

The intention was to base the simulations on the rainfall depth duration frequency (DDF) curves (figure 4.8) determined by Buishand and Wijngaard (2007) for the De Bilt, the Netherlands. The distance between the study sites and De Bilt is about 10 km. Wijngaard *et al.* (2005) stated that, for short duration events, the data from De Bilt is representative for other locations in the Netherlands. Therefore the data from De Bilt is used for the first inflow simulation.

Figure 4.7: Lateral inflow simulation with a gutter system

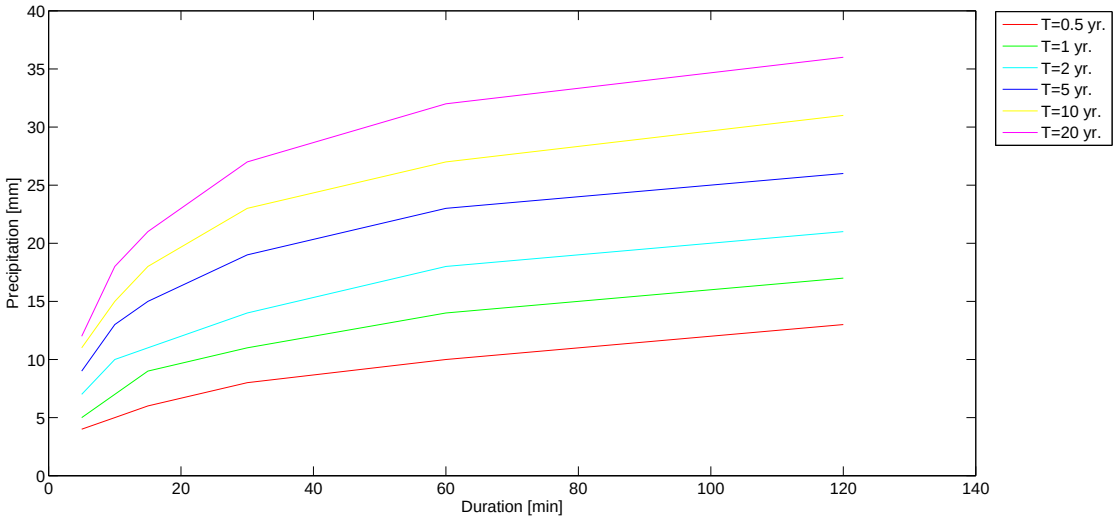

Figure 4.8: Rainfall DDF curves De Bilt, the Netherlands (source: Buishand and Wijngaard (2007))

However after doing the T=0.5 storm for 1 hour (simulation 1 and 2), it turned out that the total volume of water pumped after 30 min was sufficient to fill the swale. Also the lateral inflow facilities (gutters) were not suitable for these large discharges. Based on these observation it was decided to lower the discharges. The pump characteristics (maximum discharge and accuracy in setting the discharge) were the bases for the other simulations. The simulations are summarized in table 4.4. Simulation 3,4 and 5 were done in steps. For these simulations the values are given for the individual steps. The total inflow volume is given in [mm] and is calculated for the area that is connected to the swale (0.2 ha).

Table 4.4: Simulated events

Sim.	Duration [min.]	Type of inflow	Qin [m^3/hour]	Qin [l/(s*ha)]	Vin,tot [m^3]	Vin,tot [mm]
1	52	head	16.9	23.5	14.68	7.3
2	60	lateral	13.8	19.1	13.78	6.9
3	30+35+43	head	0.9+1.3+1.3	1.2+1.8+1.9	0.44+0.76+0.96	0.22+0.38+0.48
4	35+41+36	lateral	0.7+1.1+1.2	1.0+1.6+1.7	0.41+0.77+0.73	0.21+0.39+0.37
5	17+29	head	18.6+11.5	25.8+16	5.26+5.57	2.6+2.8
6	60	lateral	12	16.6	11.98	6
7	60	head	9.2	12.8	9.19	4.6

As mentioned before the same event was simulated twice, head vs. lateral inflow. The events belong together as the discharge is in the same range. The discharges were not exactly the same because it was impossible to set the discharge of the pump accurately. Simulation 1 and 2 form a pair. Simulations 3 and 4 and simulations 6 and 7 also belong together.

5

MEASUREMENT RESULTS AND ANALYSIS

The data presented in this chapter was obtained by doing measurements. Data validation was done and will also be described in this section.

In this study in total 18 events (events 21-38) were observed of which 7 are artificial inflow simulations (events 32-38). Together with the data collected by Donkers (2010) (events 1-20), 38 events are analyzed. The data of Donkers (2010) only include discharge measurements.

5.1. DATA VALIDATION

Water level measurements (for determining discharge) and groundwater level recordings are validated on the bases of manual observations, estimations of runoff coefficients and consistency between inflow water level and precipitation.

Air pressure compensation
Before the data validation a problem with the air pressure compensation needed to be solved first. The data from the mini divers (groundwater levels) are compensated with the air pressure measurements done at the office of the municipality of Utrecht. The office is located about 3.2 km away from the study site. The Keller divers (inflow and outflow) were compensated with the air pressure measured at the swale.

The problem occurred with the Keller divers. First, after analyzing the data it turned out that the air pressure sensor of the Keller devices was under water in cases the water level in the inflow and outflow box was at an certain level or above. This resulted in (large) errors in the air pressure recordings. The second issue is the relative big difference between the air pressure measured at the inflow and the outflow.

The two issues above made it clear that the recordings of the air pressure by the Keller divers could not be trusted. Other sources of air pressure were used to compare the inflow and the outflow air pressure measured at the site. The other sources include observations at the office of the municipality of Utrecht and measurements done by the Royal Netherlands Meteorological Institute (KNMI) in De Bilt. The town of De Bilt is about 10 km away from the Castellumknoop swale. Figure 5.1 shows the air pressure at different locations.

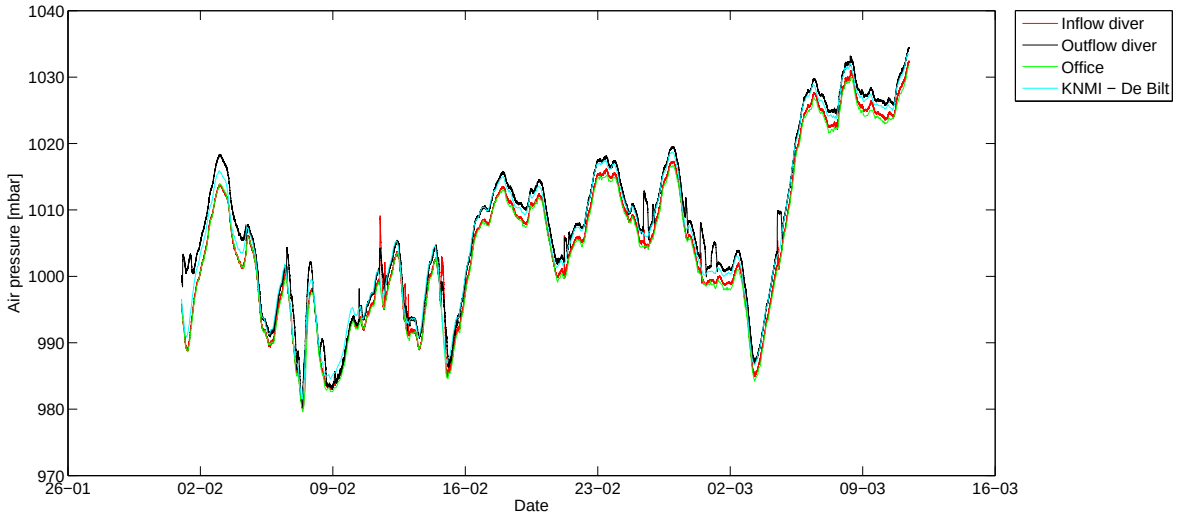

Figure 5.1: Air pressure measured at different locations

The figure shows that the measurements by the KNMI are closer to the outflow air pressure. The office values however are closer to the inflow air pressures. Because the office is closer to the site than De Bilt, it is more reasonable to assume that the air pressure at the inflow (and thus also at the office) are closer to the real air pressure than the outflow and KNMI values.

Observation well P011E (figure 4.5) is a shallow well located within the cross section of the swale. When the swale is dry, the well will also be dry and the diver would record the air pressure. To determine the air pressure that is closest to the real values the inflow and office air pressures are compared to the values recorded in the dry observation well , figure 5.2. In this analysis it is assumed that the air pressure at the dry observation well is the real air pressure. This is supported by the data validation based on manual recordings, see figure A.4 in Appendix A. The recordings in observation well P011E are very close to the manual recordings.

The difference is not constant and shows an increasing trend in time. During the measuring period, no changes in the measuring set-up or equipment were observed that could explain these changes. Sometimes the inflow air pressure deviates more than the office air pressure and vice versa.

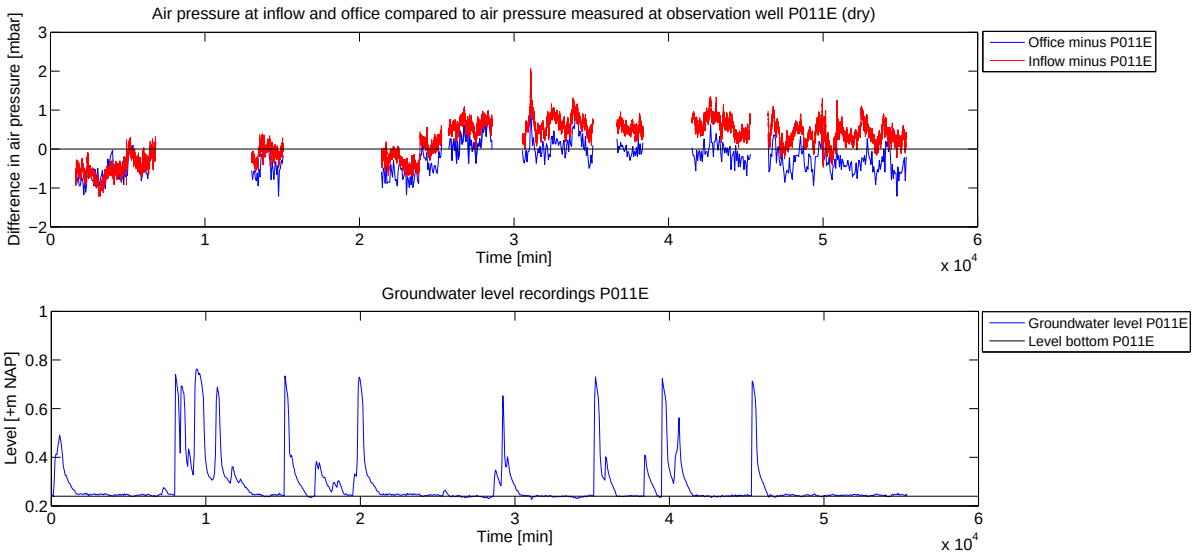

Figure 5.2: Air pressure comparison of inflow, office and observation well P011E (dry)

The median absolute difference of the office air pressure is 0.3 mbar while for the inflow this value is 0.5 mbar. The deviation of both air pressures with respect to the air pressure measured at the dry observation well are similar and considered small.

Considering this small deviation and the fact that the air pressure at the inflow is missing reliable values at times that the sensor was under water makes it reasonable to use the air pressure at the office in further analysis. The influence of the necessary linear interpolation of the hourly data of the office air pressure to minute values (for discharge determination) is considered small since large deviations in air pressure are not expected on an one minute time scale. It is expected that filling in the missing values of the inflow air pressure is more sensitive to errors but this can not be supported with numbers since the observation well P011E is not dry at these times.

The difference in water levels between compensation with the office air pressure and the inflow air pressure is shown in figure 5.3. The figure shows the water level based on the inflow air pressure minus the water level based on the office air pressure. The times that the air pressure sensor of the inflow was underwater are not taken into account.

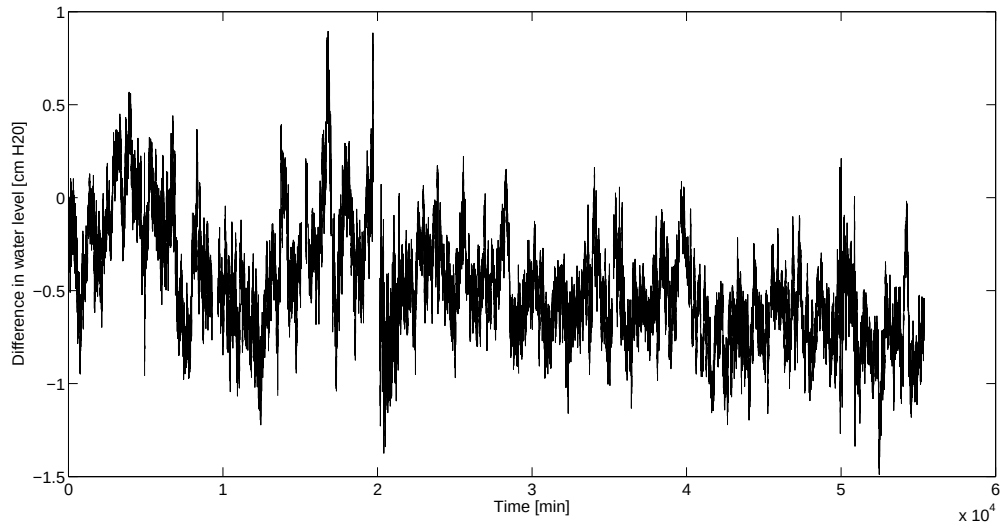

Figure 5.3: Difference in water level based on inflow air pressure and office air pressure

The figure shows that most of the time the water levels with office air pressure compensation are higher than for the inflow air pressure compensation. This was also expected since the air pressures at the inflow are almost always higher than the office values (figure 5.2). The minimum difference is almost zero while the maximum positive difference is +0.89 cm H2O and the maximum negative value is -1.49 cm H2O. The median absolute difference is equal to 0.5 cm H2O. This proves that the influence of the air pressure can be quite significant and this should be taken into account in further analysis.

Comparison with manual observations
After compensation with the appropriate air pressure the observations could be compared to the manual observations. All the recordings were compensated with the office air pressure. For the groundwater level recordings the difference between the recorded and the manual observed value is not allowed to be more than +/− 5 cm. Within this bandwidth the municipality of Utrecht assumes the recording to be acceptable. In this way the errors in the manual observations and the air pressure compensation are within reasonable limits.

All the figures of the validation are shown in Appendix A. All groundwater levels recordings were within the limits except from P011H. The difference between the recordings and the manual observations is about 5.8 cm. The groundwater levels for P011H are therefore shifted down with 5.8 cm (figure 5.4).

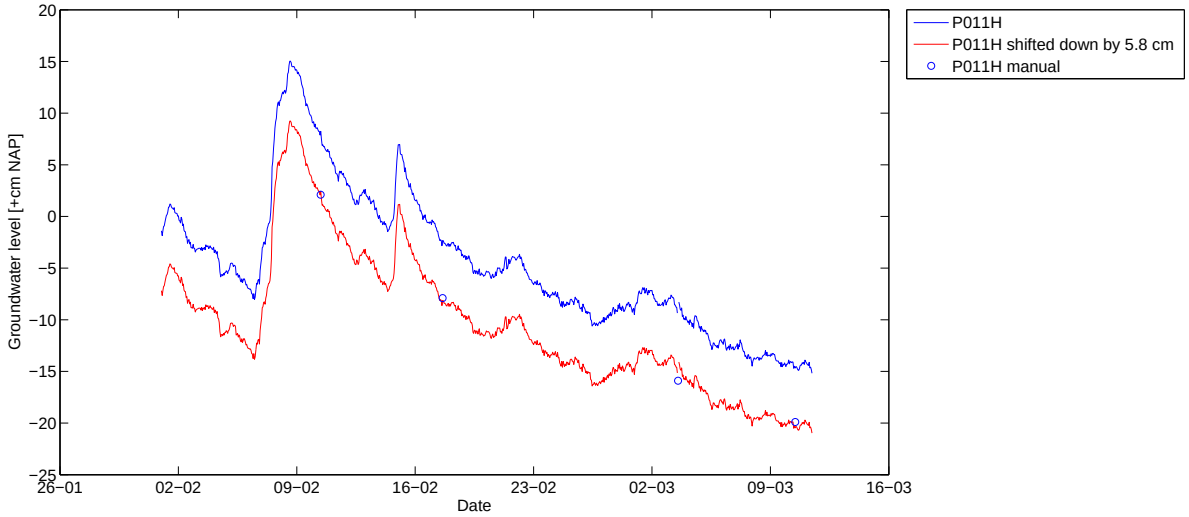

Figure 5.4: Shifted groundwater levels of observation well P011H

The water levels for discharge calculations were not within the 1 cm limits. The manual observations for the inflow are 3 cm higher (figure 5.5), while the manual inflow values are 3 cm lower (figure 5.6). This suggests that there is a shift in the recordings.

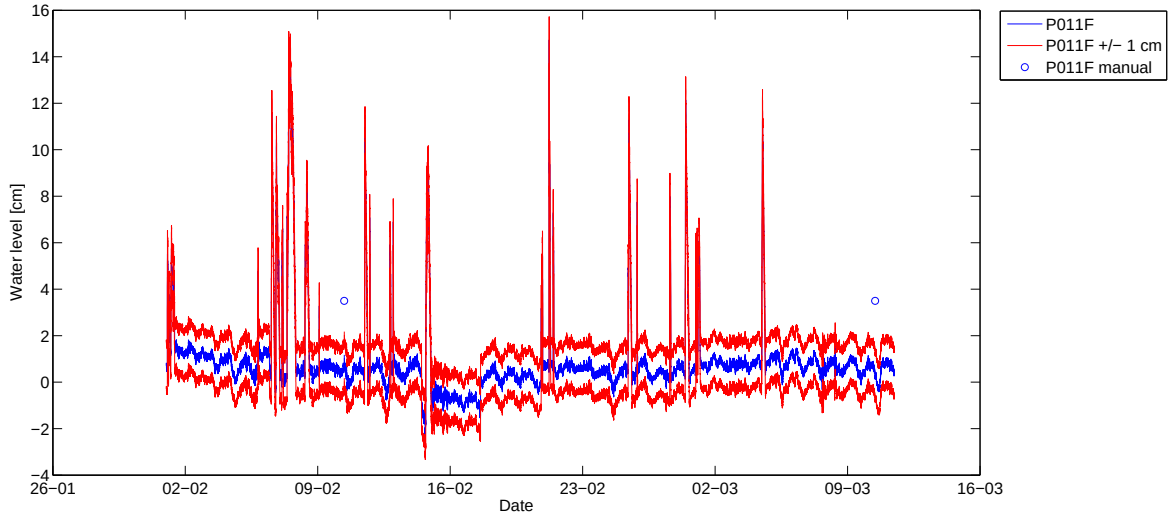

Figure 5.5: Recorded water levels P011F (inflow) in comparison with manual observations

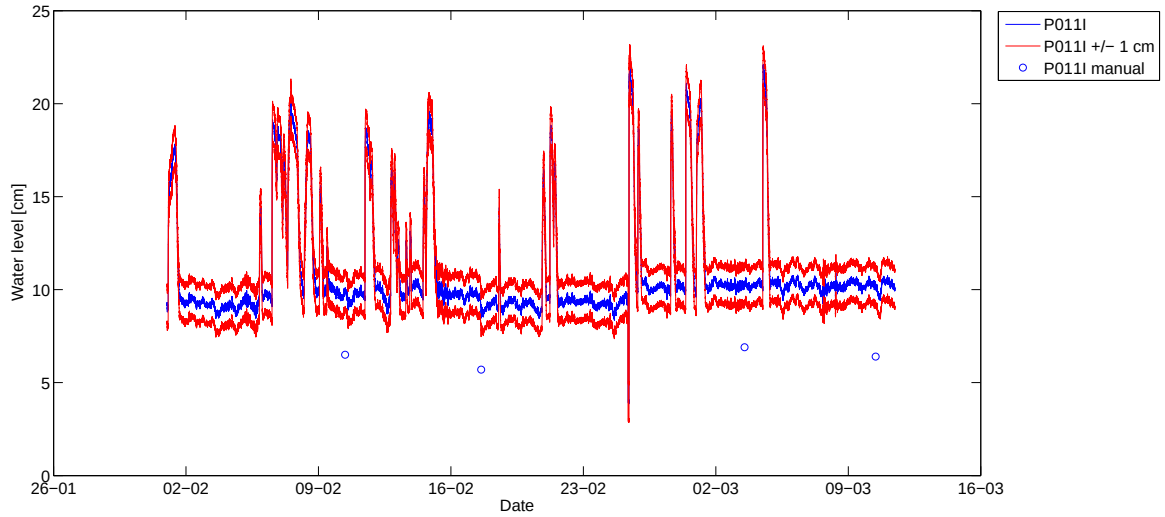

Figure 5.6: Recorded water levels P011I (outflow) in comparison with manual observations

Because the impact of an error in the water levels could have a significant impact on the discharge determinations extra calibration tests were done to test the Keller divers., In this test the divers were placed in a bucket and the water level was changed. The relationship between the diver values and the manual recorded values is shown in figure 5.7 and figure 5.8.

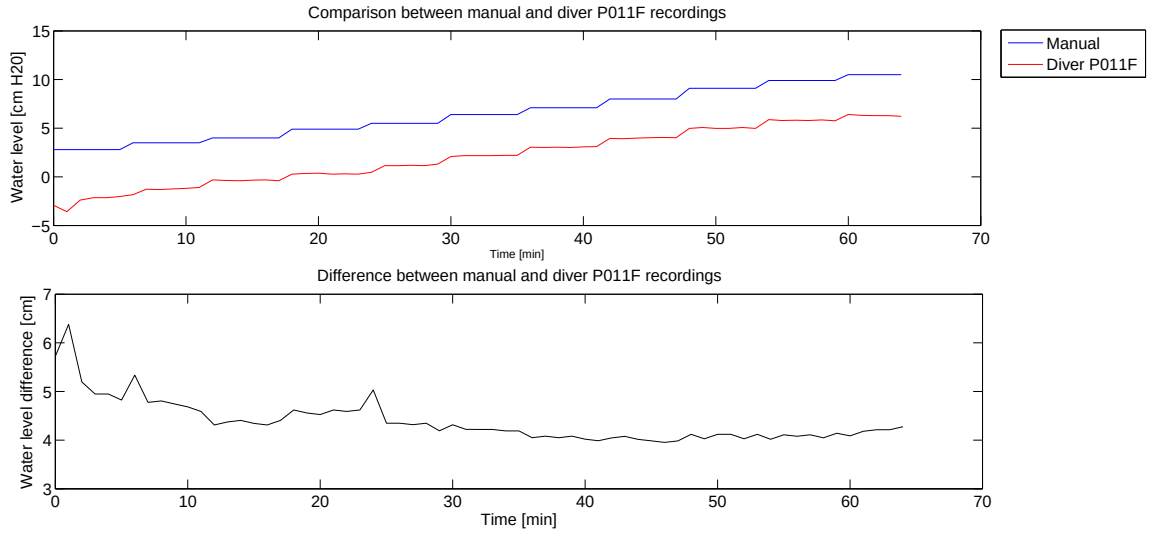

Figure 5.7: Extra calibration test inflow water level recordings

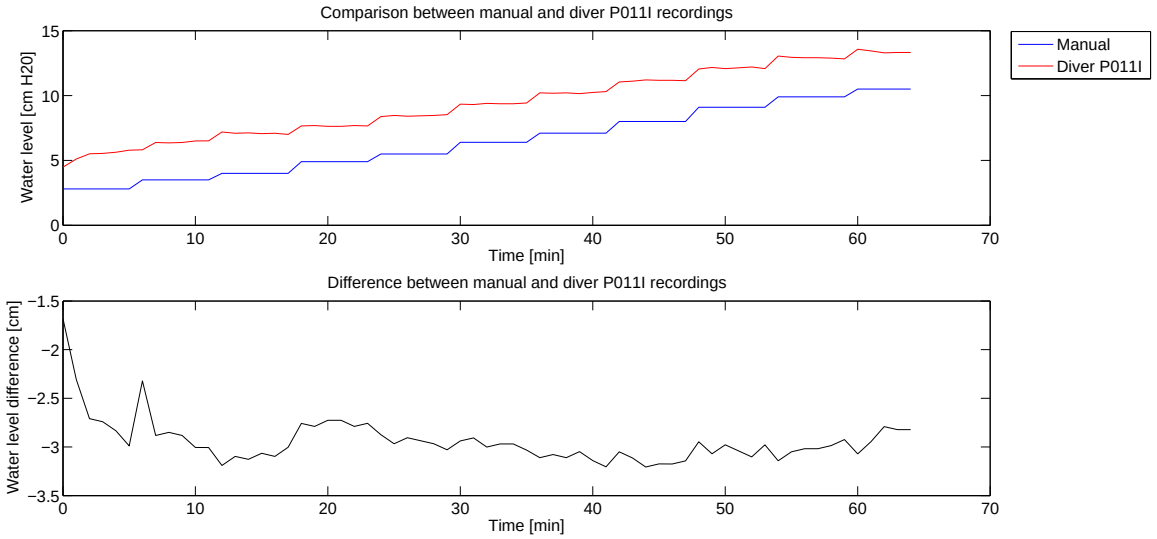

Figure 5.8: Extra calibration test outflow water level recordings

Taking into account the variability in water levels due to the air pressure compensation and the fact that for water levels lower than 3 cm, the diver is not fully submerged, the extra calibration test of the outflow water level recordings confirmed the shift in the outflow water levels (figure 5.8). The raw data of the outflow water level is thus shift downwards with 3 cm. The inflow test does not show a clear shift. The manual recordings of the extra calibration test show a shift of between +6 cm and +4.2 cm. This is more than the +3 cm that was found with the two manual recordings as shown in figure 5.5. The extra calibration test has more points for comparison with the manual recordings so an upward shift of +4.2 cm is more likely. The value is chosen based on the rather constant values at the end of the test (figure 5.7). This shift resulted in a water level almost always above the weir level at the inflow. This means there was flow into the swale constantly, which is definitely not possible based on visual observations of periods without inflow.

The extra calibration test for the inflow showed however that the diver was indeed recording water levels that were too low. The magnitude of the upward shift was not confirmed. Since the upward shift of 4.2 cm is unrealistic it was decided to shift the water levels up with 3 cm. This shift results in more reliable water levels than the 4.2 cm. The figures of the water levels used in this study are shown in Appendix B.

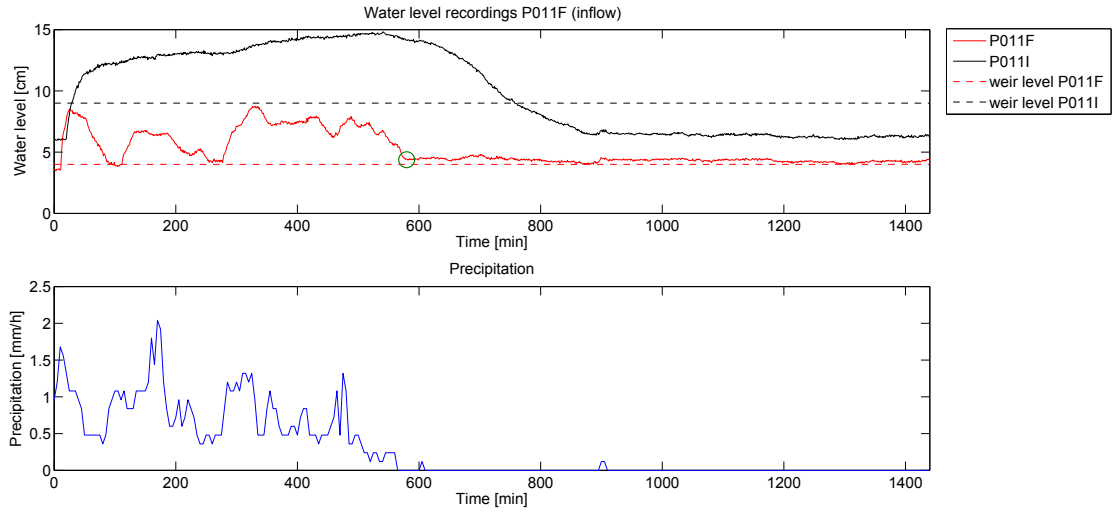

Figure 5.9: Event 21 - Moment that the inflow calculations are stopped in case of a no-flow level above the weir level

The no-flow level at the end of an inflow event is determined on basis of the transition from falling water to constant water level and the precipitation data. In some of the events this no-flow level (circled in figure 5.9) is just above the weir level. The discharge calculations are stopped at this point. And the recorded discharge is thus zero.

Runoff coefficients and inconsistent inflow water level recordings
The runoff coefficients of the natural events are determined as well. Figure 5.10 shows the coefficients against the precipitation volume of the events. The dots are labeled with the event number. The coefficients are based on the precipitation volume that falls on impervious area. Because radar data is used and the inflow volume contains uncertainties, the calculated values of the runoff coefficient (C) are just estimations.

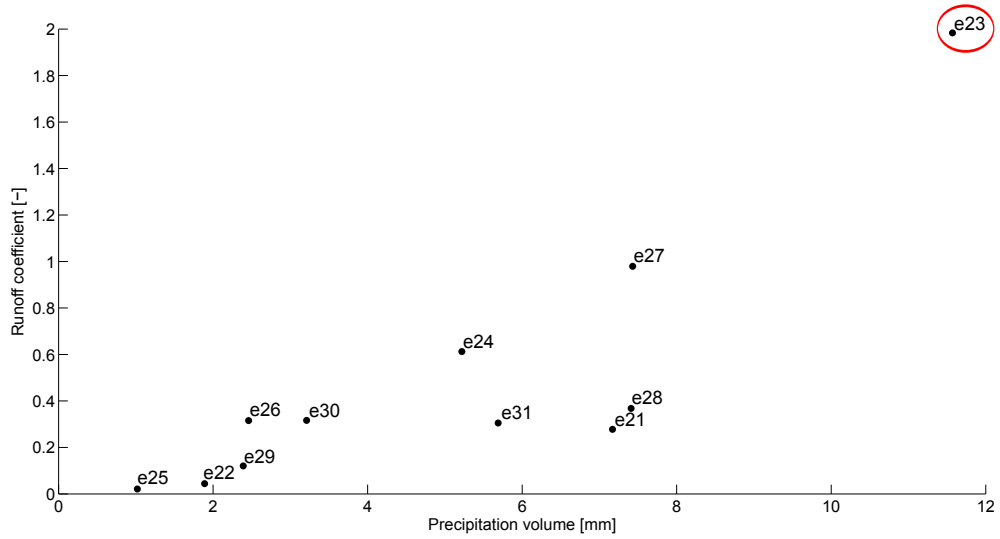

Figure 5.10: Estimation of runoff coefficient against total precipitation volume

The inflow volume of event 23 is almost twice as much as the precipitation volume (marked red in figure 5.10). This is very unlikely. The other events show more reliable values taken into the account the uncertainties in inflow and precipitation measurements. Event 23 is not considered in the analysis of this study.

The last validation step is the check if the inflow water levels look consistent with the precipitation data. The graphs of the water levels of the inflow and outflow and the precipitation are shown in Appendix B.

The inflow measurements of events 22,23,25,26 and 30 do not look consistent with the precipitation data. However if the uncertainty in the precipitation is taken into account, only event 25 (figure 5.11) shows a big difference between the inflow and the precipitation pattern.

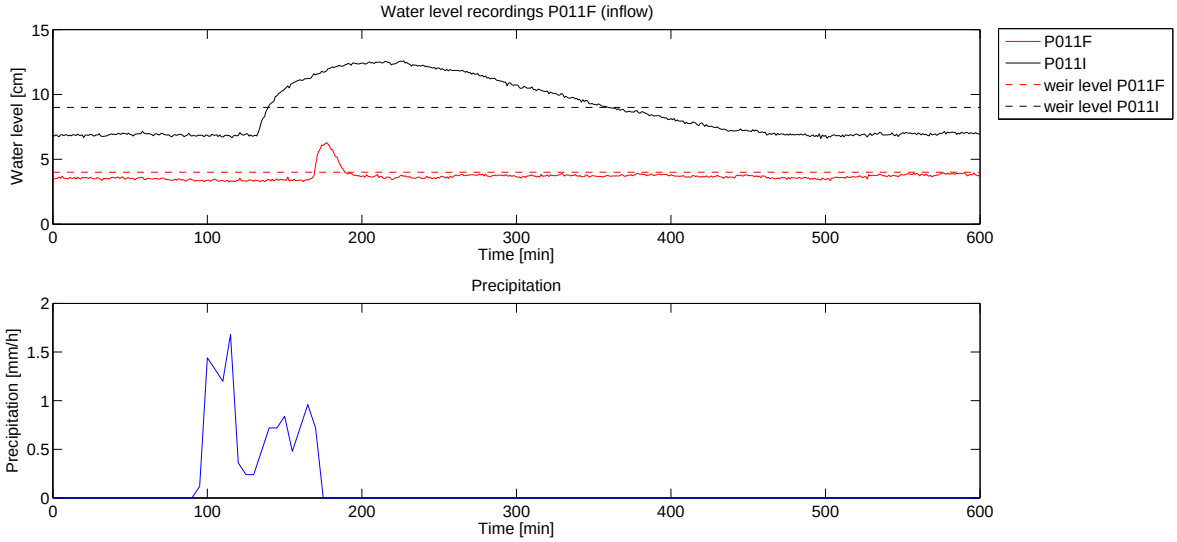

Figure 5.11: Event 25 - Water levels and precipitation

Conclusions validation of the data
The data collected for this study show a high level of uncertainties in the water levels for the inflow and outflow discharge calculations. These uncertainties are caused by the fact that the pressure diver was measuring water levels that were low. A shift in the water levels is present. The magnitude of the shifts however is not known because the extra calibration test showed different results from the manual observations. Another uncertainty in the inflow water levels is caused by the fact the shift that is applied (+ 3 cm) for the inflow water levels is based on just two points in time. It is possible that the shifts are not constant in time. Unfortunately no data is available to proof which shift is correct.

Based on estimations of the runoff coefficient and consistency of the inflow data with the precipitation event 23 and 25 are not considered in the analysis described in the next paragraph.

5.2. RESULTS AND ANALYSIS

This section concerns the results and analysis of the measured data.

5.2.1. INFILTRATION

The infiltration capacity of the top layer and the saturated hydraulic conductivity is determined in this study.

Infiltration capacity
The measured infiltration capacity over the last 5 years is shown in table 5.1. The values given in the table are the average of 3 measurements at one location within the swale.

Table 5.1: Infiltration capacity [m/d]

Date	1	2	3	4	5	6	Average
29/5/2009	0.52	2.86	8.23	2.71	2.61	2.71	3.27
06/04/2010	3.02	5.90					4.46
16/02/2011	3.20	6.64	13.96	11.92	10.52	10.40	9.44
04/05/2012	8.60	9.16	21.79	18.04	19.02	22.25	16.48
03/10/2012	8.96	9.12	17.12	17.72	20.33	20.51	15.63
20/12/2013	5.34	-	-	-	-	-	5.34
24/03/2014	13.49	6.79	10.84	-	-	-	10.37

The measurements of the 6^{th} of April 2010 is described in (Donkers, 2010). The other measurements are done by the municipality. As can be seen in the table the results show a large variability with the location of the experiment. The difference between the minimum and the maximum value on one day is between 2.88 m/day and 13.65 m/day. This large difference can be the result of the variability of the soil of the top layer and possible inconsistent installation of the rings.

The infiltration capacity also changes over time. In 2009 the top layer was replaced. A larger infiltration capacity should be expected because of a new top layer since this was the purpose of the replacement. This is not what the results show. The measurements done by Donkers (2010) do not show an significant increase in infiltration capacity. An explanation can be the different soil moisture conditions at the time the measurements were done. A saturated soil has an infiltration rate equal to the saturated hydraulic conductivity. The flow is gravity driven. Before saturation of the soil the infiltration rate is greater than the hydraulic conductivity because the soil suction also contributes to the flow. Other explanation can be the possible inconsistencies in executing the test by different persons and the exact location of tests.

An explanation can be that the tests were performed by different persons. Also, as mentioned before, the location of measurements can have an impact. An increase is however visible in 2011 and 2012. The measurements in 2013 and 2014 were done for this study. The average value for this study is equal to 9.1 m/day. This is lower than the value in 2012 and can be explained by clogging and compacting of the top layer.

Saturated hydraulic conductivity of the native soil
The hydraulic conductivity of the native soil was also determined. In the past the municipality of Utrecht (falling head test) and Donkers (2010) (water balance - Darcy's law) determined this value as well. The values were between 0.09 m/day and 0.36 m/day for the falling head test and 0.076 m/day to 0.135 m/day for the Darcy method (Donkers, 2010).

The analysis for this study made use of the average of the values measured in observation well P011J and P011C (if possible) for the groundwater level in the swale. The level in the aquifer is an average of the value measured in observation well P011B and P011G. In total 3 events were used for this analysis with a duration of more than 1000 min. This to minimize the effects of fast processes. The values that were found are 0.04 m/day, 0.07 m/day and 0.37 m/day. These fluxes are downwards. These values are consistent with the values determined before.

5.2.2. PRECIPITATION

The precipitation data that is used in this study was calibrated by HydroNet with data from rainfall stations of the KNMI and of HydroNet itself. The radar data is shown in figure 5.12.

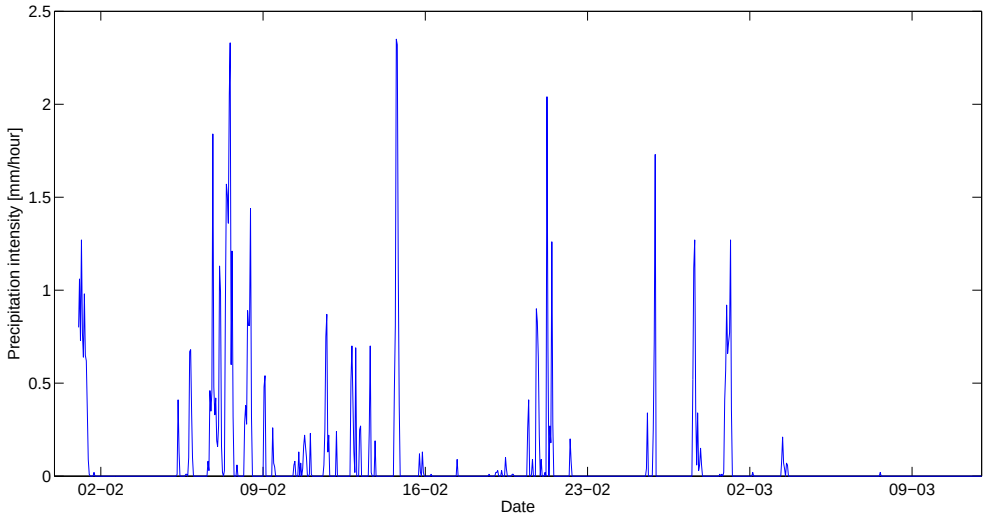

Figure 5.12: Rainfall intensity measured at HydroNet cell 129A185

The daily sums of the precipitation are shown in figure 5.13. Comparison is made with the closest KNMI station in De Bilt. This measuring station is about 10 km away from the study site. On three days precipitation is observed in one station while there is no rain measured at the other. This can be caused by the spatial variability of precipitation. The daily values of the radar data do not show very big differences with the De Bilt values.

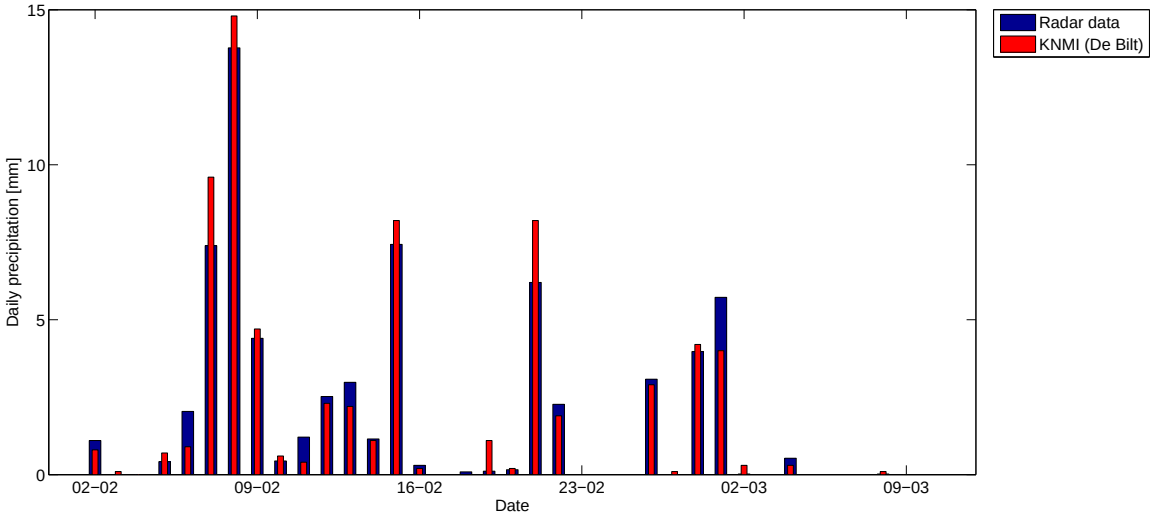

Figure 5.13: Daily precipitation amounts of HydroNet cell 129A185 and KNMI station De Bilt

The precipitation that was observed in the measuring period is considered to be light to moderate. In comparison, the KMNI considers heavy rainfall as 25 mm/day or 10 mm/hour (KNMI, 2012). The maximum daily sum recorded in this study is about 13 mm. The maximum hourly rainfall sum measured with the radar is about 2.3 mm.

5.2.3. SWALE PERFORMANCE

The results of the measurements of groundwater levels, inflow and outflow is presented in this section. The graphs of the inflow, outflow and groundwater levels of the events that are considered in the analysis are shown in Appendix C.

Groundwater levels
The groundwater recordings are shown in figure 5.14 (inside the swale) and figure 5.15 (outside the swale).

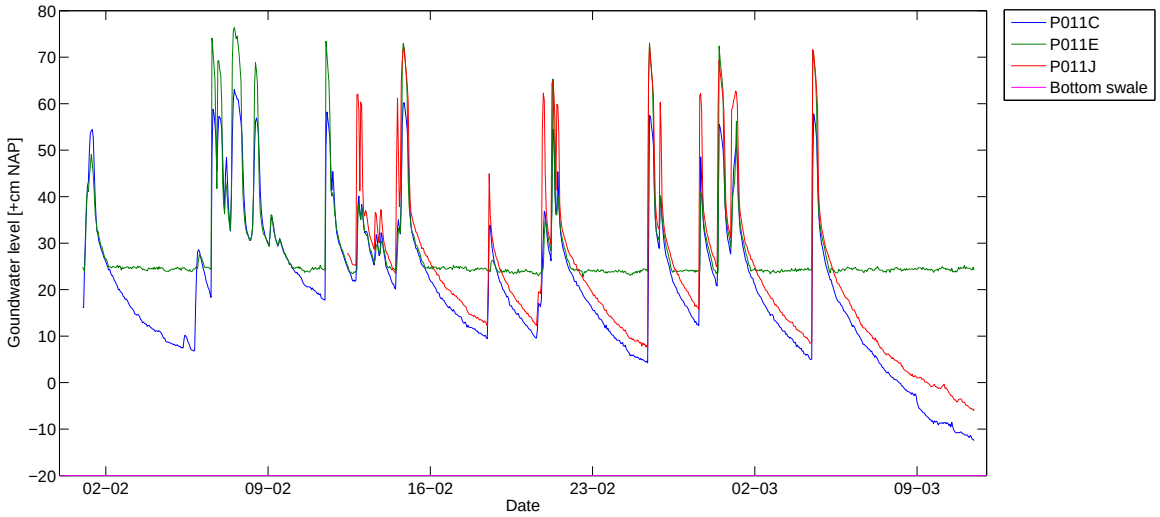

Figure 5.14: Groundwater level recordings observation wells inside the swale

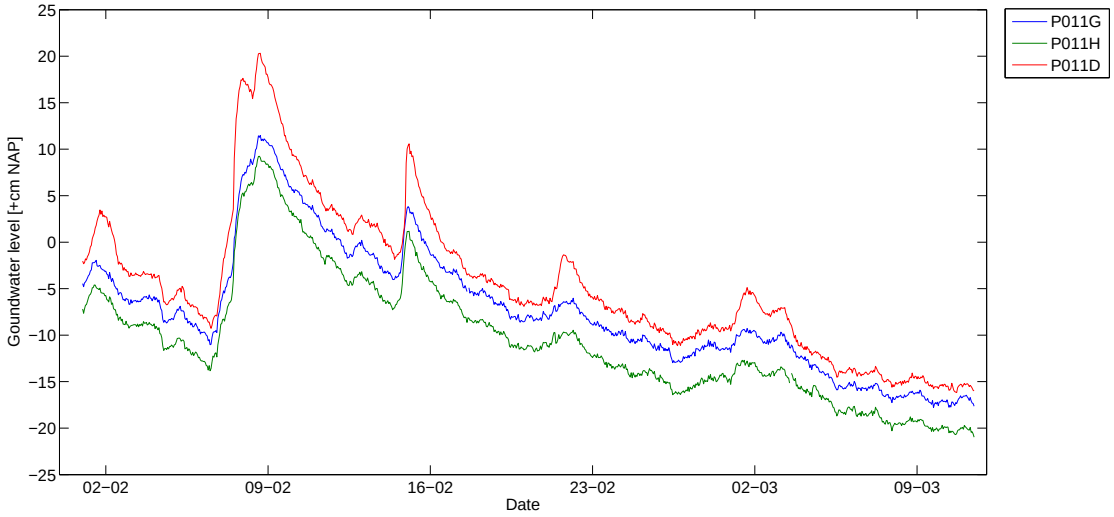

Figure 5.15: Groundwater level recordings observation wells outside the swale

The figures shows clearly that the response of the water levels inside the swale is large compared to the response of the groundwater levels outside the swale. The maximum rise of the groundwater levels inside the swale is more than 50 cm for all observation wells. For outside the swale this number is less than 17 cm. The median values of the rise in the observation well inside the swale are higher than 25 cm while the outside equivalents are lower than 2 cm.

Figure 5.14 also shows that the swale is never dry. At the end of the measuring period it looks like the swale is running dry. After almost 7 days of dry weather and no inflow, the swale is however not completely dry. The level measured in the observation wells located in the swale are also always higher than the surrounding groundwater levels. This means a gradient that enables downward flow and thus infiltration.

The events and simulations are divided into groups based on the initial water level in the swale at the start of an event or simulation. The groundwater level in observation well P011C is used for this.

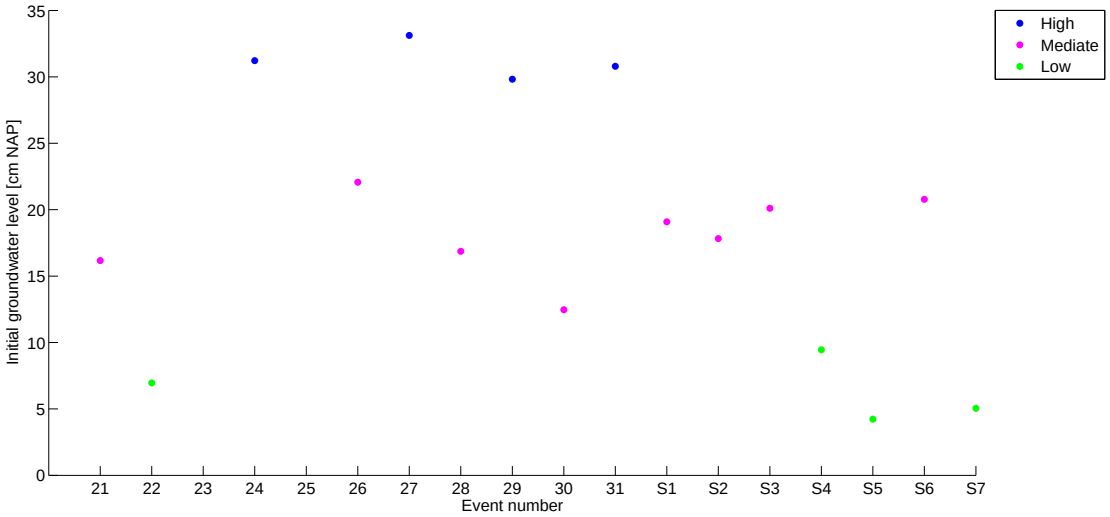

Figure 5.16: Classification of events based on initial groundwater level

Events with initial groundwater levels higher than +30 cm NAP are classified as high. The mediate class consists of initial groundwater levels between +10 cm NAP and +25 cm NAP. The events with low initial groundwater levels are those with an initial level lower than +10 cm NAP, figure 5.16.

Key performance indicators
The six key indicators that are included in the analysis are:

1. Volume reduction
   The difference between the inflow volume and the outflow volume divided by the inflow volume [%]
2. Outflow delay (A)
   The time between the start of the inflow and the start of the outflow [min.]
3. Peak reduction (B)
   The difference in the peak inflow and the peak outflow divided by the peak inflow [%]
4. Peak delay (C)
   The time between the inflow peak and the outflow peak [min.]
5. Emptying time (D)
   The time that is needed for the water level in observation well P011E to drop from the maximum level to the bottom of the well [min.]
6. Time to overflow (E)
   The time between the start of the inflow and the start of the overflow [hr]

Examples that illustrate the indicators are shown in figure 5.17 to 5.19. A comparison is also made between the data collected by Donkers (2010) (old data) and the natural events and simulation of this study (new data).

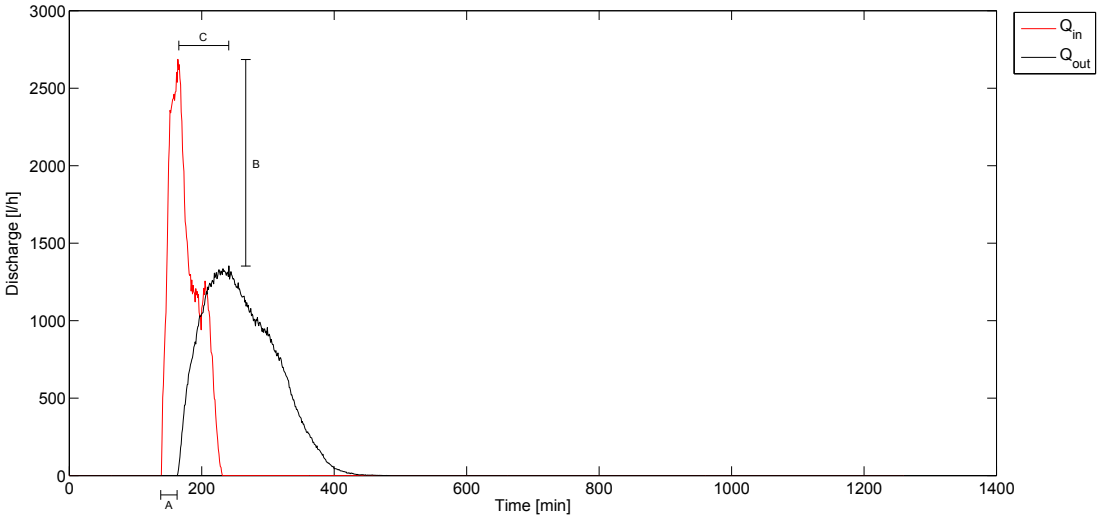

Figure 5.17: Performance indicators - Outflow delay, peak reduction and peak delay

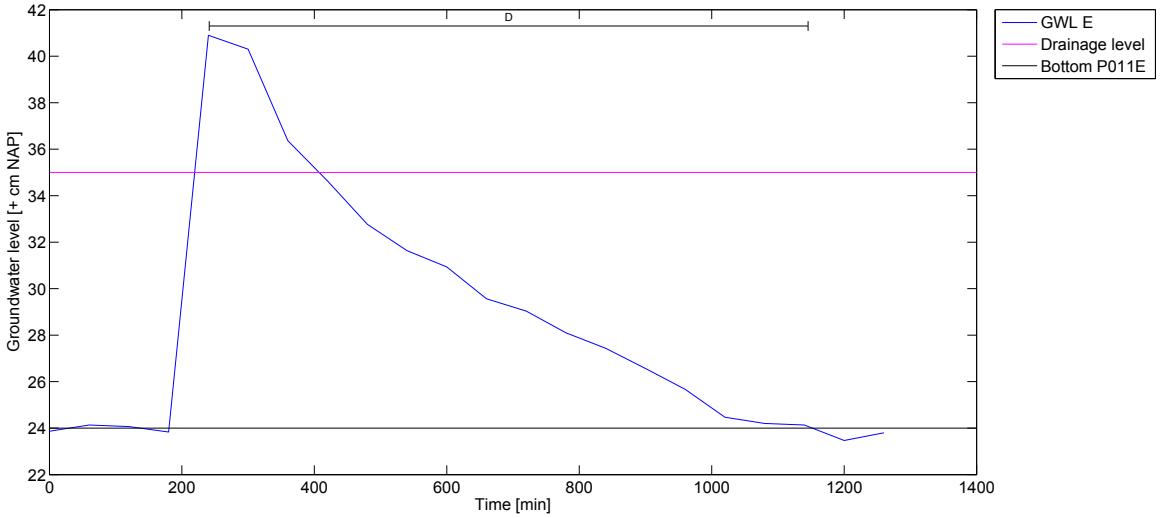

Figure 5.18: Performance indicator - Emptying time

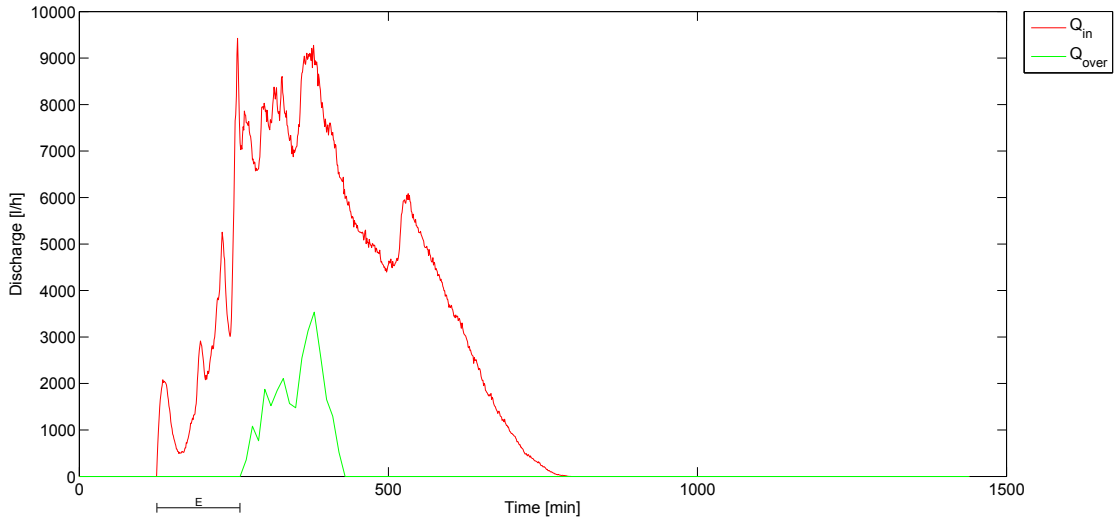

Figure 5.19: Performance indicator - Time to overflow

Volume reduction

The volume reduction in liters is shown in figure 5.21. The numbers in this figure are based on the inflow and outflow recordings only. The volume of precipitation that directly falls on the swale is not taken into account because the precipitation data is measured by radar. The extracted volumes from this data are considered to be inaccurate and are only used as estimations.

Figure 5.20 shows the volume reduction as a percentage of the total inflow volume. The results show a large variability. This variability was also present in the data of Donkers (2010).

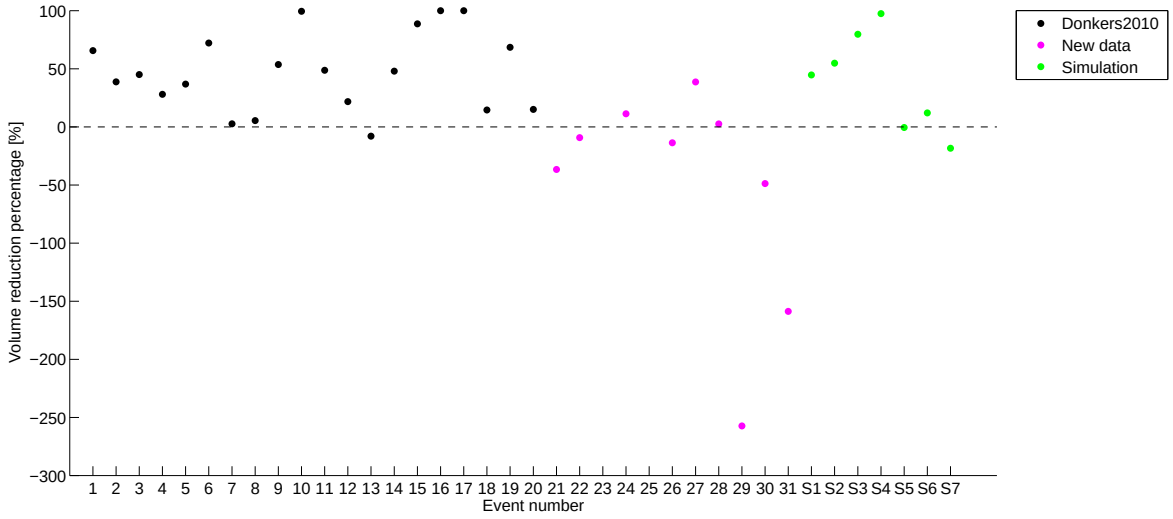

Figure 5.20: Relative volume reduction

Event 13 (Donkers2010) has a negative volume reduction. It is unknown what the reason is since only inflow and outflow data is available for the old data.

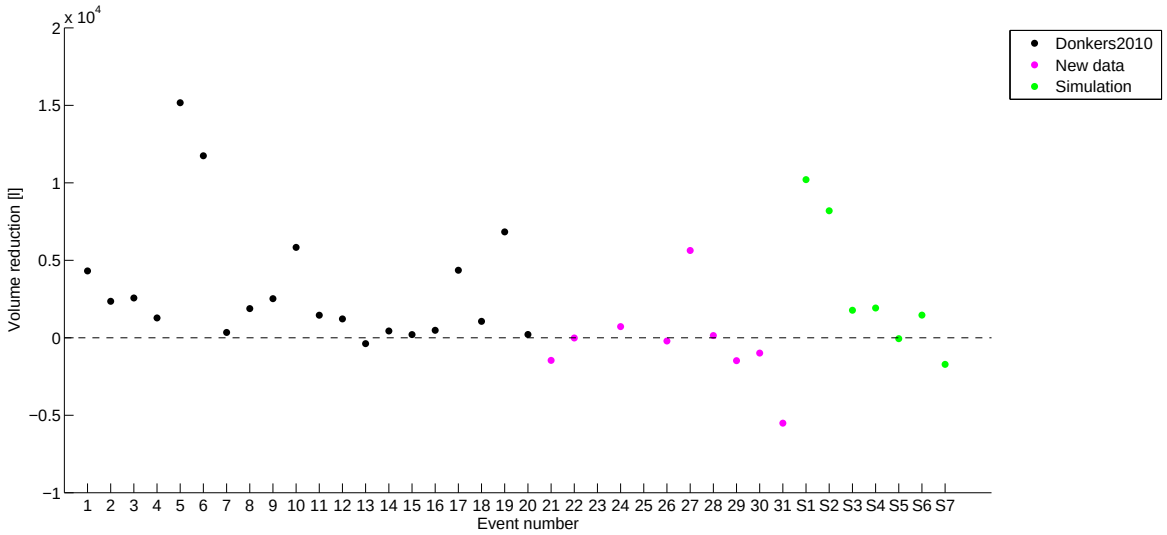

Figure 5.21: Absolute volume reduction

The new data shows a negative volume reduction for seven events. An outflow surplus can be caused by drainage of the aquifer beneath the swale. This is however unlikely since the head in the swale is always higher than the head in the aquifer beneath.

Another reason can be the direct precipitation on the swale. The outflow surplus of event 22 and 26 and simulation S5 is small (less than 250 l). Taken into account the estimations of the precipitation that directly falls on the swale, the volume reduction becomes positive. It is likely that this is the reason for the negative volume reduction for these events. Events 21,29,30 and 31 and simulation 7 show a much larger outflow surplus, more than 900 l. Estimations of precipitation that directly falls on the swale is not enough to make the volume reduction positive (still more than 500 l. outflow surplus). The direct precipitation can not be the cause of the outflow surplus.

The (large) uncertainties in the inflow measurements can also be a reason. This is likely for the events with a outflow surplus of more than 900 l. Figure 5.21 and 5.20 show that the volume reduction of event 29 and 31 are much more off than the other events with outflow surplus. The outflow surplus for event 31 is even more than 4800 l. Event 29 and 31 are therefor excluded from further analysis.

The values range between -50% and 100% for all events. The median value for the new data is 7% while for the old data this is 46%. Not taken into account all the negative volume reductions result in a median volume reduction of 41% for the new data.

Because there is an uncertainty in all measurements, it was decided to multiply the inflow and the outflow volume with factors 1.1,1.2,1.3,0.9,0.8 and 0.7. The error bands that are created this way, incorporate errors up to 30%.

Figures 5.22 and 5.23 shows the effects on the volume reductions of the events considered in the analysis. The effects of changing inflow or outflow are low for the higher volume reductions. As the volume reduction becomes smaller, the effects of errors in the measurements become larger.

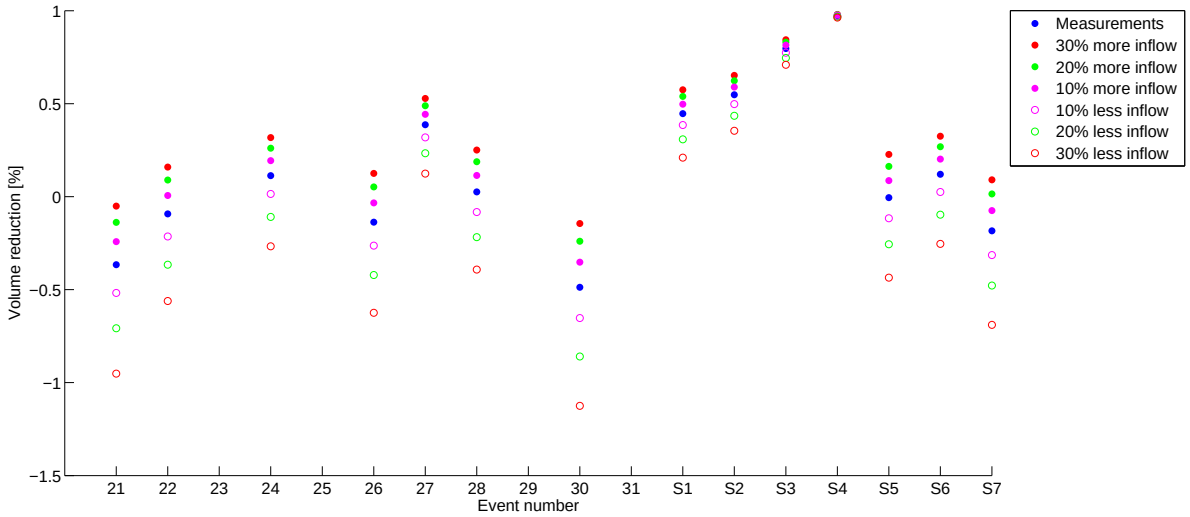

Figure 5.22: Effect of changing inflow on volume reduction

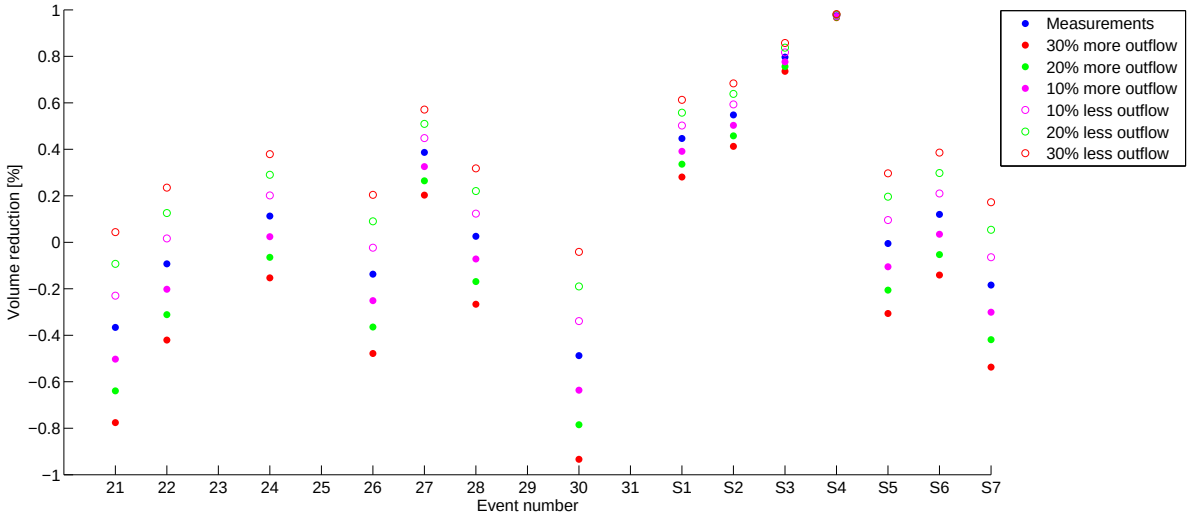

Figure 5.23: Effect of changing outflow on volume reduction

There is no clear relation found between the volume reduction and other parameters like total inflow volume, duration of the inflow, average inflow intensity or peak inflow. This was also concluded by (Donkers, 2010). The new data also does not show any relation between the initial groundwater level and the volume reduction, as shown in figure 5.24.

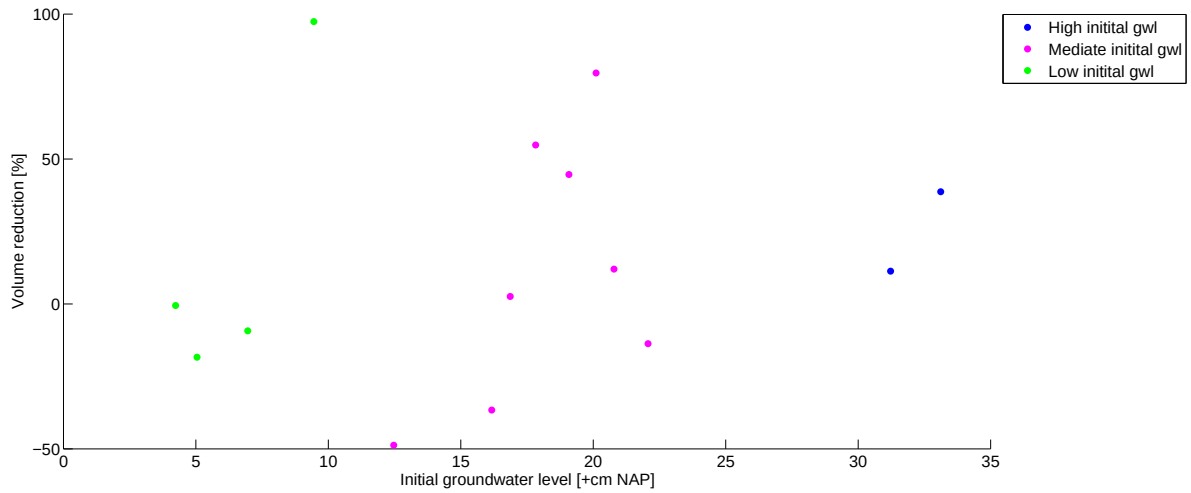

Figure 5.24: Relative volume reduction against initial groundwater level

Outflow delay

The outflow delay is shown in figure 5.25. Two events (24 and 27) show a negative outflow delay. This is probably caused by the high initial groundwater levels (31 and 33 cm NAP) of these events. These levels are close to the drainage level at +35 cm NAP. It is plausible that direct precipitation in these events caused groundwater levels to reach the drainage level before the inflow to the swale started. Event 16 and 17 (old data) have no outflow and thus no outflow delay.

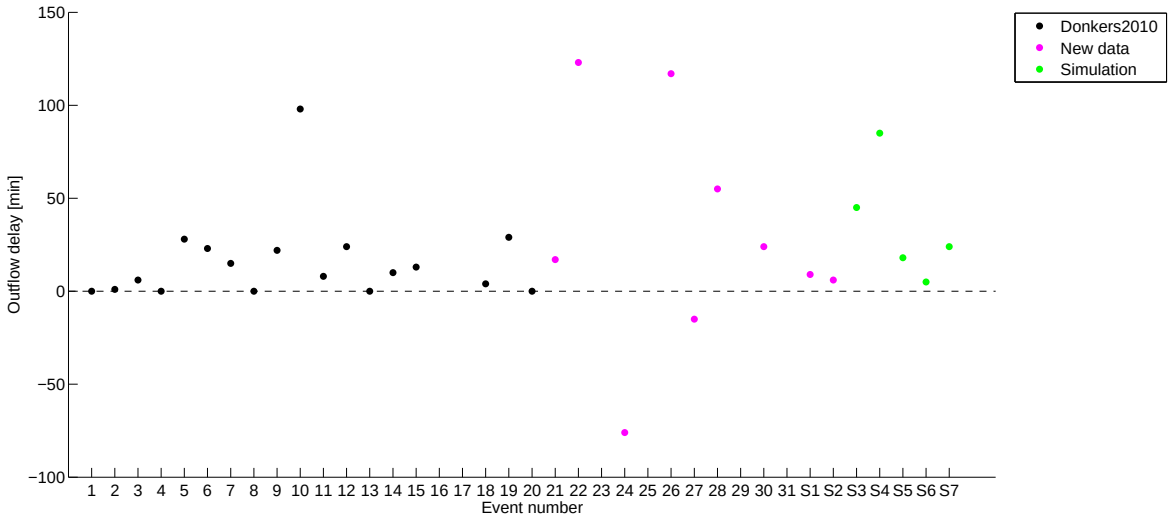

Figure 5.25: Outflow delay

The values for outflow delay range between -76 and 123 min for all events. For the old data the range is between 0 and 98 min. The outflow delay is between 0 min and 30 min in 75% of the events. It can be concluded that the outflow starts fairly quickly after the inflow has started. The median outflow delay for all data is 14 min. The new data has a median outflow delay of 21 min., while the outflow delay measured in the previous study is only 9 min. The new data thus shows a longer outflow delay than the old data.

The outflow delay of the events with a small outflow surplus (22,26 and simulation 5) do not show abnormal values. This is also the case for the other events with a negative volume reduction. There is no clear relation found between the outflow delay and other parameters like total inflow volume, average inflow intensity or peak inflow. This was also concluded by Donkers (2010).

Figure 5.26 shows the outflow delay against the average inflow. The initial groundwater levels are indicated with different colors and the numbers indicate the initial groundwater level in +cm NAP. It can be seen that for more or less the same average inflow intensity the events with a lower initial groundwater level have a larger outflow delay. Except for the events indicated with 16 and 17 as initial groundwater level. Also for events with similar initial groundwater levels the outflow delay decreases with increasing average inflow intensity. This was expected and the timing of the inflow and outflow measurements seem not to be off.

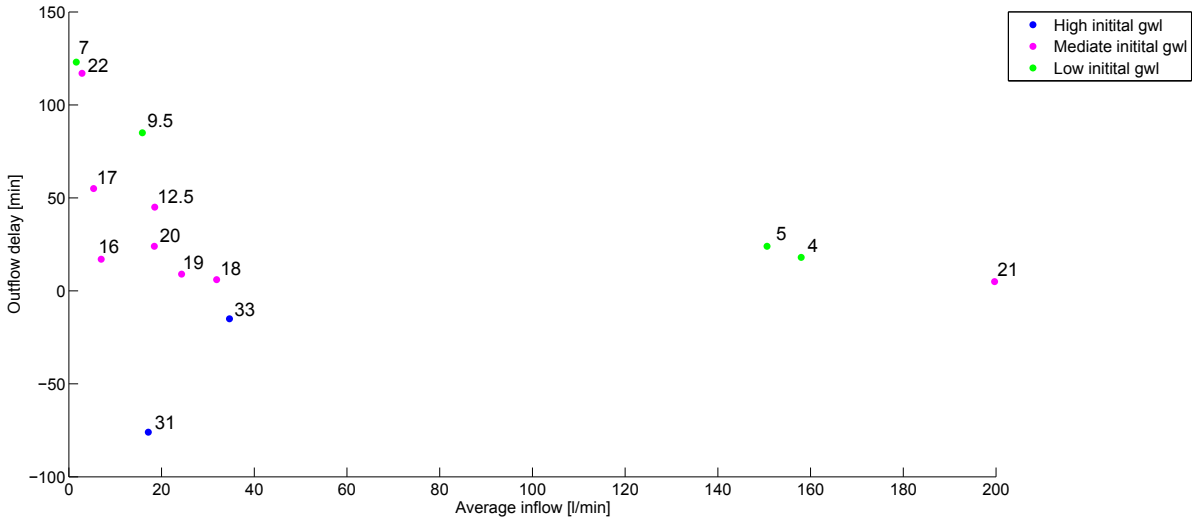

Figure 5.26: Outflow delay vs initial groundwater level

Peak reduction

The peak reduction as a percentage of the peak inflow is shown in figure 5.27.

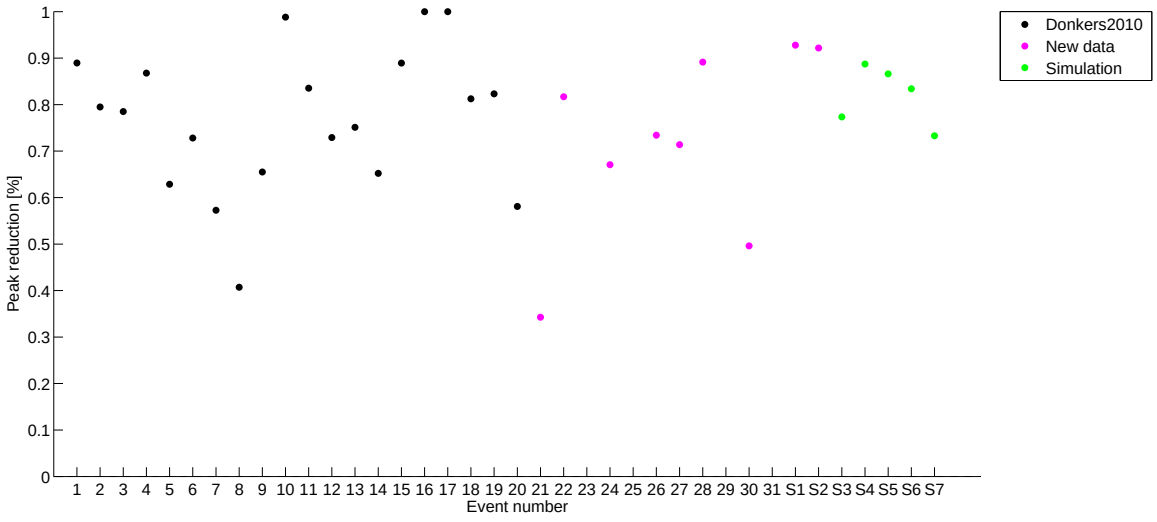

Figure 5.27: Peak reduction percentage

The peak reduction in general is large, in 85% of the events the peak outflow is only 60% or smaller of the peak inflow. The new data is consistent with the old data. The values range between 34% and 100%. The median values of the new and the old data is both 79%. Figure 5.28 shows the absolute peak reduction plotted against the peak inflow.

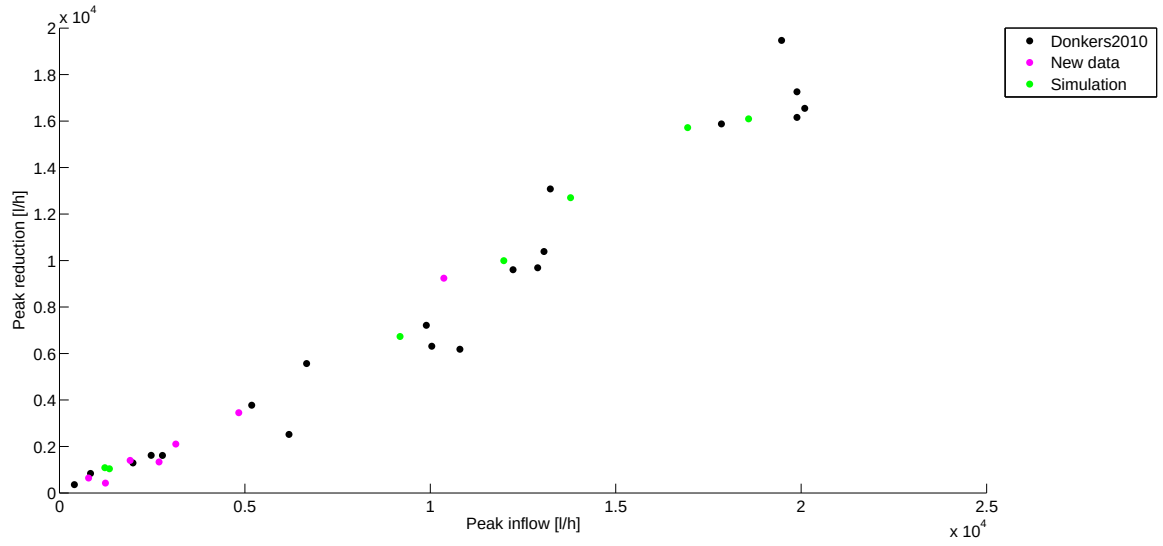

Figure 5.28: Absolute peak reduction against the peak inflow

A linear trend between the two parameters is present in the data. An increasing peak inflow causes a larger peak reduction. However this trend is gone when not the absolute peak reduction is considered but the relative peak reduction as was considered earlier in this section. This is shown in figure 5.29.

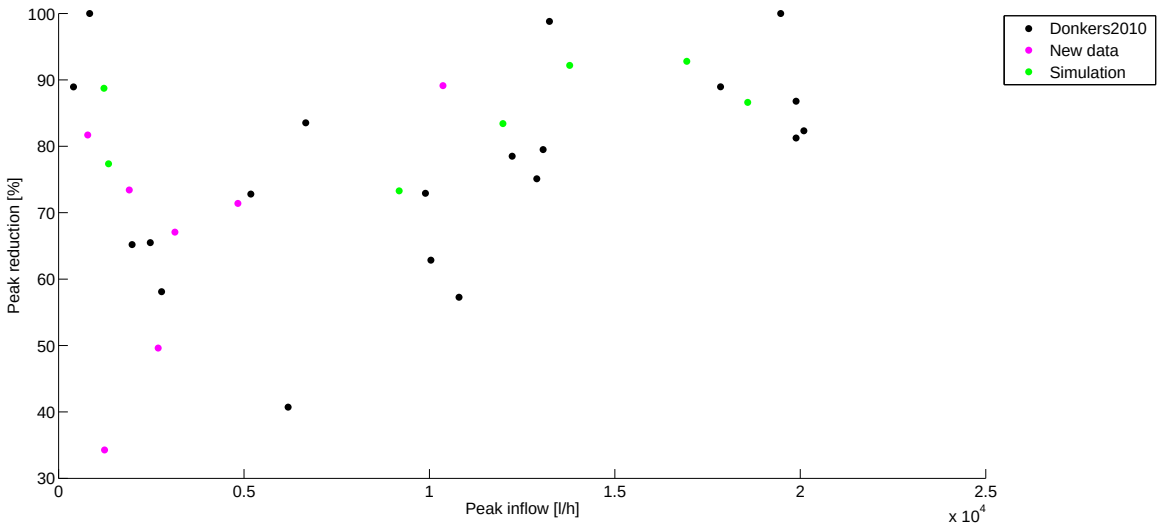

Figure 5.29: Relative peak reduction against the peak inflow

Peak delay

Figure 5.30 shows the peak delay for all considered events. Event 26 has a negative peak delay. This means the peak outflow was earlier than the peak inflow. This can be explained by the two inflow and outflow peaks present in the event, see figure 5.31. The second peak in the inflow causes a lower peak in the outflow.

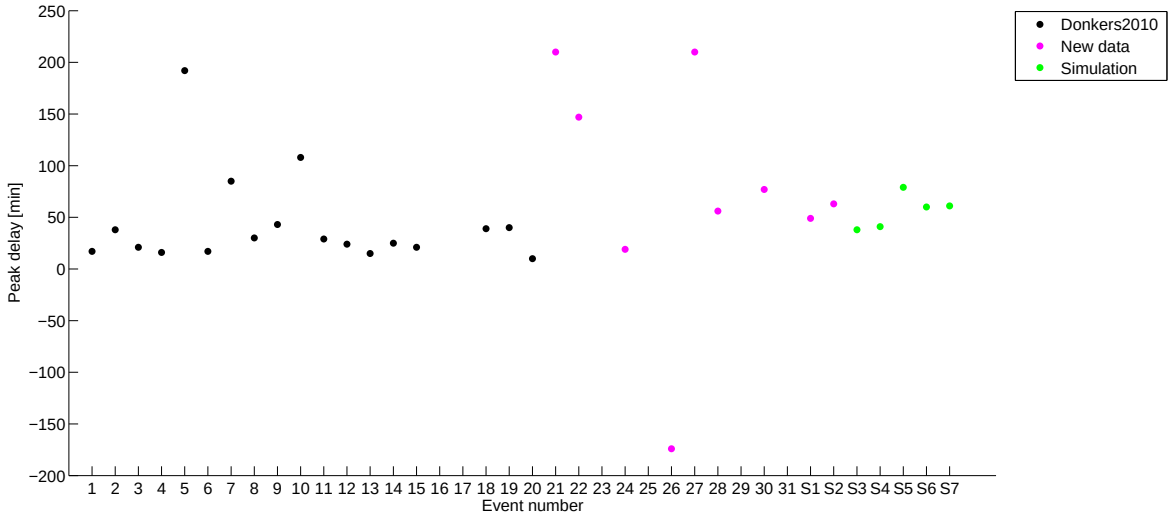

Figure 5.30: Peak delay

The peak delay for all the events is between -174 min and 210 min, figure 5.30. More than 60% of the events have a peak delay lower than 60 minutes. The median value for all events is 40 min. The median value for the old data is 27 min. and for the new data the median value is 61 min.

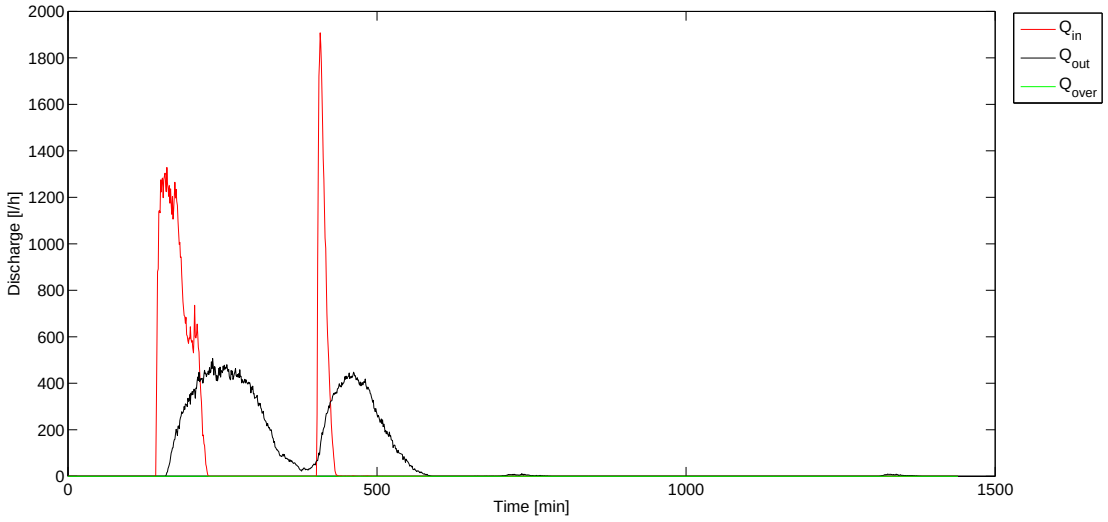

Figure 5.31: Event 26 inflow and outflow

Emptying time

The emptying time here is an indication of the time need to empty the top 40 cm of the swale (subsurface part). This is recorded by observation well P011E (sensor height 40 cm below surface level). The emptying time of the entire subsurface part of the swale is not determined because the swale is never completely dry, figure 5.14.

The emptying time is only determined for the new data since no groundwater level data is available for the old data. In total seven events had a groundwater level below the sensor height before the start of the next event. These events are considered in the determination of the emptying time, figure 5.32.

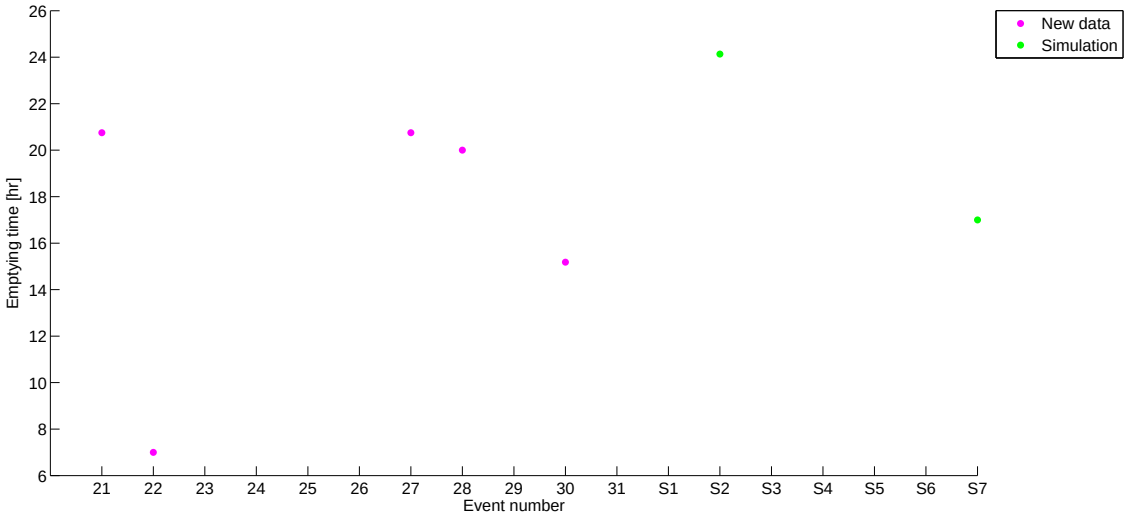

Figure 5.32: Emptying time

The emptying time varies between 7 hours and just over 24 hours. The median emptying time is 20 hours while the average is a little less than 18 hours.

Time to overflow
During the measuring period an overflow situation was recorded in 4 simulations (S1,S5,S6,S7), figure 5.33. No data on overflow situations was available for the old data. The time to overflow is the same as the time needed to completely fill the storage of the swale below and above surface level.

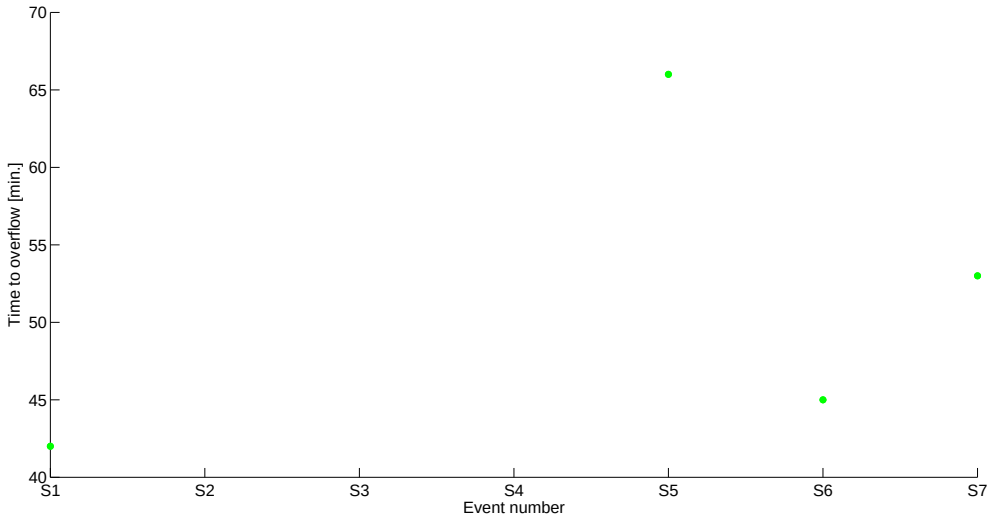

Figure 5.33: Time to overflow

When an overflow situation occurred, the minimum time to overflow was 42 minutes, while the maximum time was 66 minutes. This is quite quick. The average time to overflow is a little more than 51 minutes. The median value is 49 minutes.

Figure 5.34 shows the total inflow volume of the all the events of the new data. Simulations 1,5,6 and 7 all have a relative high inflow volume. Figure 5.35 shows that the average inflow intensity is high for simulations S5,S6 and S7.

This can be an explanation that an overflow situation occurred. The average inflow intensity of simulation 1 is not that high and the time to overflow is relative short compared to other simulations. A reason could be the relative high (mediate class) initial groundwater levels for simulation 1.

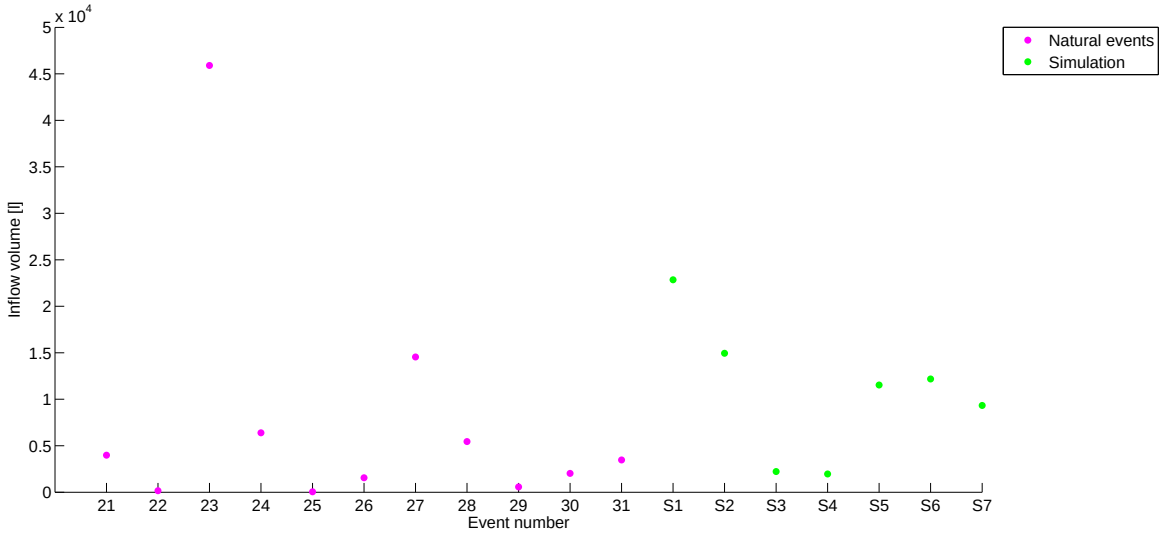

Figure 5.34: Total inflow volume

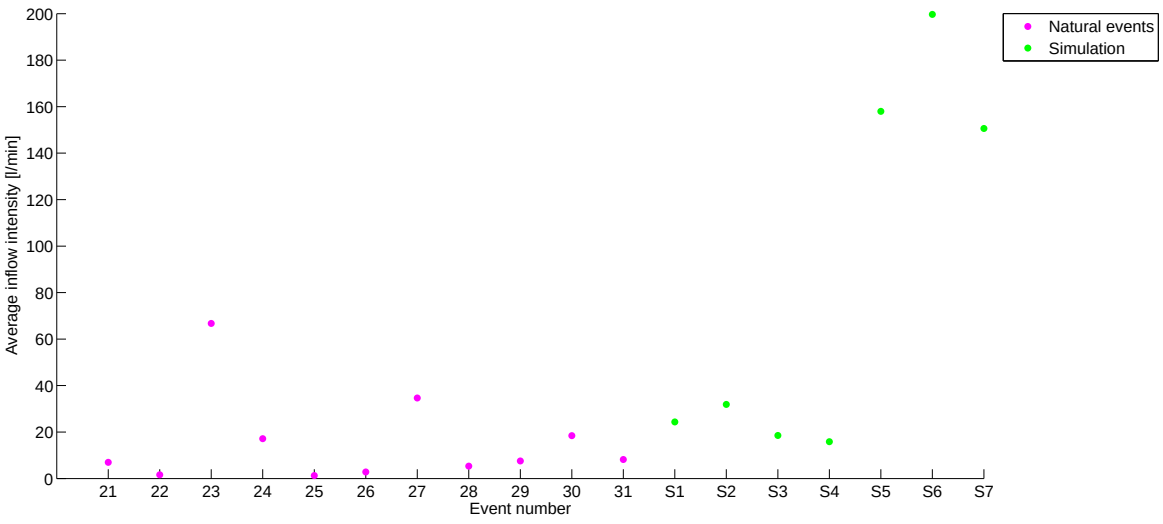

Figure 5.35: Average inflow intensity

Difference between head inflow and lateral inflow

In order to compare the performance of the same swale with head inflow and lateral inflow three simulation events were done twice. One time with an head inflow and once with lateral inflow as described in paragraph 4.3. This will be referred to as simulation couples. The results of the different simulations are shown in table 5.2.

Three of the simulated events did not have an overflow situation. These simulations are marked with 'no overflow' in table 5.2. The simulations with the case that the top 40 cm of the swale did not run dry before the next event happened are marked with 'not empty'. For one event the top 40 cm of the swale was dry the entire time and is marked with 'no water'. Also it needs to be remarked that the simulations of couple 1 are influenced by rainfall within a couple of hours after the simulation.

The inflow due to precipitation during the lateral inflow simulation has entered the swale at the head of the swale. The inflow in simulation 2 is not always lateral.

The outflow delay is different for the head inflow compared to the lateral inflow. The outflow delay is larger for the lateral inflow for two of the three simulation couples (2 and 3). The outflow delay for the lateral simulation is for couple 2 almost two times and for couple 3 almost five times larger than for the equivalent head inflow simulations. The larger outflow delay for the lateral inflow was expected since in case of head inflow the water is ponding at the inflow of the swale. The water (at the beginning) is not divided over the entire swale and the drainage level is reached earlier at the head of the swale. This causes the drain to discharge earlier than in case of lateral inflow. The outflow delay for the lateral inflow simulation is smaller than for the head inflow in couple 1. The difference (3 min) however is small and the outflow delay is considered to be equal.

The volume reduction of the lateral inflow simulation is larger than for the head inflow in two of the three simulation couples (1 and 2). The difference is 10% (couple 1) and 17% (couple 21). Nothing can be said about the third couple since the outflow is larger than the inflow. The difference in volume reduction was also expected for the same reason as for the outflow delay. With the lateral inflow there is more time before the discharge starts and the water has more time to infiltrate.

The peak reduction does not show to be sensitive to the inflow type. The results show no conclusive relation. The peak delay is larger for lateral inflow simulations for all couples. For couple 2 and 3 the difference however is small and the peak delay is assumed to be equal.

Table 5.2: Head vs lateral inflow simulations

Parameter	Head 1	Lateral 1	Head 2	Lateral 2	Head 3	Lateral 3
Simulation number	1	2	3	4	6	7
Inflow volume [l]	22848	14947	2224	1967	12182	9338
Duration inflow [min]	939	469	120	124	61	62
Average inflow [l/min]	24	32	19	16	200	151
Outflow volume [l]	12640	6754	452	51	10691	11042
Duration outflow [min]	1139	680	191	79	570	495
Average outflow [l/min]	11	10	2	1	19	22
Outflow delay [min]	9	6	45	85	5	24
Overflow volume [l]	6.5	no overflow	no overflow	no overflow	27.9	12.5
Duration overflow [min]	20				30	20
Average overflow [l/min]	0.3				0.9	0.6
Time to overflow [min]	42				45	53
Peak inflow [l\h]	16938	13783	1347	1223	11982	9185
Peak outflow [l\h]	1221	1078	305	138	1988	2453
Peak reduction [%]	93	92	77	89	83	73
Peak delay [min]	49	63	38	41	60	61
Volume reduction [%]	45	55	80	97	12	-18
Emptying time [min]	not empty	1448	not empty	no water	not empty	1020

Nothing can be said about the emptying time of the top 40 cm of the swale since there is no couple with two values for the emptying time. Also, for the time to overflow it is hard to make any conclusions. For couple 1 the lateral inflow did not have an overflow while the head inflow had but this could also be explained by the total inflow volume that was much smaller for the lateral inflow simulation. Overflow situations were present for both simulations of couple three and the time to overflow for the lateral inflow is larger. But one comparison is not enough to conclude the influence of lateral inflow on the time to overflow.

5.3. CONCLUSIONS

The results of this study show that the emptying of the swale is slow process. In the 5.5 weeks of the measuring period the swale did not become dry. At the end of the measuring period the swale was getting drier and drier but after about seven days of dry weather conditions the swale was not completely dry. The water level in the swale was about 10 cm above the swale bottom level. The groundwater levels outside the swale show a much smaller reaction to inflow than the groundwater levels inside the swale.

The volume reduction is defined as the difference between inflow and outflow divided by the inflow volume. For this study it was found that the volume reduction is highly variable and not dependent on inflow intensity or peak inflow. Taken into account only the events with a positive volume reduction, the median value is equal to 41%.

The outflow of the swale is active quite shortly after the inflow started. In 75% of the events the outflow delay is shorter than 30 minutes with a median value of 21 minutes. The outflow delay seems to increase with a deeper groundwater level.

The relative peak reduction of the swale considered is defined as the difference between peak inflow and peak outflow divided by the peak inflow. In 85% of the events more than 40% of the inflow peak is 'lost'. The median values of the data measured is about 79%. The peak reduction of the swale is large. The absolute peak reduction (difference peak inflow and peak outflow) shows a linear relation with the peak inflow. However the relative peak reduction does not show this trend.

The peak delay is defined as the time between the peak inflow and the peak outflow. The peak delay is shorter than one hour for more than 60% of the events. The median value for the peak delay is 61 minutes.

The emptying time of the swale only considered the first 40 cm below surface level since the entire swale never ran dry during the measuring period. For the analysis only seven events were considered since these events had a groundwater level below the sensor level before the next event started. The median emptying time is about 20 hours.

The time between the start of the inflow and the start of the overflow is defined as the time to overflow. Four events were considered in this analysis. The median time to overflow is 49 minutes. A combination of a high initial groundwater level, high average inflow intensity and high total inflow volume seem to be reasons for overflow situations.

In general it can be concluded that the performance of the swale has not decreased in 4 years. The volume reduction and peak reduction show similar results as 4 years ago. It can be concluded that the influence of possible occurred clogging of the top layer is small. The peak delay is even larger for this study. The median peak delay is more than two times bigger for this study. This is an improvement of the performance.

For this swale the lateral inflow seems to perform a little better or at least equal to the head inflow. Improvement in outflow delay and volume reduction is found. This increase in performance can be explained by the fact that less water is ponding at the head of the swale at the beginning of the event. The water is more divided over the swale and the drainage level will be reached not as fast as in case of a head inflow.

6

MODELING

This chapter concerns the modeling. The modeling exercise consists of two parts.This first model is referred to as the swale model and will simulate the performance of an individual infiltration swale. The second part is an urban drainage model and simulates the effects of infiltration swales on the surface water system of an urban catchment.

6.1. SWALE MODEL

The swale model consists of an 1D unsaturated zone module (MetaSwap) and a 3D groundwater module (Modflow). For practical reason it was decided to only model a cross-section. A 2D model has less computational time and runoff in lateral direction is hard to model. This makes the groundwater model 2 dimensional for the saturated zone and one dimensional for the unsaturated zone. The measurements described earlier in this report are being used to validate the model.

6.1.1. MODEL APPROACH

The model consists of a MetaSwap and Modflow module. The two models are linked to each other by means of the exchange of heads. .

The swale model will be used for two purposes. The first purpose is to model the effects of different initial moisture conditions at the start of an event. This will be achieved by applying different starting heads and corresponding soil moisture profile in the unsaturated zone at the start of the same event. The difference in drain discharge will tell something about effects of the initial conditions.

The second purpose is to create different inputs for the urban drainage model. Storms applied to the swale model and the outcome of these runs will be applied to urban drainage model. In this way different storm can be used in the urban drainage model, to study the performance on an urban catchment scale.

6.1.2. THEORY

Modlfow module
The Modflow model is a finite-difference ground-water model. The model is based on the equation 6.1 for the three-dimensional (3D) movement of water through soil. An extensive description of the model can be found in (Harbaugh, 2005).

$$\frac{\partial}{\partial x}\left(K_{xx}\frac{\partial h}{\partial x}\right)+\frac{\partial}{\partial y}\left(K_{yy}\frac{\partial h}{\partial y}\right)+\frac{\partial}{\partial z}\left(K_{zz}\frac{\partial h}{\partial z}\right)+W=S_s\frac{\partial h}{\partial t} \tag{6.1}$$

where:

K_{xx}, K_{yy} and K_{zz}	= hydraulic conductivity along the x, y, and z coordinate axes [L T^{-1}]
h	= head [L]
W	= volumetric flux per unit volume representing sources and/or sinks of water [T^{-1}]
S_s	= specific storage of the porous material [L^{-1}]
t	= time [T]

The analytical solution is of the form h(x,y,z,t). However an analytical solution is rare. The numerical method that is used by Modflow for solving the equation is the finite-difference model. Where the continuous system is discretized in points in space and time and the partial derivatives are replaced by terms calculated from the head difference between the points (Harbaugh, 2005).

The finite-difference equation is found by applying the continuity equation to each cell: the sum of all flows into and out of the cell is equal to change in storage of that cell. Equation 6.2 shows the mathematical representation (Harbaugh, 2005).

$$\sum Q_i = SS\frac{\Delta h}{\Delta t}\Delta V \tag{6.2}$$

where:

Q_i	= flow rate into a cell [L^3 T^{-1}]
SS	= specific storage [L^{-1}]
Δ h	= change of head [L]
Δ t	= time step [T]
Δ V	= volume of the cell [L^3]

SS is the finite difference specific storage term and is defined as the volume of water that can be injected per unit volume of aquifer material per unit change in head. The right-hand side of equation 6.2 is the change in storage (volume change) over a time step Δt given a change in head (Harbaugh, 2005).

The finite difference approximation of the continuity equation for cell i,j,k is given in equation 6.3 (Harbaugh, 2005).

$$\begin{aligned} &CR_{i,j-1/2,k}(h_{i,j-1,k}-h_{i,j,k})+CR_{i,j+1/2,k}(h_{i,j+1,k}-h_{i,j,k})\\ &+CC_{i-1/2,j,k}(h_{i-1,j,k}-h_{i,j,k})+CC_{i+1/2,j,k}(h_{i+1,j,k}-h_{i,j,k})\\ &+CV_{i,j,k-1/2}(h_{i,j,k-1}-h_{i,j,k})+CV_{i,j,k+1/2}(h_{i,j,k+1}-h_{i,j,k})\\ &+P_{i,j,k}h_{i,j,k}+Q_{i,j,k}=SS_{i,j,k}(\Delta r_j\Delta c_i\Delta v_k)\frac{\Delta h_{i,j,k}}{\Delta t} \end{aligned} \tag{6.3}$$

where:

CR,CC and CV	= hydraulic conductance for row, column and vertical direction [L^2 T^{-1}]
h	= head [L]
P	= head dependent external inflow [L^2 T^{-1}]
Q	= head independent external inflow [L^3 T^{-1}]
$\Delta r_j \Delta c_i \Delta v_k$	= volume of a cell [L^3]
$\Delta h/\Delta t$	= approximation for head derivative [L T^{-1}]

Superscript i,j,k are the row, column and layer index resp. The $-1/2$ and $+1/2$ superscripts indicate the region between the nodes and is not the value half-way between the nodes. The hydraulic conductance is defined as the product of the hydraulic conductivity and the cross-sectional area of flow divided by distance between two nodes. The external inflow into a cell is divided into a head dependent inflow and head independent inflow. An example of head dependent inflow is infiltration from a river. Head independent inflow is for example recharge from a well.

The head derivative is approximated by means of the backward-difference approach as shown in equation 6.4. This approach is numerically stable and errors introduced diminish in time (Harbaugh, 2005).

$$\frac{\Delta h_{i,j,k}}{\Delta t} \cong \frac{h^m_{i,j,k} - h^{m-1}_{i,j,k}}{t^m - t^{m-1}} \tag{6.4}$$

where:
h = head [L]
t = time [T]

The superscript indicate the moment in time and thus t^{m-1} is preceding t^m.

MetaSwap module
The MetaSwap model is coupled with the Modflow unit by means of h-link. Heads are used as shared state variable that alternately is updated by model A (MetaSwap) and model B (Modflow).

The unsaturated flow in MetaSwap is assumed to be within parallel vertical columns. The horizontal flows are therefore assumed to be in the saturated zone (Van Walsum *et al.*, 2012). For the unsaturated zone the model is based on steady-state solutions to the Richards' equation. The unsteady flow of the Richards' equation is replaced by two ordinary partial differential equations. The first is for the variations in the vertical column and the other is used for variation in time by using the water balance. This results in a quasi steady state model.

The steady state flow equation for an one dimensional situation with root water extraction is shown in equation 6.5 (Van Walsum *et al.*, 2012):

$$\frac{d}{dz}\left(K(\phi)\left(\frac{d\phi}{dz}+1\right)\right) - \tau(\phi,z) = 0, \qquad 0 \geq z \geq h \tag{6.5}$$

where:
z = elevation, taken positively upwards [L]
h = groundwater elevation [L]
ϕ = pressure head [L]
$K(\phi)$ = hydraulic conductivity as function of pressure head [L T^{-1}]
$\tau(\phi,z)$ = depth- and head-dependent extraction term for root water uptake [$L^3 L^{-3} T^{-1}$]

Solutions of equation 6.5 for different combinations of groundwater levels, flux density at the soil surface and root water uptake are stored in a database of steady state profiles. Dynamics are simulated by the transition between two steady state profiles. A water balance for one time step is formulated and the (only) steady state profile satisfies the water balance determines a profile for the water content (Van Walsum *et al.*, 2012).

Evaporation/transpiration
Evapotranspiration are divided into four terms (Van Walsum *et al.*, 2012):

1. crop transpiration
2. canopy interception evaporation
3. soil evaporation
4. ponding evaporation

The approach is given by equation 6.6 (Van Walsum *et al.*, 2012):

$$T_p + E_{s,p} = (E_{s,p} + K_{ew})ET_0 \tag{6.6}$$

where:

T_p = potential crop transpiration [L T^{-1}]
$E_{s,p}$ = potential soil evaporation [L T^{-1}]
K_{ew} = basal crop coefficient [-]
K_{cb} = evaporation coefficient of a wet bare soil, partly shielded by vegetation [-]
ET_0 = reference crop evaporation [L T^{-1}]

The reference evaporation is calculated with the simplified Makkink equation.

Ponding
Water stored on the soil surface are schematized into micro and macro storage. The micro storage are small depressions in the soil surface and do not run dry after inundation. Macro storage contains water that can flow freely over the soil surface. Macro storages run dry after inundation. The infiltration rate is limited to a infiltration capacity.

6.1.3. MODEL LAYOUT

The model layout is shown in figure 6.1.

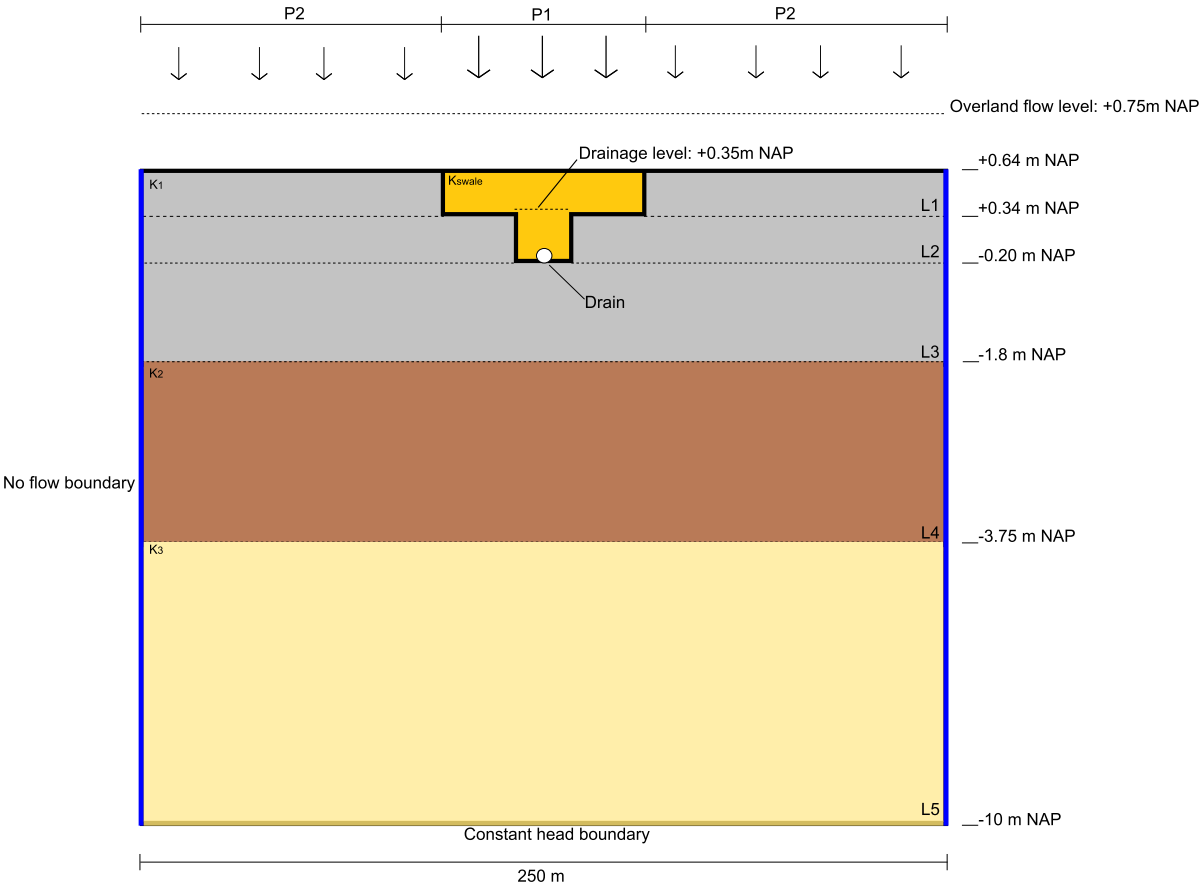

Figure 6.1: Infiltration swale model layout

The cellsize of the model is 0.5x0.5m. Model parameters are defined by validating the model results with the measurements. This is done with a trial and error method.

Swale
The swale dimensions in the model are based on the Castellumknoop swale and has a width of 2.5 m. The vertical part of the T-shape is 50 cm wide (real swale 45 cm). The surface level is set at +0.64 m NAP. This value is based on the average surface level at the observation wells in the swale. The chosen surface level is equal to the surface level at observation well P011C.

Boundary conditions
The sides of the model consists of no flow boundaries. The bottom boundary condition is a constant head boundary. The head in this layer is equal -0.13 m NAP. The constant head value was found based on measurements of heads in the aquifer near the swale.

Soil types
The model consists of 5 model layers. The first two layers are applied to create the T-shape of the swale. The native soil consists of three different soil types. The soil profile is shown in table 6.1. An isotropic soil profile is assumed. The values for the permeability are found by trial and error.

Table 6.1: Soil profile model

Layer	Soil type	K [m/d]
Swale		
L1 and L2	coarse sand	43.2
Native soil		
L1,L2 and L3	silt	0.05 (L1,L2) and 0.15 (L3)
L4	loamy sand	3.5
L5	unknown	4.32

The soil type of the aquifer in the fifth layer is unknown and the permeability is found by trial and error.

Precipitation, swale inflow and evaporation
The swale inflow is modeled by means of extra precipitation on the cell that represent the swale. The swale inflow is divided by the area of the swale to get a flux in mm/day. The sum of this flux and the precipitation (P2) yields the precipitation on the swale (P1). The precipitation (P2) only is also applied to the cells outside the swale. The precipitation data is radar data with a temporal resolution of 5 minutes.

Evaporation values are daily values for De Bilt acquired from the KNMI database. The values are based on the Makkink equation.

Drain
The drain is located at the bottom of the swale, at -0.20m NAP. The drainage level is set at +0.35m NAP. This is consistent with the situation at the Castellumknoop swale. The drain conductance is found by means of trial and error and is equal to 2.5 m^2/d. The equivalent drain resistance would than be around 0.15 days.

Overland flow
The overland flow level is set at +0.75 m NAP. This is consistent with the overflow level of the Castellumknoop swale. A resistance of the overland flow is set at 0.10 days based on expert judgment.

MetaSwap parameters
The MetaSwap parameters are summarized in table 6.2.

The landuse types used by MetaSwap are predefined and give the factors for actual evaporation calculations. The soil fysical units include the database of steady-state profiles that is used by MetaSwap. Soil Fyscial Unit (SFU) 23 that was used for the swale belongs to the sandy soils (coarse sand). For the surrounding soils SFU 23 was chosen which is a silty soil. The characteristics are shown in table 6.3.

[1] Full description can be in Wösten *et al.* (2012)

Table 6.2: MetaSwap parameters

Parameter	Value
Rootzone depth	50 cm
Landuse type	grass
Soil Fysical Unit [1]	
-swale	36
-surroundings	23
Ponding depth	500 m.

Table 6.3: Main characteristics Soil Fysical Units

Characteristic	Value
Unit 23	
vertical resistance	2.4 days
transmissivity	8,932 cm^2/d.
Unit 36	
vertical resistance	0.8 days
transmissivity	24,131 cm^2/d.

The ponding depth is set at a large value in order to let Modflow (Overland flow package, OLF) simulate the overflow of the swale.

6.1.4. INITIAL SOIL MOISTURE CONDITIONS

The initial soil moisture conditions that are studied are shown in table 6.4. The levels are indications of the starting heads and can differ a little.

Table 6.4: Initial moisture conditions

Classification	Head [+ m NAP]
High	0.20
Average	0.00
Low	-0.20
Deep	-0.40

The initial conditions were created by running the model for 3 months with precipitation data. The heads at every time step were stored. These heads were then changed (to create the initial moisture conditions of table 6.4) and used as fixed heads in the next run in order to get the corresponding moisture profile in the unsaturated zone. The end values of heads and soil moisture conditions are used as starting values for the runs to study the effects of the initial conditions.

Design storm Bui08 is used as input for all scenarios. Figure 6.2 (Rioned, 2012) shows the design storm. The storm has 5 min time interval and the duration is 60 min. The total volume of the event is 19.8 mm and the return period is equal to 2 years.

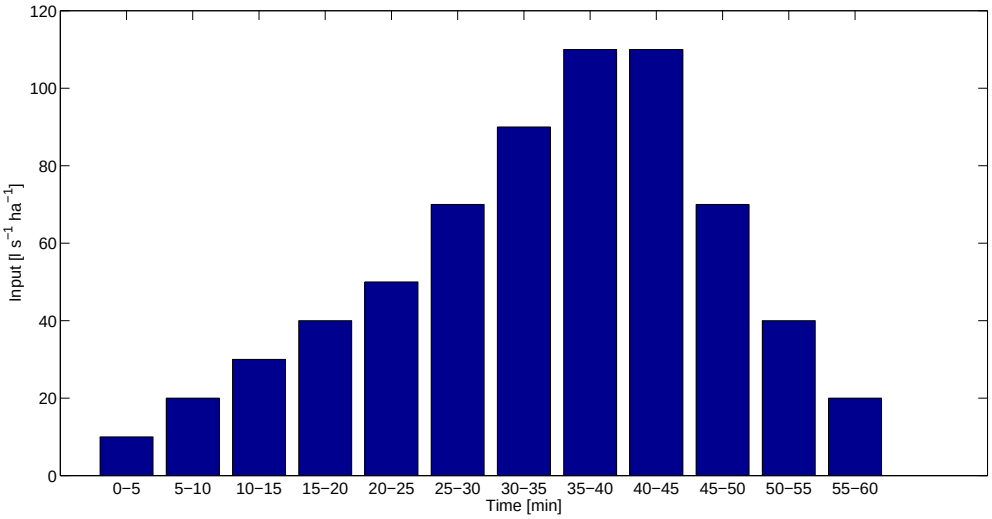

Figure 6.2: Design storm Bui08, T= 2 year

6.2. URBAN DRAINAGE MODEL

The urban drainage model is based on an existing Infoworks model for Schepenbuurt, a neighborhood in the city of Utrecht. The model is one dimensional pipe network model.

6.2.1. MODEL APPROACH

The model is used to model the effects of infiltration swales on the surface water system that the sewer is connected to.

The approach is shown in figure 6.3. Storms used as input for the swale model will be used for the urban drainage model as well. The reference situation does not contain any swales. The only input is the predefined storm. The contributing area of the manholes are all 0.2 ha., the size of the contributing area of the Castellumknoop swale.

The model then is adapted with a certain percentage of infiltration swales. The manholes that are not connected to a swale will have the same input as in the reference situation. The other manholes will be disconnected from their contributing area and a pump is connected. The pump discharge will represent the outflow of the swale (drain discharge and overflow) determined with the swale model.

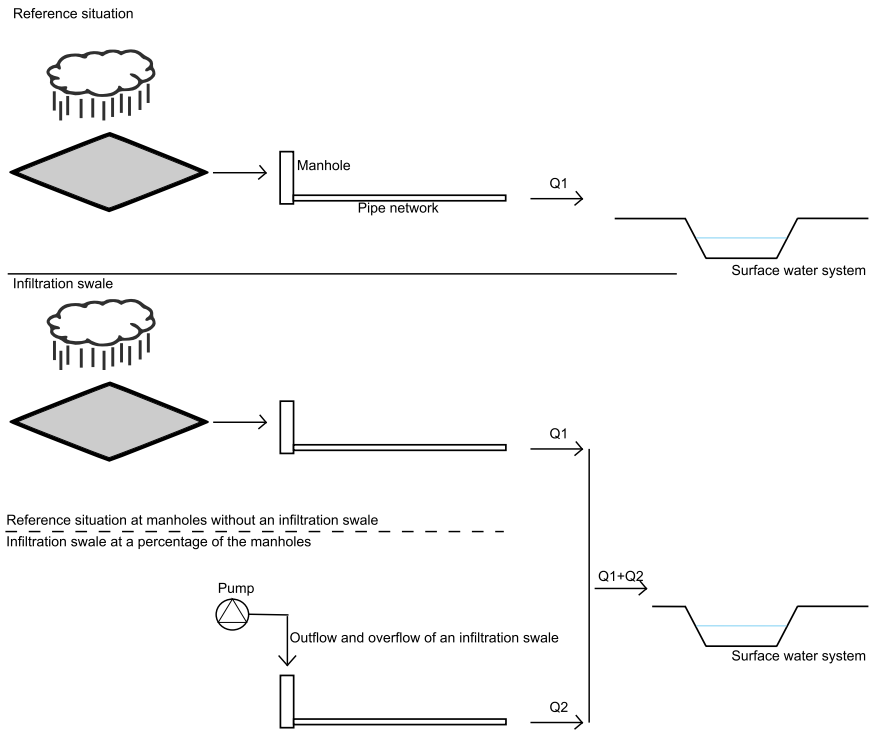

Figure 6.3: Urban drainage model schematization

The effect on the surface water system is related to the flow on the surface water that is calculated with the model in the reference situation and the model runs with infiltration swale included. Different scenarios will be considered.

6.2.2. MODEL CHARACTERISTICS

The model layout is shown in figure 6.4. The numbers in the figure indicate the manhole numbers.

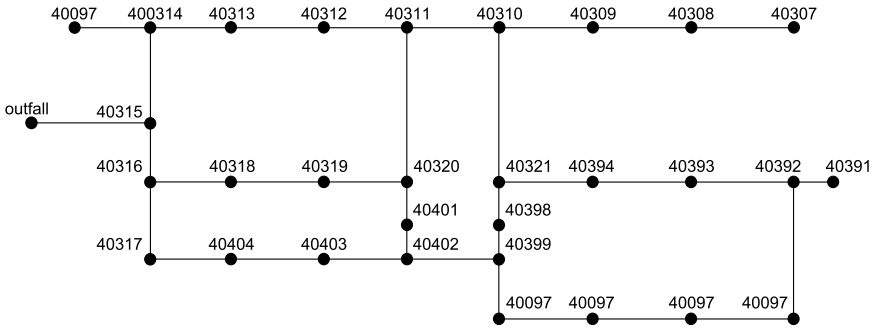

Figure 6.4: Urban drainage model layout

The model characteristics are summarized in table 6.5.

Table 6.5: Urban drainage model characteristics

Characteristic	
Total subcatchments	30
Total contributing area	5.8 ha.
open imperverious, flat	77%
roof, inclined	23%
Total pipe length	1838m
Pipe diameters	160-600 mm
Number of manholes	35
Number of outfalls	1
Timestep	5 min.

The model has a free outfall and this outfall is located on the lowest point of the system.

6.2.3. SCENARIOS

The scenarios used for the urban drainage model are shown in table 6.6

Table 6.6: Urban drainage model scenarios

Scenario	Area percentage swales [%]	Contributing area [ha.] Swale	Other
Reference situation			
Reference	0	0	5.8
Infiltration swales present			
$Swale_{10}$	10.3	0.6	5.2
$Swale_{20}$	20.7	1.2	4.6
$Swale_{30}$	31.0	1.8	4
$Swale_{40}$	41.4	2.4	3.4
$Swale_{50}$	51.7	3	2.8
$Swale_{60}$	62.1	3.6	2.2
$Swale_{70}$	72.4	4.2	1.6
$Swale_{80}$	82.8	4.8	1
$Swale_{90}$	93.1	5.4	0.4
$Swale_{100}$	100.0	5.8	0

Design storm Bui08 is used as input for all scenarios. An description of the design storm can be found in the previous section.

7

MODELING RESULTS AND ANALYSIS

The data presented in this chapter was obtained by the modeling exercise. The MetaSwap-Modflow model was validated with the measurements described in chapter 5.

7.1. SENSITIVITY ANALYSIS AND BEST FIT

A sensitivity analysis of the swale model was done. This was done to identify the most influential parameters. These parameters were changed and the model results were fitted to the observations by trial and error.

7.1.1. SENSITIVITY ANALYSIS

The parameters that were used in the sensitivity analysis are:

1. hydraulic conductivity of swale and native soil of all layers
2. drain conductance
3. storage coefficients of all layers

The analysis is based on visual effects on the output time series of the heads. A reference run was done to compare the influence of changing a parameter. The parameters of the reference run and the changes in value for the sensitivity analysis are shown in table 7.1.

Table 7.1: Reference model run

Parameter	Reference run	Value in sensitivity analysis
Kswale	43.2 m/day	4.32 m/day
K1		
-L1	0.06 m/day	0.6 m/day
-L2	0.06 m/day	0.6 m/day
-L3	0.06 m/day	0.6 m/day
K2	3.50 m/day	0.35 m/day
K3	43.2 m/day	4.32 m/day
Drain conductance	2.5 m2/day	5 m2/day
Storage coefficient		
-L2	0.001	0.1
-L3	0.001	0.1
-L4	0.001	0.1
-L5	0.001	0.1

All the events and simulations were used as input during the sensitivity analysis. Although not all measurements were trusted fully, it was decided to include them in the input because leaving them out would have caused the swale to recover while in reality the swale was influenced by inflow.

The focus in this analysis is on the heads in the swale since these are the most important factors for the drain and overflow discharge.

Hydraulic conductivity of the swale soil (Kswale)
The swale soil is permeable. To study the influence it was decided to make the conductivity of the swale soil ten times smaller, at 4.32 m/day. The effect on the heads in the swale is shown in figure 7.1.

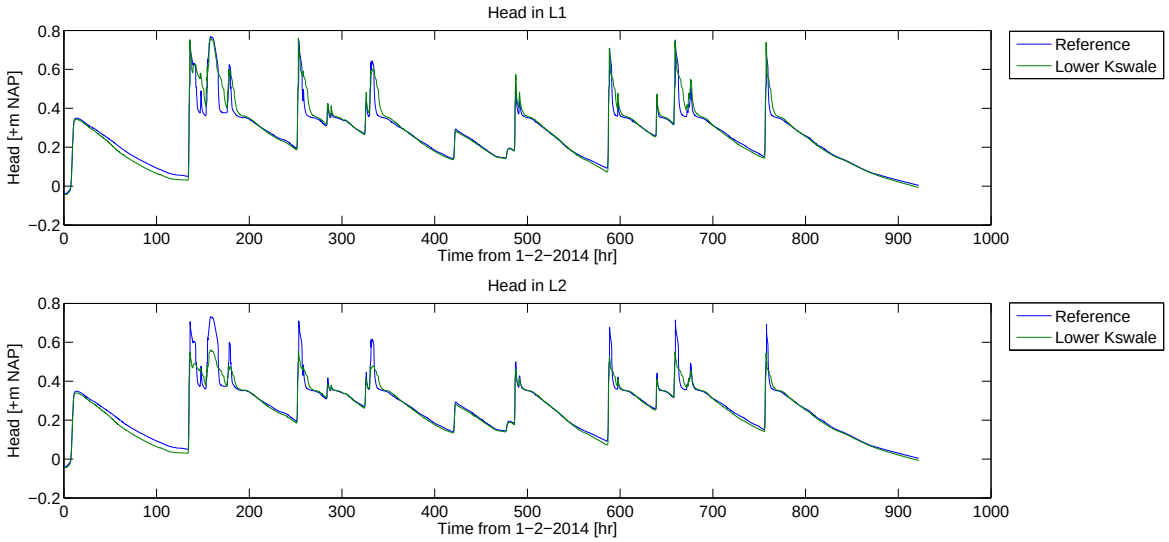

Figure 7.1: Hydraulic conductivity of swale soil -heads L1 and L2

The effects of a less permeable swale soil can be noticed especially when heads are dropping above the drainage level (+0.35 m NAP). This process is slower than in the reference situation. The effect is however small. Also the peaks of the head in layer 2 seem to be lower than in the reference situation.

Hydraulic conductivity of the first native soil layer (K1)
The first native soil layer (L1,L2,L3 in the model) is not very permeable. Therefor it was decided to make the hydraulic conductivity ten times higher, at 0.6 m/day. The result is shown in figure 7.2.

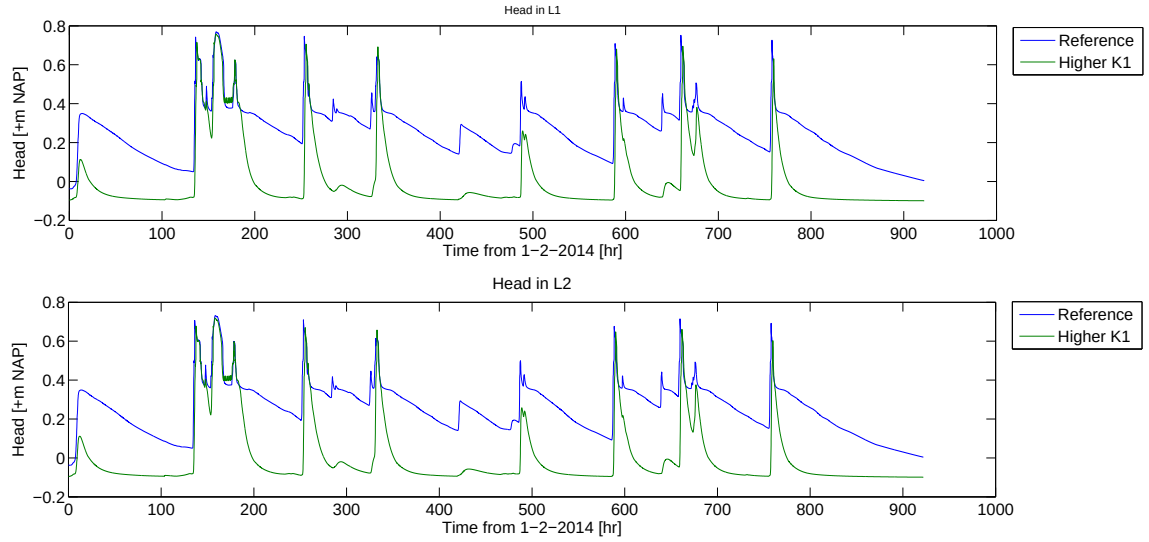

Figure 7.2: Hydraulic conductivity of first native soil layer -heads L1 and L2

The figure shows that the effect is quite large. The biggest difference is that the heads drop much faster and the heads drop also to a much lower level. The peaks are not influenced much by the change.

Hydraulic conductivity of the second native soil layer (K2)
The second native soil layer (L4) is not as permeable as the swale but more permeable than the first native soil layer. The hydraulic conductivity was lowered ten times to 0.35 m/day. The result is shown in figure 7.3.

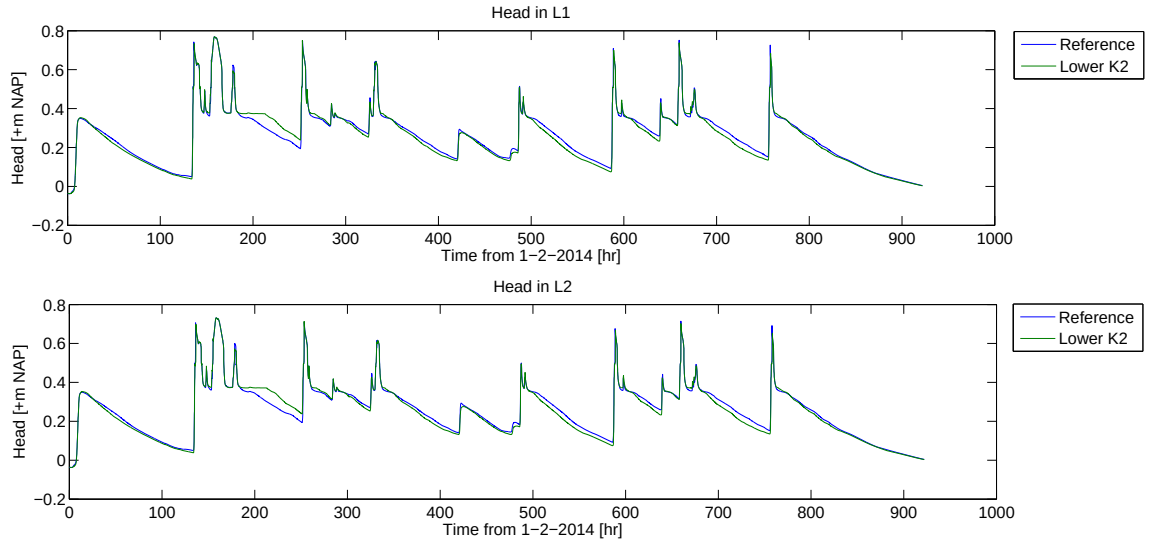

Figure 7.3: Hydraulic conductivity of second native soil layer -heads L1 and L2

The figure shows that the effect on the peaks is small. Heads that are below the drainage level differ a bit more but the difference is not as significant as the changes in hydraulic conductivity of the first native soil layer.

Hydraulic conductivity of the aquifer (K3)
The effects of the hydraulic conductivity of the aquifers is very low as shown in figure 7.4. In this figure the hydraulic conductivity is ten times smaller than in the reference run.

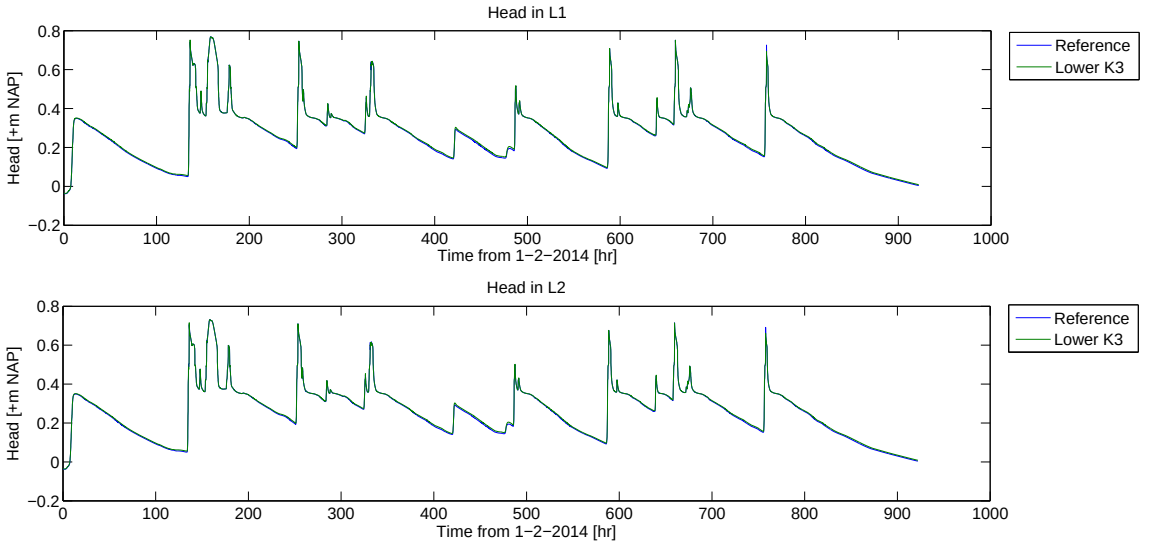

Figure 7.4: Hydraulic conductivity of the aquifer -heads L1 and L2

Drain conductance

The drain conductance is inverse proportional to drain resistance. The effects of drain resistance twice as low as in the reference situation is shown in figure 7.5.

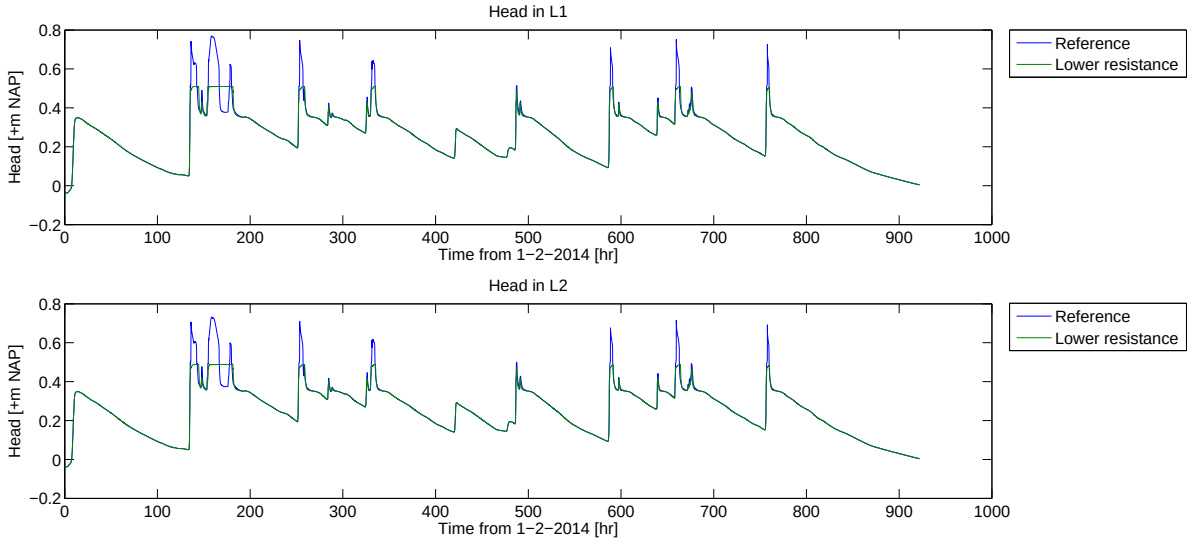

Figure 7.5: Drain conductance -heads L1 and L2

As can be seen in the figure lowering the drain resistance shows an aberrant behavior. Peaks are cut off above +0.50 NAP. No physical explanation can be found to explain this behavior.

Storage coefficient of layer L2,L3,L4,L5

The storage coefficient of the lower four layers is multiplied with 100 to 0.1. The results of a changing storage coefficient is shown in figure 7.6.

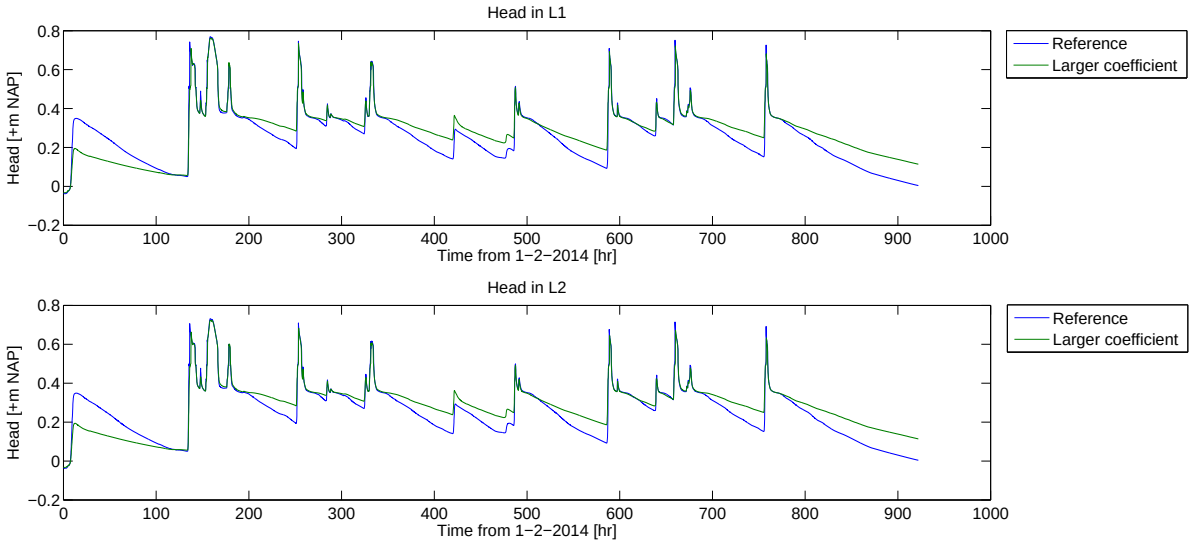

Figure 7.6: Storage coefficient of the L2,L3,L4,L5 -heads L1 and L2

The figure shows that the dynamics of emptying the swale is much slower than in the reference situation.

7.1.2. BEST FIT

Based on the sensitivity analysis the most sensitive parameters were the hydraulic conductivity of the first native soil layers and the storage coefficients. The best fit was found by trial and error and the parameter set is shown in table 7.2.

Table 7.2: Best fit parameter set

Parameter	Value
Kswale	43.2 m/day
K1	
-L1	0.05 m/day
-L2	0.05 m/day
-L3	0.15 m/day
K2	3.50 m/day
K3	4.32 m/day
Drain conductance	2.5 m2/day
Storage coefficient	
L1	0.15
L2	0.1
L3	0.1
L4	0.1
L5	0.1

The heads in the swale calculated with the model compared to the measured values is shown in figure 7.7. The horizontal parts in the observed groundwater levels of P011E (upper part of figure 7.7) is the sensor level. Only water level above this level are measured.

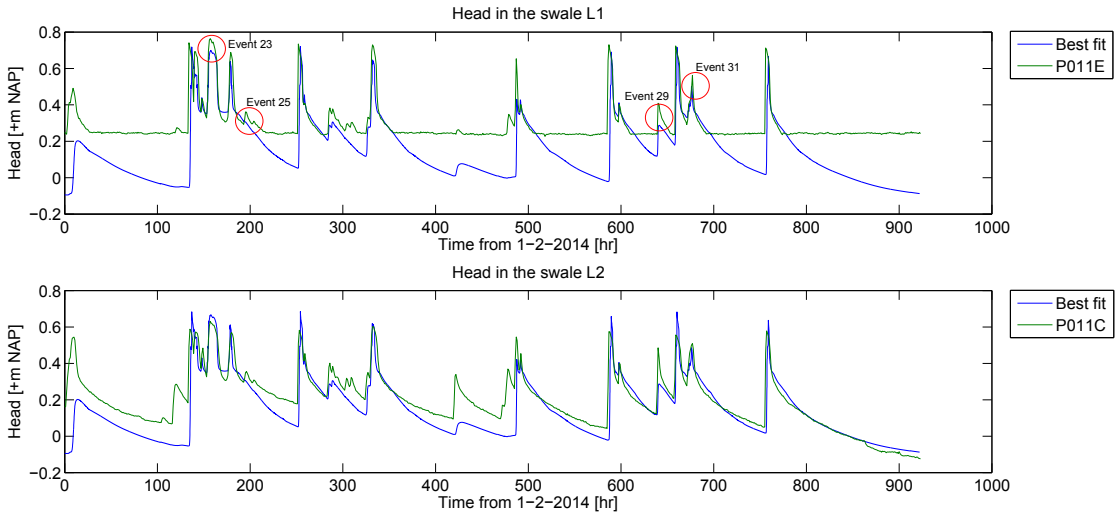

Figure 7.7: Best fit - heads in L1 and L2

The red circles in figure 7.7 indicate the events with large uncertainties that were measured, as described in chapter 5. The figure shows that the modeled values are reasonably well compared to the observed values.

Generally the process of emptying of the swale is modeled well, especially at the end of the measuring period. Also the peaks are modeled quite well at first sight.

Only when details are considered the model is not performing that well. Figure 7.8 shows a detail of two peaks. The response of the modeled heads is lagging behind with 1 hour or more. This is in almost all events the case. It also shows that the modeling of the peaks in detail is hard and in almost all the cases there is a difference in magnitude and timing of the peak. This makes it almost impossible to get the overflow of the swale right since it is highly depended on the heads (water levels) and the timing of the peaks.

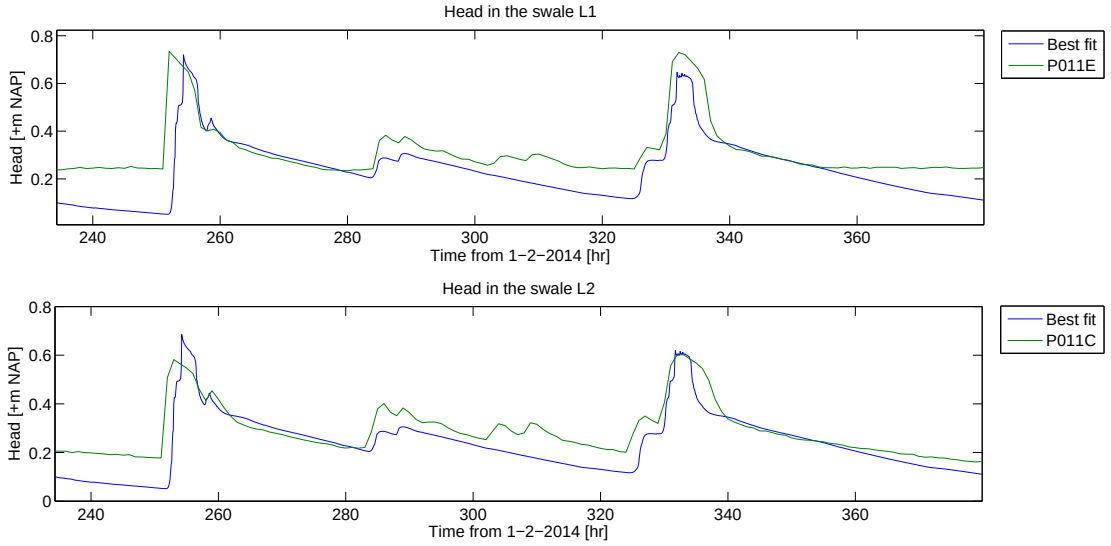

Figure 7.8: Best fit detail

Figure 7.9 shows the modeled and observed drain discharge and overflow. The same as for the heads in the swale layers counts for the drain discharges. The modeled overflow does not perform that well. Since the drain discharge and the overflow are very depended on the heads it was expected that the results would be like this.

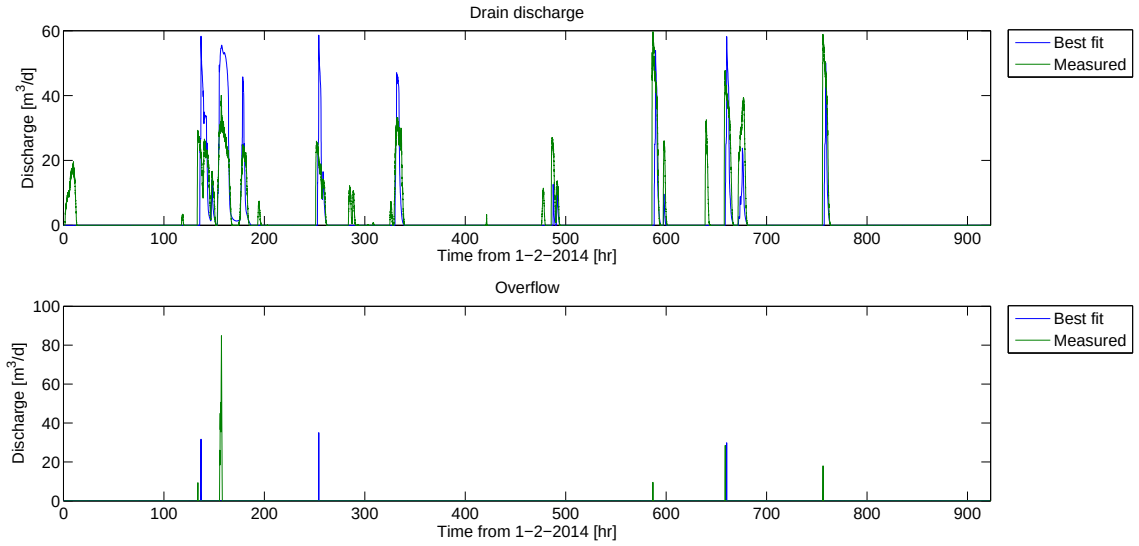

Figure 7.9: Best fit drain discharge and overflow

The cumulative overflow and drain volume is shown in figure 7.10. The total drain discharge is about 70% of the observed drain discharge. Taken also into account the uncertainties in the observed drainage volume it is considered to be reasonably good. The modeled overflow is just 7% of the observed value.

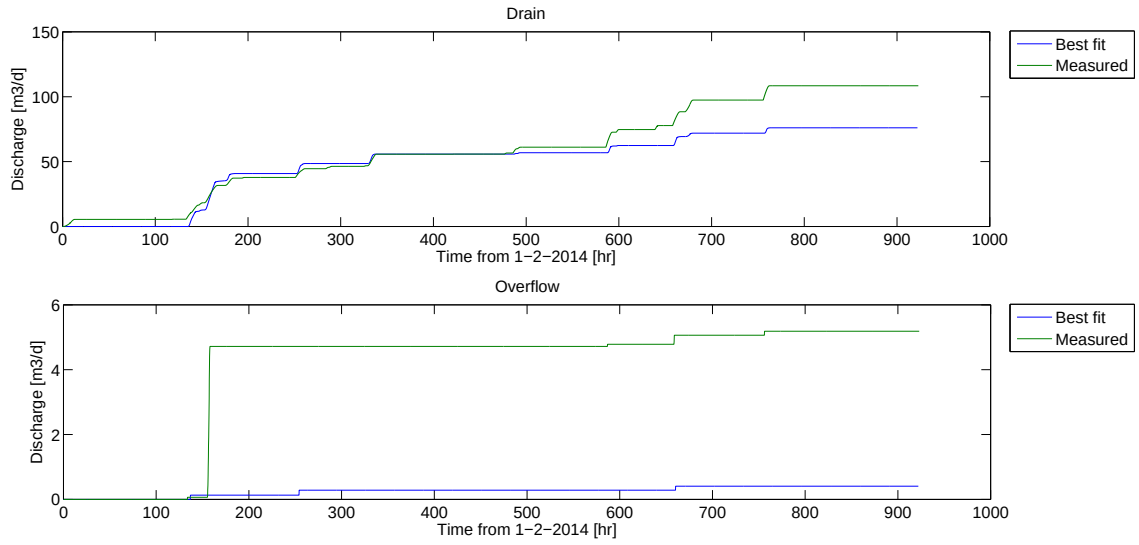

Figure 7.10: Best fit cumulative drain and overflow volume

7.2. RESULTS AND ANALYSIS

This section considers the results of the models runs used to determine the effects of the initial condition and the performance of infiltration swales on an urban catchment.

Because the swale model as described in the previous section was not able to get the overflow right it was decided to use a standard design storm with a short return period. The design storm Bui08 (return period of 2 years) is used. The output of the swale model is also used as input (pump discharge) of the urban drainage model.

7.2.1. SWALE MODEL

The swale model is used to study the effects of the initial soil moisture conditions. The model, the initial condition scenarios and the design storm are described in chapter 6.1.

Heads in the swale
Figure 7.11 and 7.12 show the modeled heads in the swale under different initial soil moisture conditions.

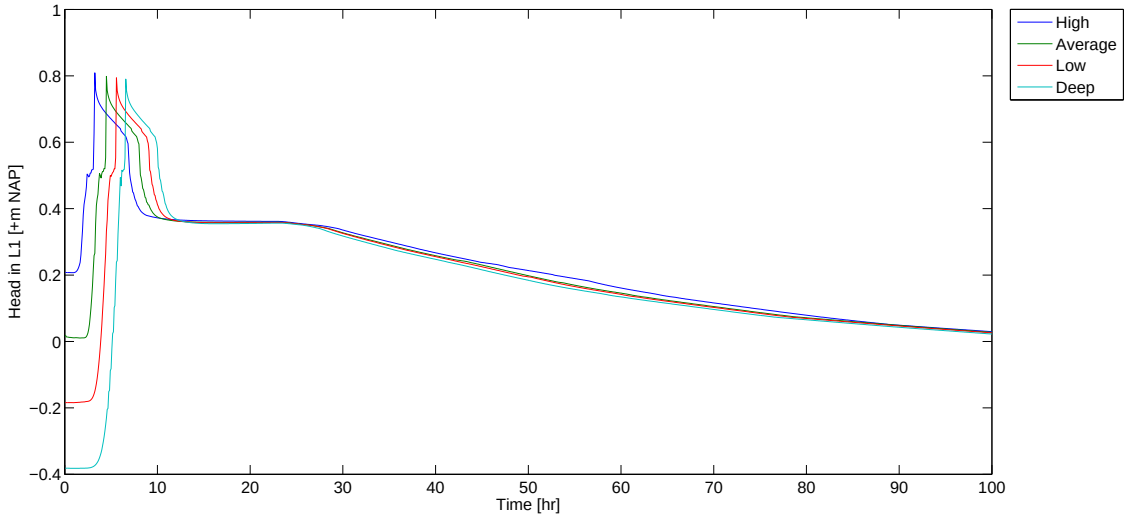

Figure 7.11: Swale model - Heads in the swale (L1) with different initial moisture conditions

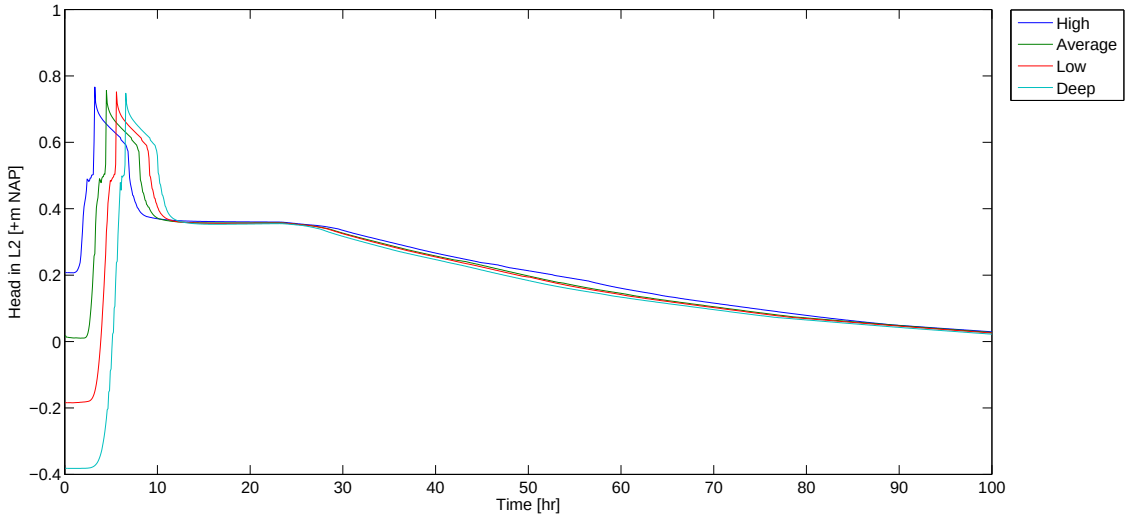

Figure 7.12: Swale model - Heads in the swale (L2) with different initial moisture conditions

The figure shows that the maximum level that is reached for all initial conditions is about the same. The difference in the maximum head between the high and deep initial condition is less than 2 cm. The small difference in storage in the vertical part of the T-shape of the swale can be an explanation. The maximum heads are lower for dryer initial conductions, which was expected since the extra storage of the deeper heads at the beginning of an event.

Drain discharge and cumulative volume

Figure 7.13 shows the model drain discharge output. Like with the heads there is not much difference between the initial conditions runs. The difference in peak heads between high and deep initial conditions is just 3 m^3/day. The difference in total drained volume for the high and the deep initial condition is 2 m^3.

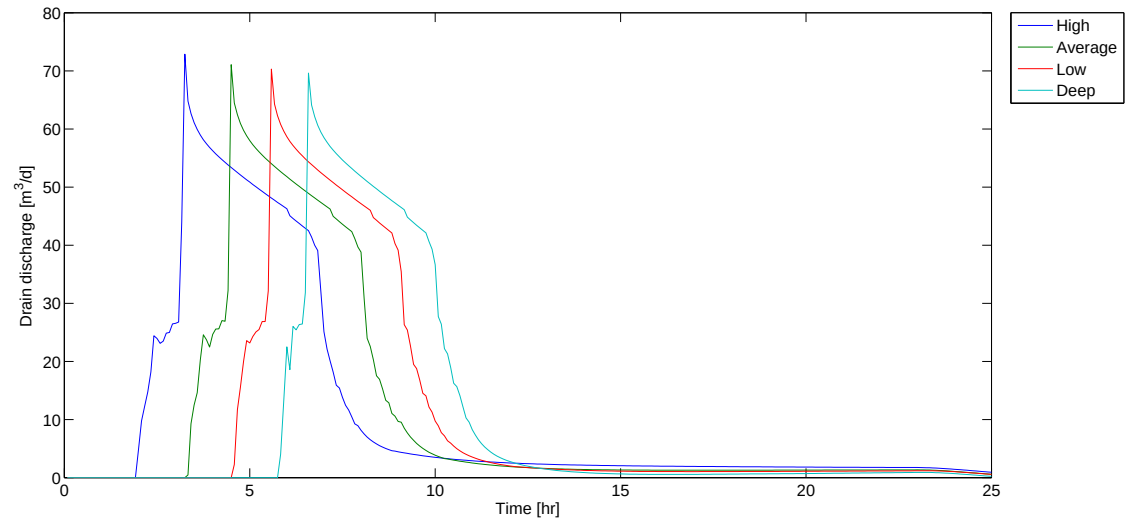

Figure 7.13: Swale model - Drain discharge

The model does show that the initial condition effects the timing of the peaks. The peak in case of the deep initial condition is more than 3 hours later than in case of the high initial condition.

The overflow modeled is shown in figure 7.14. The difference in overflow is larger and the maximum difference in peak overflow is about 330 m^3/day. The total overflow volume is 1.3 m^3 more in case of a high initial condition than with a deep initial condition.

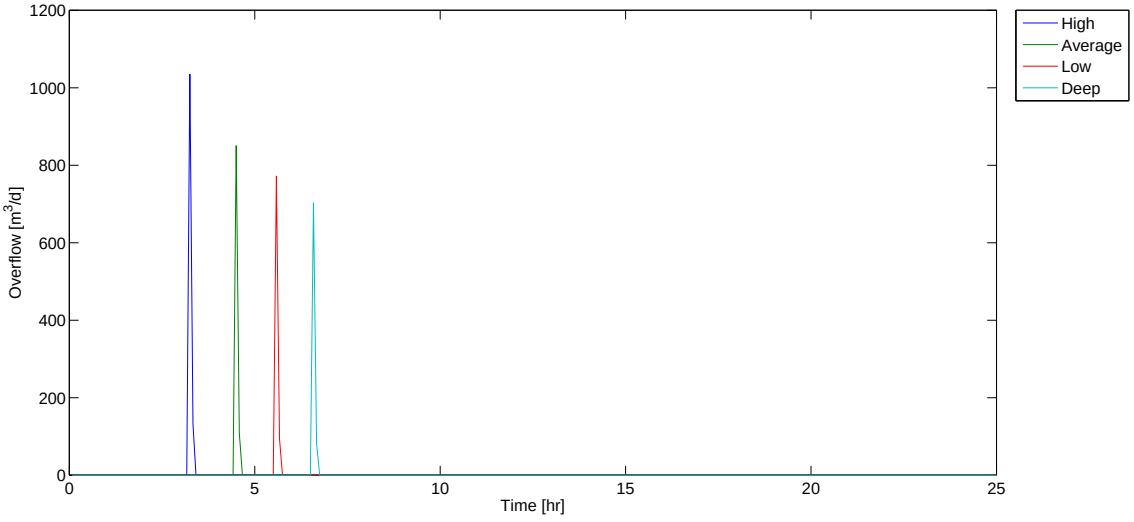

Figure 7.14: Swale model - Overflow

Figure 7.15 shows the cumulative volumes of the different runs. This volume includes the water discharged by the drain and the overflow. The cumulative volume of the input is also shown. The sudden change in slope of the outcome graphs can be explained by the relative large overflow.

As expected the lower initial conditions have a slightly better performance. The difference between the maximum and minimum initial condition on the volume reduction is about 5%.

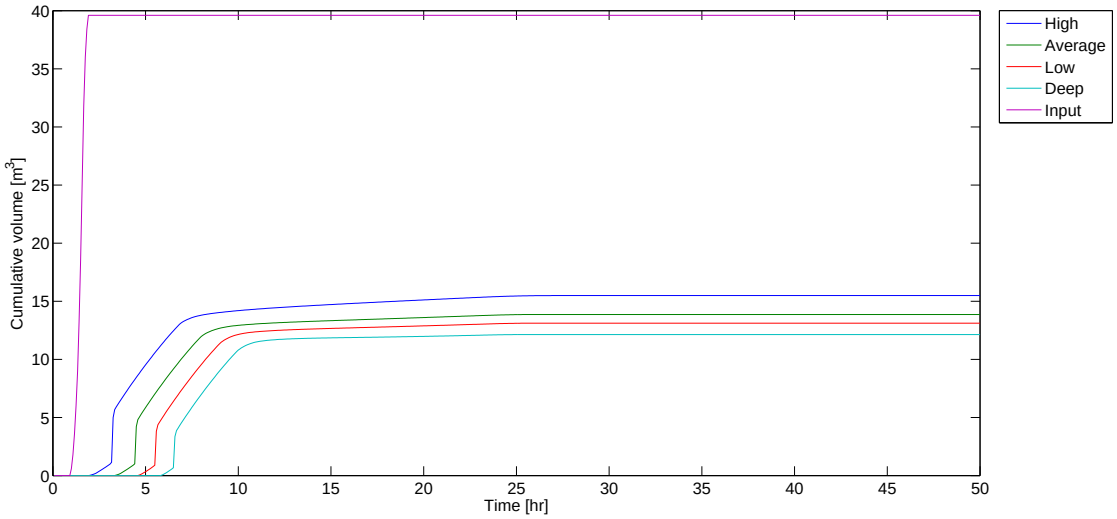

Figure 7.15: Swale model - Cumulative volume

The performance of the swale with different initial conditions is summarized in table 7.3.

Table 7.3: Swale performance under different initial conditions

Initial condition	Max. drain discharge [m^3/d]	Max. overflow [m^3/d]	Volume reduction [%]	Peak delay [min]
High	73	1035	61	100
Average	71	850	65	175
Low	70	772	67	240
Deep	70	703	69	300

7.2.2. URBAN DRAINAGE MODEL

The urban drainage model (Infoworks model) was used to model the effects of infiltration swales on an urban catchment scale. The model and scenarios are described in chapter 6.2.

Figure 7.16 shows the flow on the surface water water system that is modeled in all scenarios.

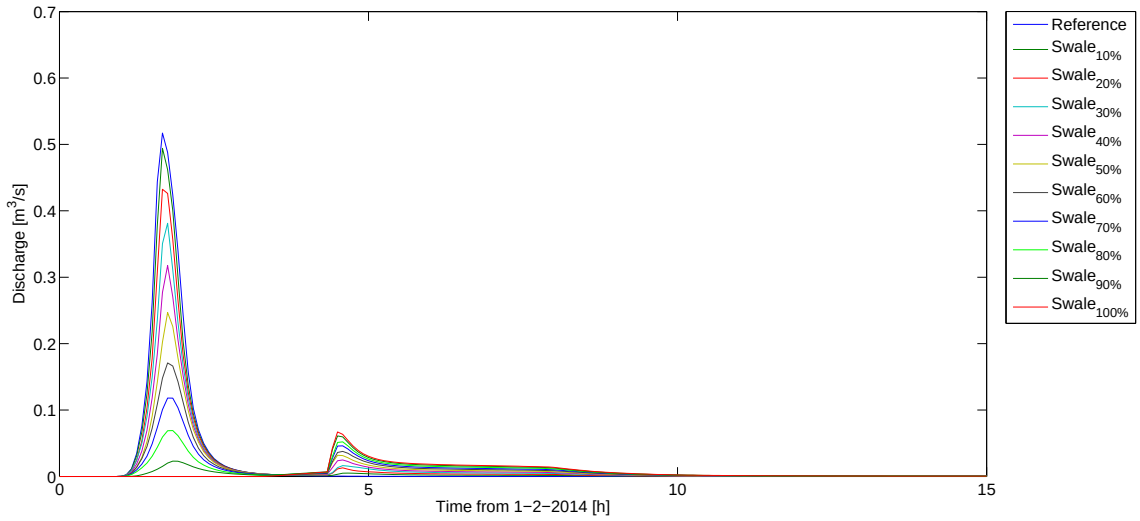

Figure 7.16: Urban drainage model - Flow onto the surface water system

Two distinctive parts can be seen in the figure. The first part is dominated by the areas without a swale and are characterized by (relative) high peaks and short time frame. The second part is dominated by the areas with a swale and the peak is flattened out and the duration of the flow is much longer. This was also expected based on the experience with a individual swale.

The timing of the peak does not change significantly with an increasing area percentage of swales. Only in case that swales are connected to 90% or 100% of the area the peak comes much later. These are the scenarios were the peak is located in the infiltration swale dominated part. In all other scenarios the peak can de dedicated to the precipitation on contributing areas. Figure 7.17 gives the peak reductions for all scenarios.

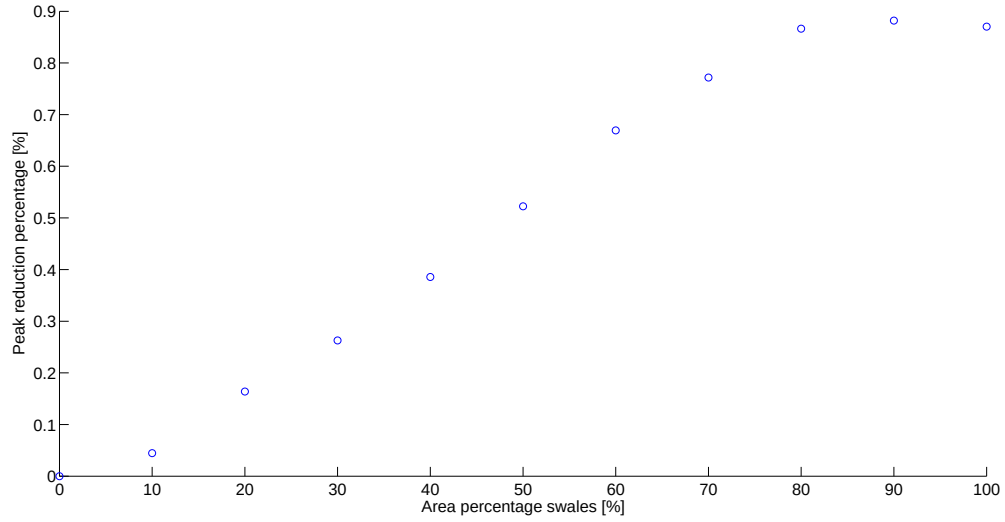

Figure 7.17: Urban drainage model - Peak reduction percentage

Figure 7.18 shows the cumulative volumes of the outfall. The reference scenarios has the largest outfall volume and the situation with only swales has the lowest volume, which was expected.

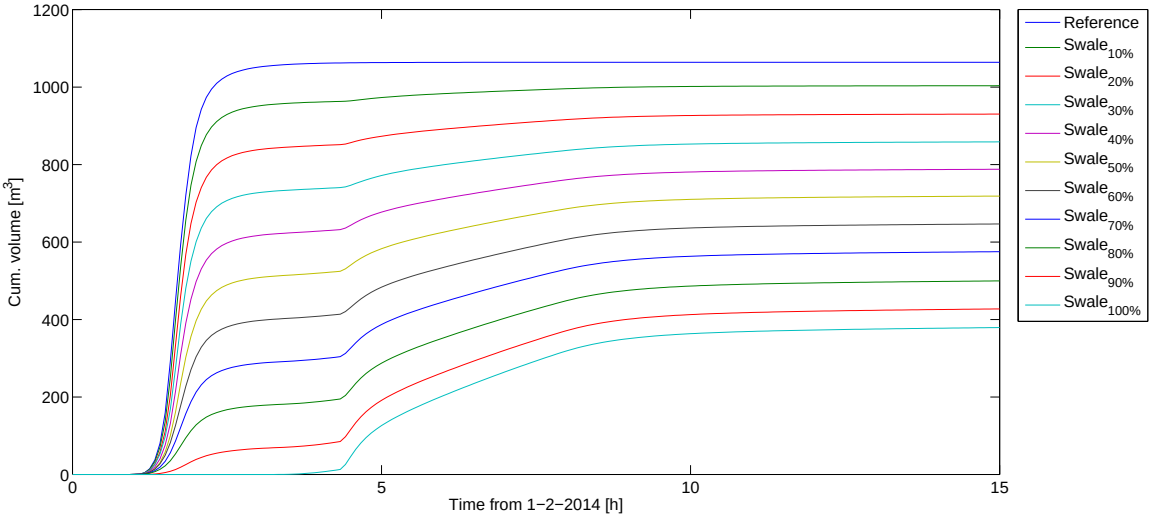

Figure 7.18: Urban drainage model - Cumulative volume

The modeled volume reduction is shown in figure 7.19. The percentages are in line with the volume reduction of an individual swale.

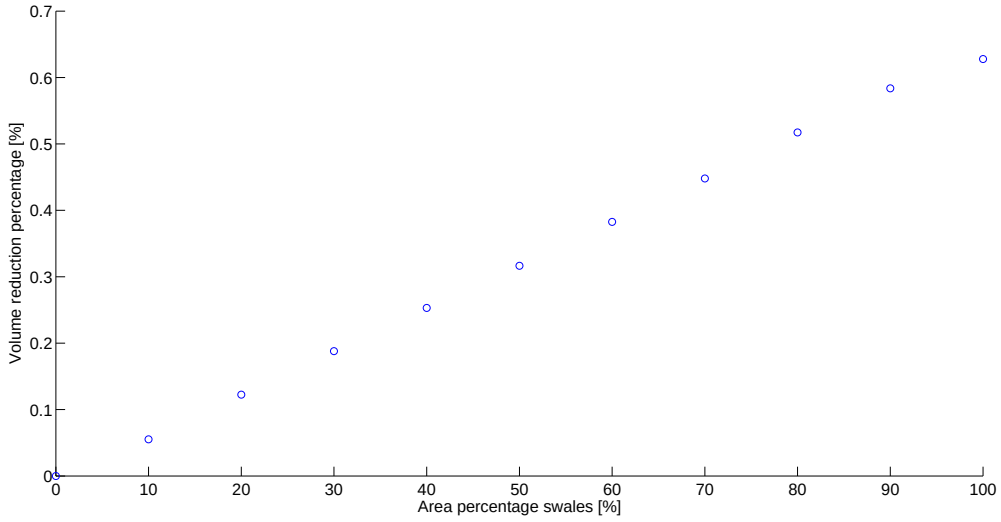

Figure 7.19: Urban drainage model - Volume reduction percentage

An overview of the maximum flood depths (thickness of water layer above surface level) and the total maximum flood volumes for each scenario is given in table 7.4.

Table 7.4: Urban drainage model - Flood depth and volume

Scenario	Flood depth [m]	Flood volume [m^3]
Reference	0.18	46
$Swale_{10}$	0.13	16
$Swale_{20}$	0.10	5
$Swale_{30}$	0	0
$Swale_{40}$	0	0
$Swale_{50}$	0	0
$Swale_{60}$	0	0
$Swale_{70}$	0	0
$Swale_{80}$	0	0
$Swale_{90}$	0	0
$Swale_{100}$	0	0

The maximum flood volumes are based on the extreme situation in the pipe network (at maximum flood depth). Flooding occurs three scenarios. The maximum flood event is the reference scenario, which was expected based on the analysis above. The table shows that an area percentage of 30% is enough to prevent flooding. The flood volume of the reference situation is about three times smaller for scenario $swale_{10}$ and about nine times smaller for for scenario $swale_{20}$.

7.3. CONCLUSIONS

The MetaSwap-Modflow model was used to determine the effects of changing initial soil moisture conditions. The model showed that the effects on the maximum head (water level) in the swale is small. Since the drain discharge is highly related to the heads in the swale also the peaks in the drain discharge are not very different.

Larger effects are noticed on the total drained volume and the outflow delay (time difference between start inflow and start drain discharge). The difference in volume reduction between a deep and high initial moisture conditions is about 10%. The peak delay and outflow delay have a difference larger than 3 hours between the deep and high initial moisture conditions.

The Infoworks model was used to determine the performance of infiltration swales on an urban catchment scale. The model showed that using infiltration swales in urban planning is beneficial. The total volume that discharges on the surface water and the peak discharge is lowered. The volume reduction is consistent with the performance of an individual swale. The peak reduction is between 4% (scenario $swale_{10}$) and 88% (scenario $swale_{90}$). The scenario with only swales performs a little less than the 90% scenario.

The model also showed that it is effective on flood control. The flooding that occurred in the reference scenario (no swales) was eliminated with an area percentage of infiltration swales of 30%.

8

CONCLUSIONS AND RECOMMENDATIONS

This chapter describes the conclusions that are drawn from the results of the measurements described in chapter 5 and the analysis of the output of the two models described in chapter 7. The conclusions will be based on the research questions described in chapter 2

8.1. MEASUREMENTS

The measurements that were done for this study contained (large) uncertainties due to shifts in the water level recordings used for inflow discharge calculations. The results of the outflow measurements (after confirmed shift) and the groundwater level recordings were within the limits of being acceptable.

The results of manual observations and an extra calibration test of the inflow pressure diver were inconclusive. Both showed that the pressure diver was recording water level that were too low. An upward shift of the data was necessary to correct the data. However the magnitude of this shift was different in both cases. Sufficient data was missing to see if the shift was constant in time or changed as well. Four events were excluded from the analysis because the results showed a large deviation from the other events, old (Donkers (2010)) and new data. The results that were included in the analysis could also contain large uncertainties but the results of these events did not show large abnormalities.

In total 34 events were considered. Seven inflow simulations, seven natural events and 20 events measured four years ago by Donkers(2010).

Quantitative performance under different weather conditions
The performance indicators were defined to answer the first research question of this study. The precipitation events in this study are considered to be low to medium intensity storms, according to KNMI classification. The maximum storm that was simulated had a return period of 6 months. This simulations showed that the swale is filled in less than 45 minutes. The storage of the swale is filled fairly quickly for this T=0.5 yr. storm. Since the storm is rather small and overflow of the system is expected to reduce the quantitative performance of the swale, it can be concluded that the swale is only effective for smaller storms. This is also found in literature.

The results of this study shows that the emptying of the subsurface part of the swale is slow process. In the 5.5 weeks of the measuring period the swale did not become dry. At the end of the measuring period the swale was getting drier and drier but after about seven days of dry weather conditions the subsurface retention part of the swale was not completely dry. The water level in the swale was about 10 cm above the swale bottom level. The groundwater levels outside the swale show a much smaller reaction to inflow than the groundwater levels inside the swale.

The volume reduction is defined as the difference between inflow and outflow divided by the inflow volume. For this study, it was found that the volume reduction is highly variable and not dependent on inflow intensity or peak inflow. Taken into account only the events with a positive volume reduction, the median value is equal to 41%. The median value for events measured for this study is 7%. This is around the value that

Donkers(2010) found (46%) four year ago. The volume reduction is consistent with the values found in literature (Davis 2008 and Abida 2006) and higher than the value found by Sabourin(2008). The data of this study does not show a relation between the initial groundwater level

The outflow of the swale is active quite shortly after the inflow started. In 75% of the events the outflow delay is shorter than 30 minutes with a median value of 21 minutes. The median value measured by Donkers(2010) is even shorter, 14 minutes. In general it can be concluded that the outflow delay is short. The outflow delay seems to increase with a deeper groundwater level.

The relative peak reduction of the swale considered is defined as the difference between peak inflow and peak outflow divided by the peak inflow. In 85% of the events more than 40% of the inflow peak is 'lost'. The median values of the data measured for this study and data from 4 years ago are 79%. The peak reduction of the swale is large. The absolute peak reduction (difference peak inflow and peak outflow) shows a linear relation with the peak inflow. However the relative peak reduction does not show this trend.

The peak delay is defined as the time between the peak inflow and the peak outflow. The peak delay is shorter than one hour for more than 60% of the events. The median value for the Donkers(2010) data is 27 minutes. For the new data this is larger, 61 minutes.

The emptying time of the swale only considered the first 40 cm below the swale's surface level since the entire subsurface part of the swale never ran dry during the measuring period. For the analysis only seven events were considered since these events had a groundwater level below the sensor level before the next event started. The median emptying time is about 20 hours.

The time between the start of the inflow and the start of the overflow on surface water is defined as the time to overflow. Four events were considered in this analysis. The median time to overflow is 49 minutes. A combination of a high initial groundwater level, high average inflow intensity and high total inflow volume seem to be reasons for overflow situations.

In general, it can be concluded that the performance of the swale has not decreased over the past 4 years. The volume reduction and peak reduction show similar results as 4 years ago. It can be concluded that the influence of possible occurred clogging of the top layer is small. The peak delay is even larger for this study. The median peak delay is more than two times bigger for this study. This is an improvement of the performance.

Inflow characteristics
For this swale, the lateral inflow seems to perform a little better or at least equal to the head inflow. Improvement in outflow delay and volume reduction is found for two of the three pairs of events. The volume reduction percentage was 10-17% larger for the lateral inflow. The outflow delay 19-40 minutes longer for the lateral inflow simulations. The increase in performance can be explained by the fact that less water is ponding at the head of the swale at the beginning of the event. The water is more divided over the swale and the drainage level will be reached not as fast as in case of a head inflow.

8.2. MODELING

The modeling exercise consisted of two parts. An individual swale model made with MetaSwap-Modflow was used to model the performance of a swale with different initial soil moisture condtions. The output of the swale model was also used for the second model, an urban drainage model in Infoworks. This model was used to determine the performance of swales on an urban catchment scale.

Initial soil moisture conditions
The MetaSwap-Modflow model was used to determine the effects of changing initial soil moisture conditions. The model showed that the effects on the maximum head (water level) in the swale is small. Since the drain discharge is highly related to the heads in the swale also the peaks in the drain discharge are not very different.

Larger effects are noticed on the total drained volume and the outflow delay (time difference between start inflow and start drain discharge). The difference in volume reduction between a deep and high initial moisture conditions is about 10%. The peak delay and outflow delay have a difference larger than 3 hours between the deep and high initial moisture conditions.

Urban catchment scale
The Infoworks model was used to determine the performance of infiltration swales on an urban catchment scale. The model showed that using infiltration swales in urban planning is beneficial. The total volume that discharges on the surface water and the peak discharge is lowered. The volume reduction is consistent with the performance of an individual swale. The peak reduction is between 4% (scenario $swale_{10}$) and 88% (scenario $swale_{90}$). The scenario with only swales performs a little less than the 90% scenario. This can be explained by the fact that the peak in outfall is caused by the areas with a swale. The $swale_{90}$ has less area connected to a swale and thus is the peak smaller.

The model also showed that it is effective on flood control. The flooding that occurred in the reference scenario (no swales) was eliminated with an area percentage of infiltration swales of 30%.

8.3. DISCUSSION

This section considers the draw-backs of the modeling exercise.

Swale model
The model only consisted of 1 cell row. This means that a cross-section of the swale was modeled and is a simplification of the real situation. The surface level is constant, while in reality this varies quite a bit in the longitudinal direction. The surface level at the first couple of meters from the inflow of the swale are much lower than the surface level that was used in the model. Extra storage in this depression is not taken into account. Furthermore flow in longitudinal direction is not taken into account. This makes the model more a swale with homogeneous lateral inflow.

The MetaSwap-Modflow model normally is used for large groundwater systems with daily or larger time step. In the model described in this report the system and the time step are much smaller. It was questionable if the model was able to cope with this. Especially since the MetaSwap steady-state profiles are based on daily values. The model seemed to be performing well in general. The details, however are not simulated that well.

The model is not calibrated and the best fit to the measurements is used. The question is if the best-fit parameter set is really the best fit. Because of the unknown (large) uncertainties in the measurements, it is hard to say how well the model performs compared to reality. A calibrated model will have the same challenges.

Evaporation in the model is a daily value and is constant over the day. In reality the evaporation has a day-night cycle. The influence of the evaporation however is considered to be small in this model since the ratio between evaporation and precipitation (inflow) is small.

Urban drainage model
The urban drainage model is not coupled to the swale. This means that there is not interaction between the sewer system and the swales. The model is not able to infiltrate water from the sewer system via the drain of the swale. In reality this is possible.

The model is fitted to the particular performance indicators of the Castellumknoop swale. A swale in a different native soil will perform differently. Moreover the area that is connected to the swale is fixed at 0.2 ha. Only one storm with the average initial soil moisture condition is used.

The influence of the surface water on which the system discharges is not taken into account. Assumed is that the surface water level is always lower than outfall level of the system.

The model scenarios as they were defined did not take into account a runoff coefficient from the area to the swale. This means losses that occur on the way from the contributing area to the swale are not taken into account. Not taken into account these losses result in a larger inflow to the swale and the sewer system.

8.4. RECOMMENDATIONS

The recommendations for further research are mainly focused on the improvement of models.

The monitoring of a swale as was done for this research could be supplemented by doing measurements on another swale. This was tried for this study as well but was not successful. Monitoring another swale could say something about the representativity of the Castellumknoop swale measurements.

Also it could be interesting to monitor a swale with different native soil conditions and with lateral inflow without artificial simulations. An isolated area with multiple swales could also be interesting to monitor to validate the urban drainage model. The performance of the individual swales and the swales together can be determined. Considerable investment in monitoring equipment and labor costs is however required for such an analysis.

The swale model described in this study might be improved by a good calibration process. The best fit found does not have to be the best fit per se. Calibration can improve the performance of the model. Also the influence of changing native soil conditions on the performance of an individual and the performance on urban catchment scale could be studied.

Coupling of the swale model with the urban drainage model will be an improvement as well. The one way interaction (swale model –> urban drainage model) only models the flow from the swale to the pipe network. It is possible for water to flow the other way in case of dry conditions. Also if the sewer network is completely full the drain of the swale will not be able discharge as much water and the flow can be from the network to the swale.

Beyond the scope of this research but interesting is the effectiveness of infiltration swales compared to the costs. Optimization of the sewer network and the urban water system. A cost benefit analysis could provide information about the feasibility of swales in an urban catchment. Different solutions can be taken into account and indicators like investment costs, hydrological performance, maintenance costs and (surface) water quality aspects could be considered.

BIBLIOGRAPHY

A. Buishand and J. Wijngaard, *Statistiek van extreme neerslag voor korte neerslagduren* (Koninklijk Nederlands Meteorologisch Instituut, 2007).

M. E. Barber, S. G. King, D. R. Yonge, and W. E. Hathhorn, *Ecology ditch: A best management practice for storm water runoff mitigation,* Journal of Hydrologic Engineering **8**, 111 (2003).

A. Semadeni-Davies, C. Hernebring, G. Svensson, and L.-G. Gustafsson, *The impacts of climate change and urbanisation on drainage in helsingborg, sweden: Combined sewer system,* Journal of Hydrology **350**, 100 (2008).

J. K. Holman-Dodds, A. A. Bradley, and K. W. Potter, *Evaluation of hydrologic benefits of infiltration based urban storm water management1,* JAWRA Journal of the American Water Resources Association **39**, 205 (2003).

D. Revitt, J. Ellis, and L. Scholes, *Review of the use of stormwater boms in europe,* Middlesex University, Middlesex (2003).

K. E. Brander, K. E. Owen, and K. W. Potter, *Modeled impacts of development type on runoff volume and infiltration performance1,* JAWRA Journal of the American Water Resources Association **40**, 961 (2004).

F. Boogaard, N. Jeurink, and J. Gels, *Vooronderzoek natuurvriendelijke wadi's: inrichting, functioneren en beheer* (STOWA, Stichting Toegepast Onderzoek Waterbeheer, 2003).

E. Donkers, *Swale Filter Drain System - Inflow-discharge relation*, Master's thesis, Delft University of Technology (2010).

E. S. Williams and W. R. Wise, *Hydrologic impacts of alternative approaches to storm water management and land development,* JAWRA Journal of the American Water Resources Association **42**, 443 (2006).

A. P. Davis, *Field performance of bioretention: Hydrology impacts,* Journal of Hydrologic Engineering **13**, 90 (2008).

H. Abida and J. Sabourin, *Grass swale-perforated pipe systems for stormwater management,* Journal of irrigation and drainage engineering **132**, 55 (2006).

J.-F. Sabourin, M. Eng, P. Eng, and H. C. Wilson, *20 year performance evaluation of grass swale and perforated pipe drainage systems.* (2008).

M. Roldin, O. Fryd, J. Jeppesen, O. Mark, P. J. Binning, P. S. Mikkelsen, and M. B. Jensen, *Modelling the impact of soakaway retrofits on combined sewage overflows in a 3 km^2 urban catchment in copenhagen, denmark,* Journal of Hydrology **452**, 64 (2012a).

M. Roldin, P. J. Binning, P. S. Mikkelsen, and O. Mark, *Distributed models coupling soakaways, urban drainage and groundwater* (DHIDHI, 2012).

Eijkelkamp, *13.17.02 RBC meetgoot - Gebruiksaanwijzing* (2014).

J. Wijngaard, M. Kok, I. Smits, and M. Talsma, *Nieuwe statistiek voor extreme neerslag,* H2O **6**, 35 (2005).

KNMI, *Factsheet regen,* (2012).

A. W. Harbaugh, *MODFLOW-2005, the US Geological Survey modular ground-water model: The ground-water flow process* (US Department of the Interior, US Geological Survey, 2005).

P. Van Walsum, A. Veldhuizen, and P. Groenendijk, *Simgro 7.2.11, theory and model implementation,* Alterra-Report **913.1**, 93 (2012).

H. Wösten, F. De Vries, T. Hoogland, H. Massop, A. Veldhuizen, H. Vroon, J. Wesseling, J. Heijkers, and A. Bolman, *BOFEK2012, de nieuwe, bodemfysische schematisatie van Nederland* (Alterra Wageningen, 2012).

S. Rioned, *Leidraad riolering*, Module C2100. Rioleringsberekeningen, hydraulisch functioneren (2012).

APPENDICES OVERVIEW

A - Data validation
Graphs of the recorded groundwater and water levels compared to manual recordings.

B - Water levels
Graphs of the measured water levels for the inflow and outflow calculations.

C - Events
Graphs of the events that were used in the analysis

A

DATA VALIDATION

This appendix includes the comparison of the recorded (ground)water levels and the manual recorded values. The figures of the different observation wells are shown in figure A.1 to figure A.9.

Graphs

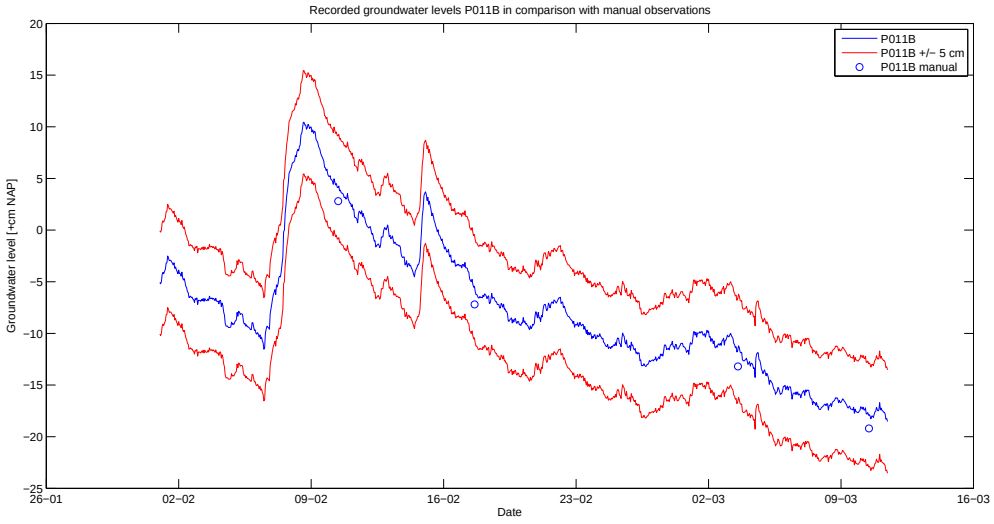

Figure A.1: Observation well P011B

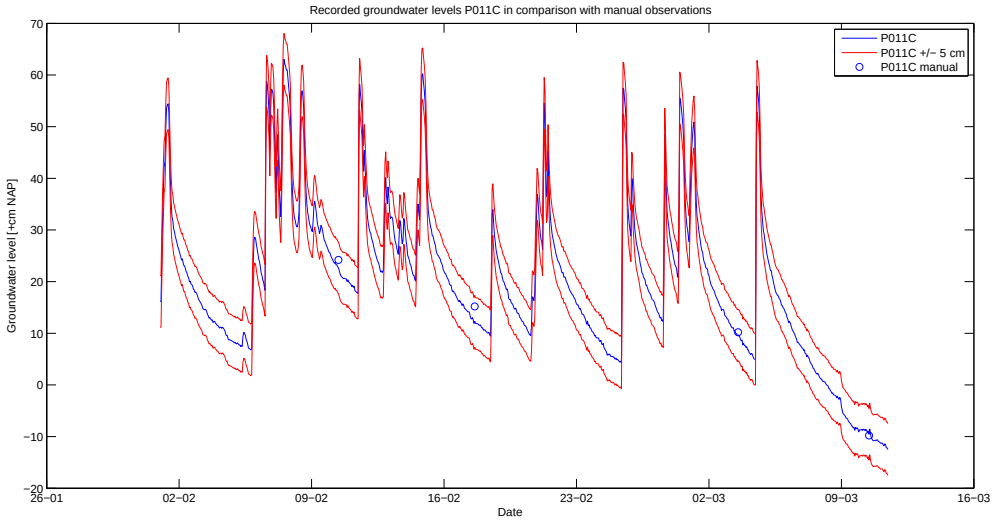

Figure A.2: Observation well P011C

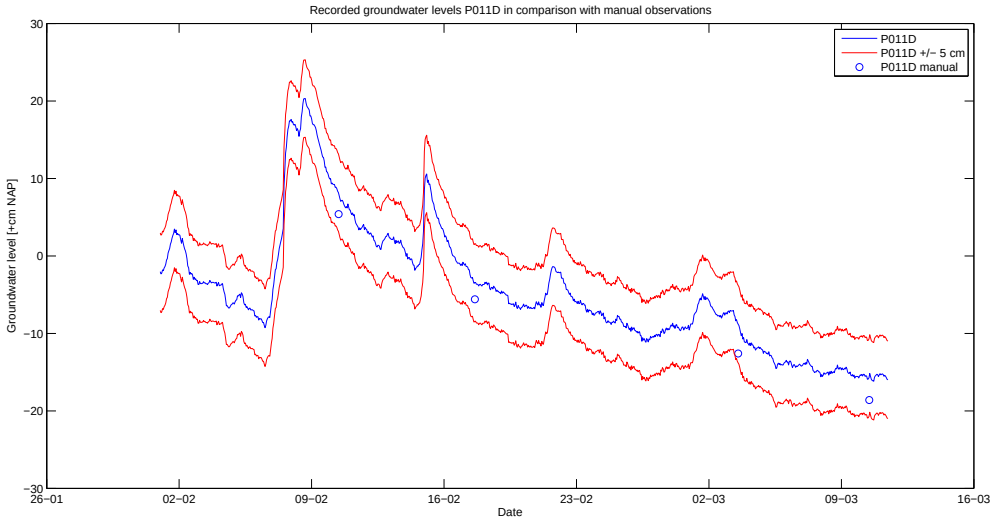

Figure A.3: Observation well P011D

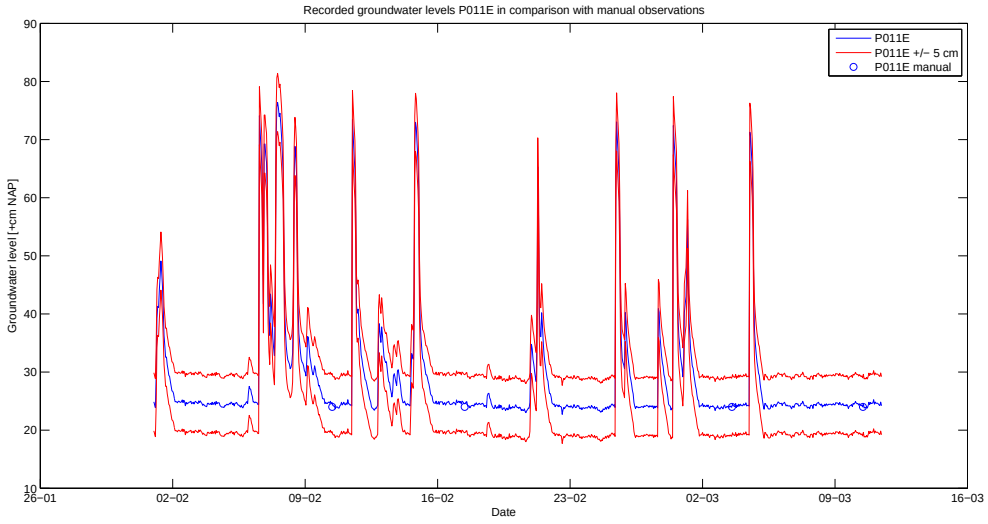

Figure A.4: Observation well P011E

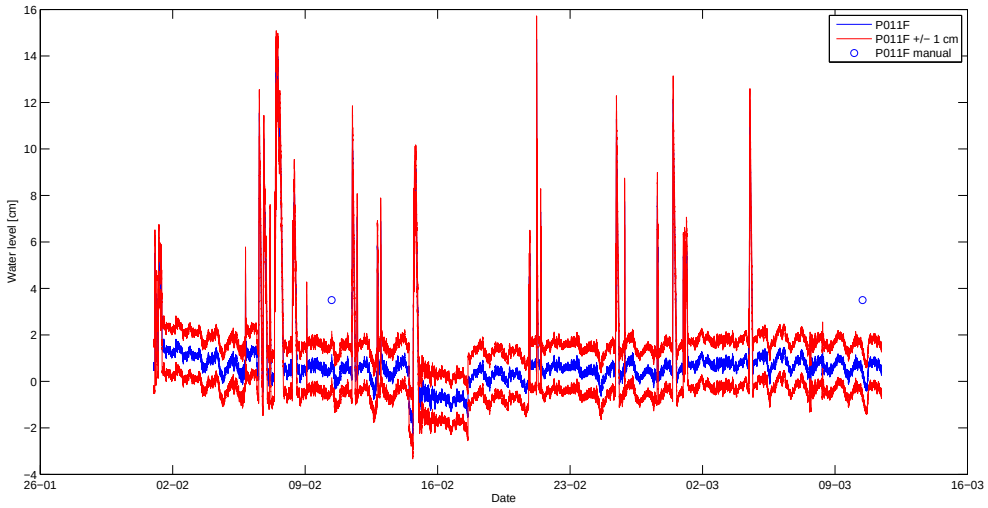

Figure A.5: Inflow P011F

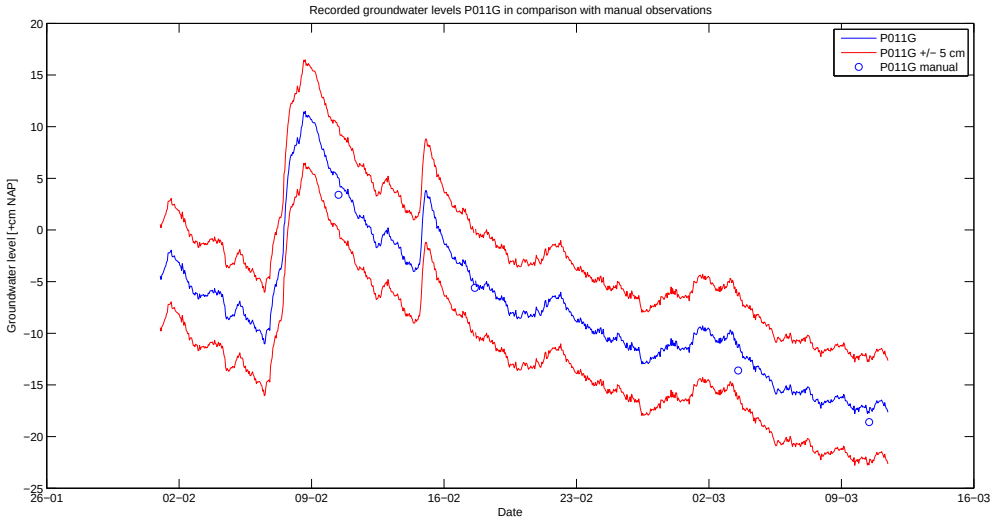

Figure A.6: Observation well P011G

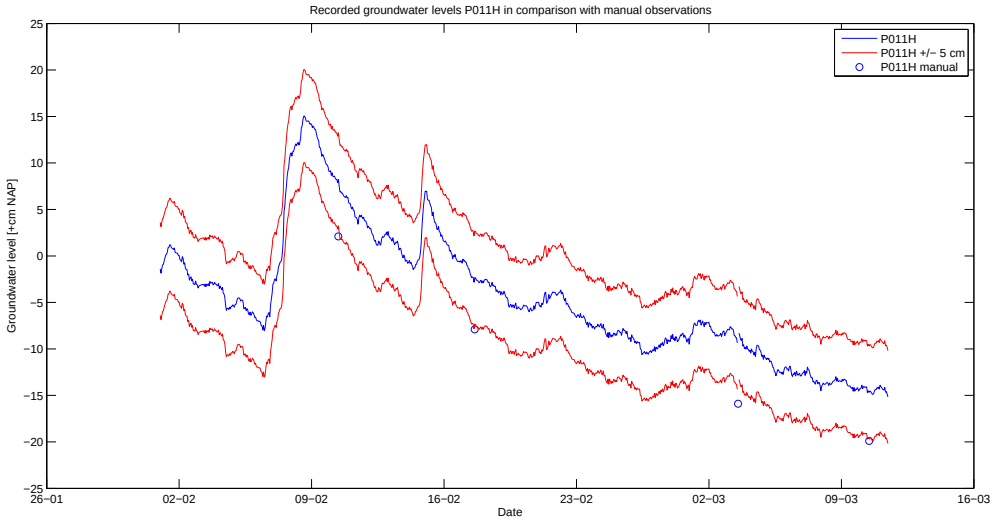

Figure A.7: Observation well P011H

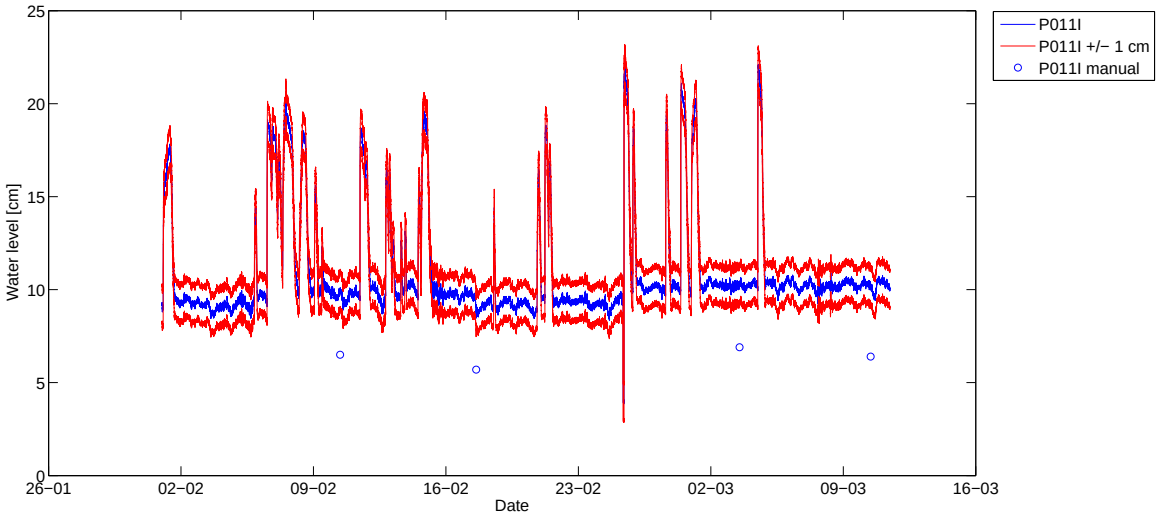

Figure A.8: Ouflow P011I

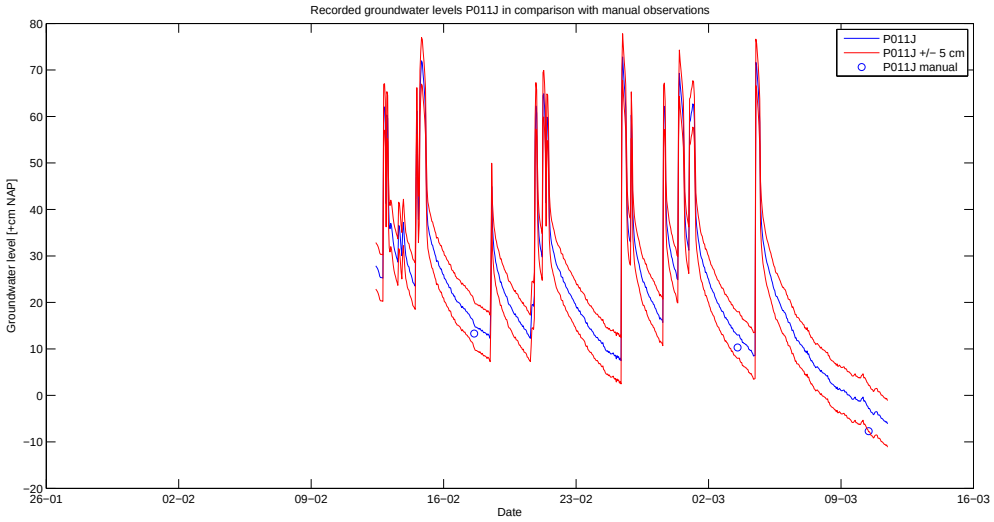

Figure A.9: Observation well P011J

B

WATER LEVELS

This appendix includes the graphs of the water levels used for inflow and outflow calculations. The inflow water levels were shifted 3 cm up and the outflow water levels 3 cm down with regard to the raw data. Inflow water levels are not used for determining the discharge of the artificial simulation 3,4,5,6 and 7. During these simulations and within the period that the outflow was active it was dry. The inflow for these simulations were purely based on the pump discharge measured.

Event 21

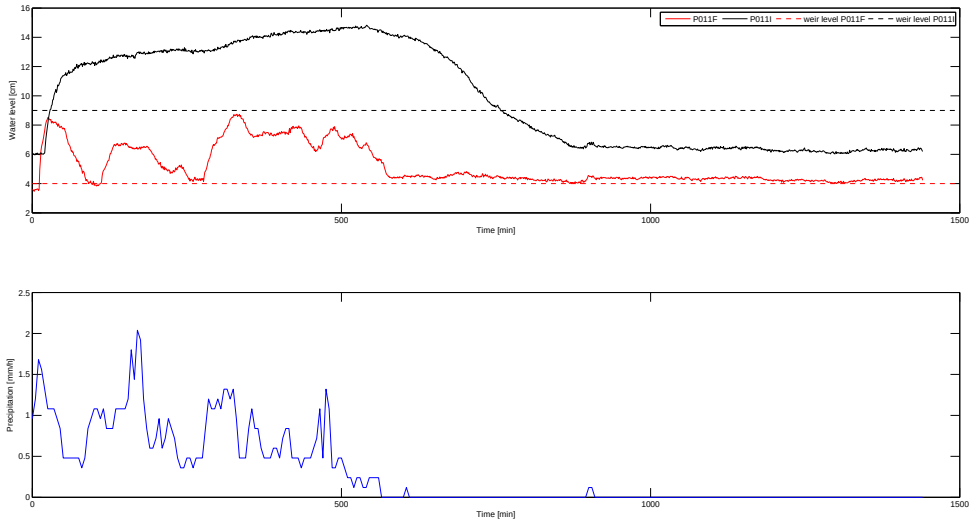

Figure B.1: Event 21 - Water levels and precipitation

Event 22

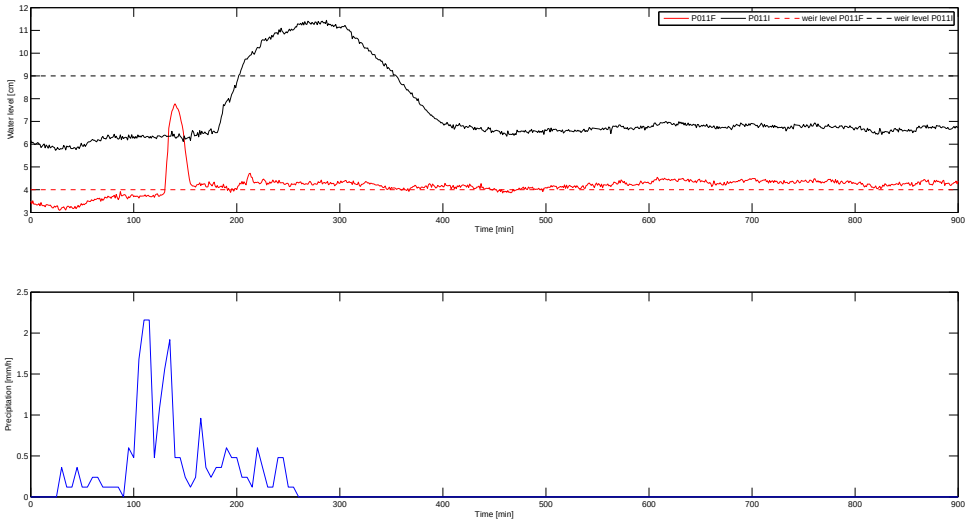

Figure B.2: Event 22 - Water levels and precipitation

Event 23

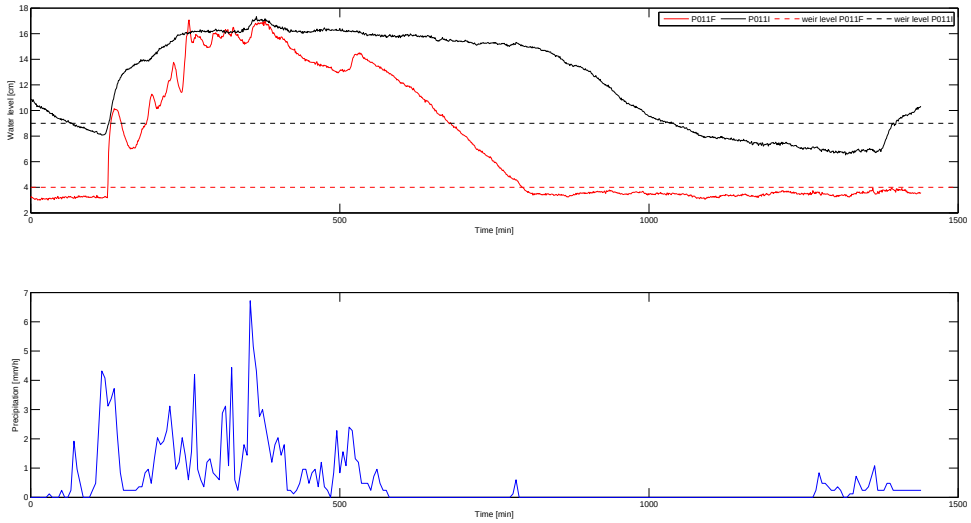

Figure B.3: Event 23 - Water levels and precipitation

Event 24

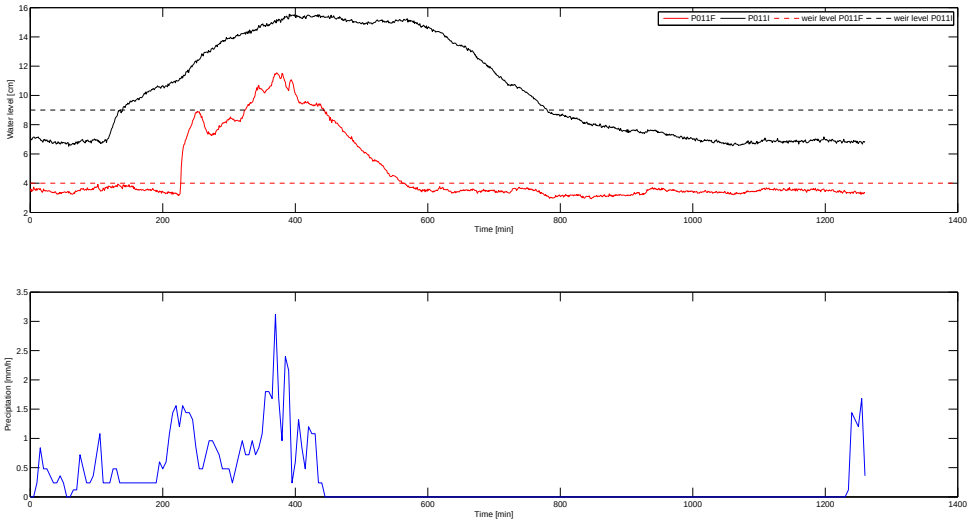

Figure B.4: Event 24 - Water levels and precipitation

Event 25

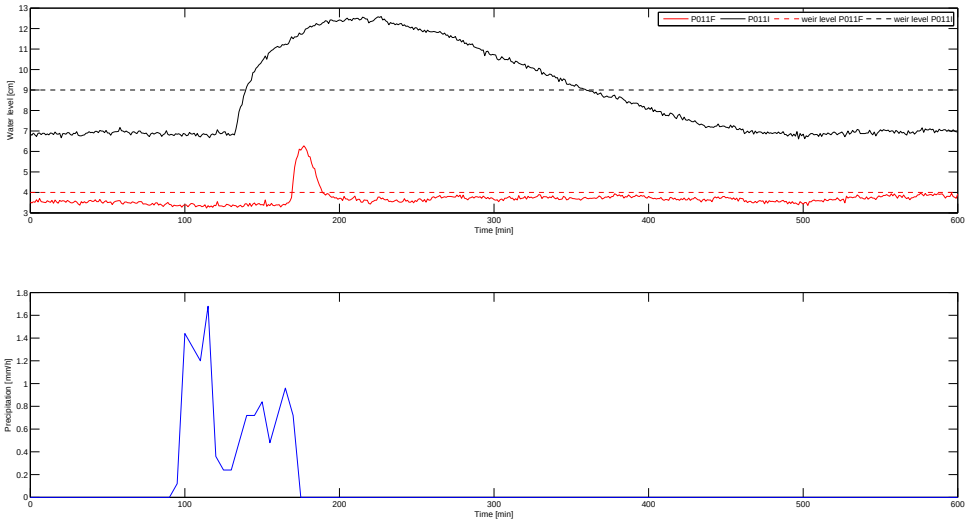

Figure B.5: Event 25 - Water levels and precipitation

Event 26

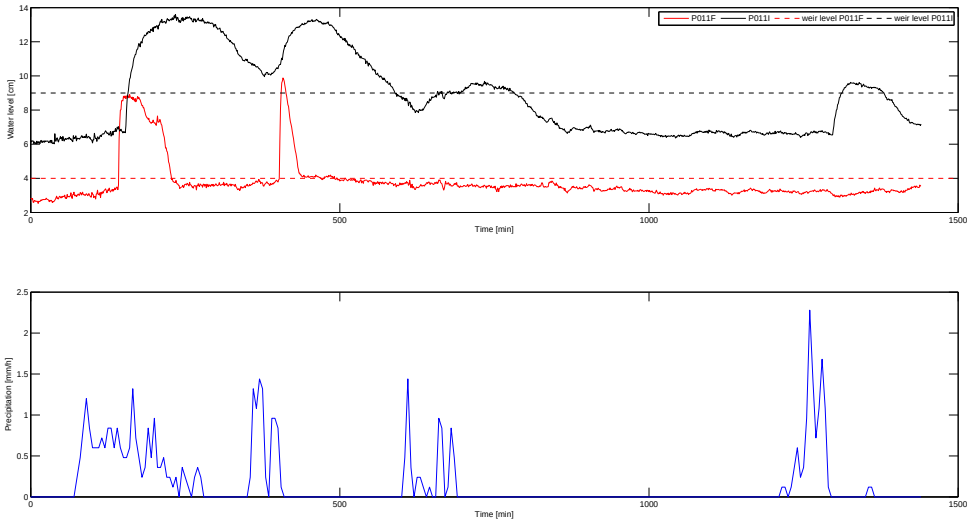

Figure B.6: Event 26 - Water levels and precipitation

Event 27

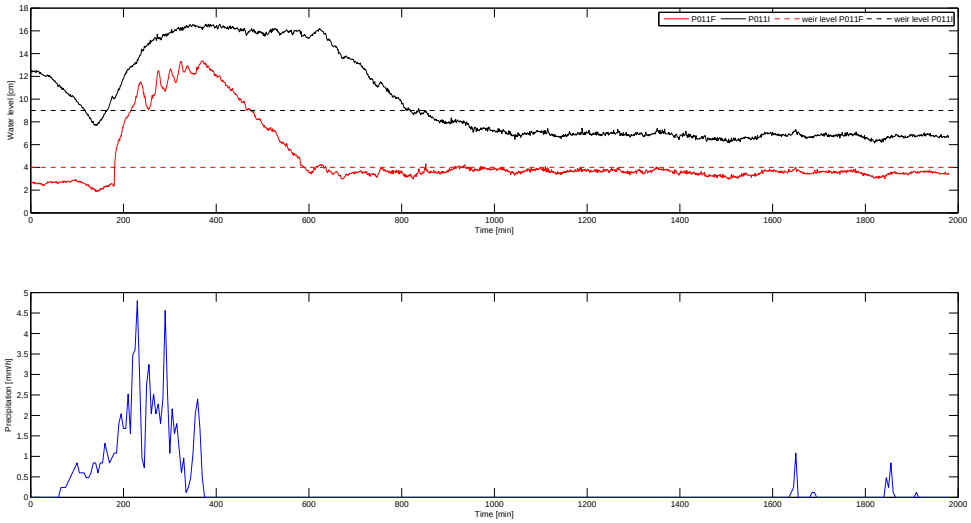

Figure B.7: Event 27 - Water levels and precipitation

Event 28

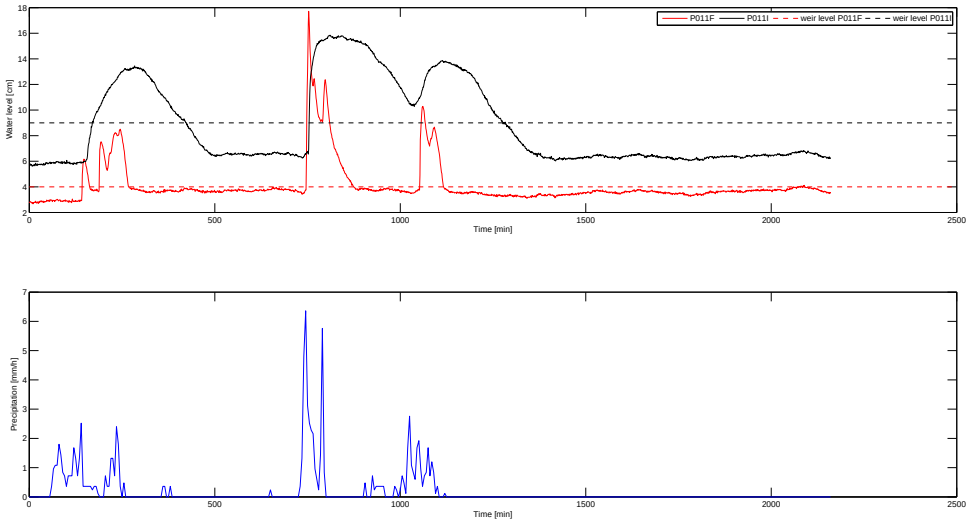

Figure B.8: Event 28 - Water levels and precipitation

Event 29

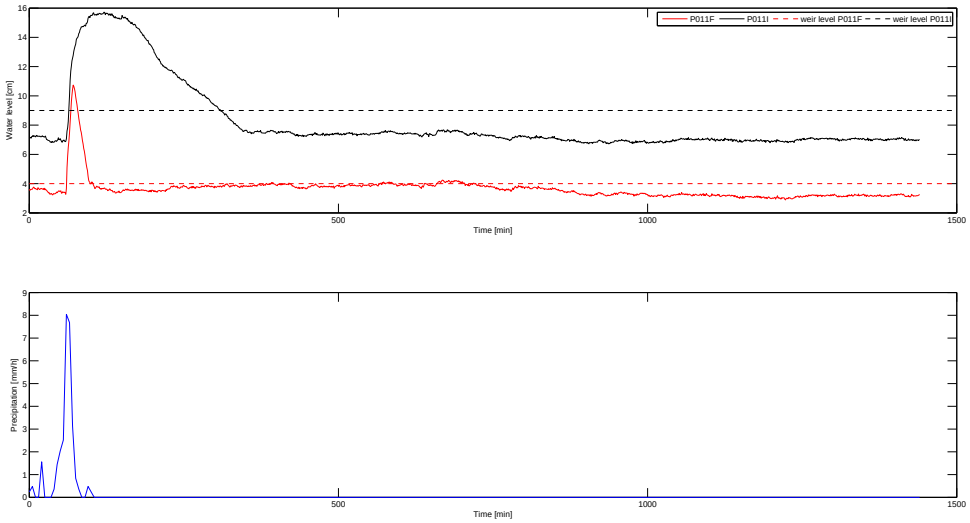

Figure B.9: Event 29 - Water levels and precipitation

Event 30

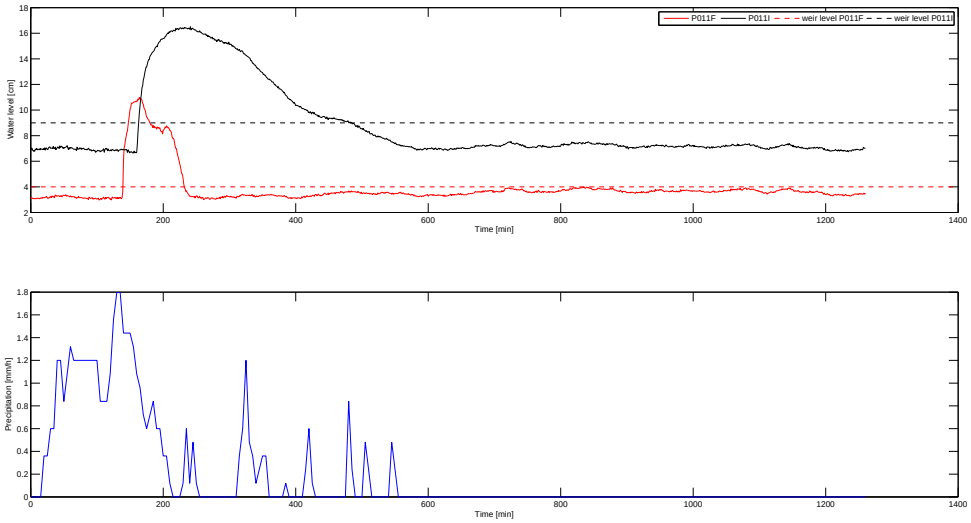

Figure B.10: Event 30 - Water levels and precipitation

Event 31

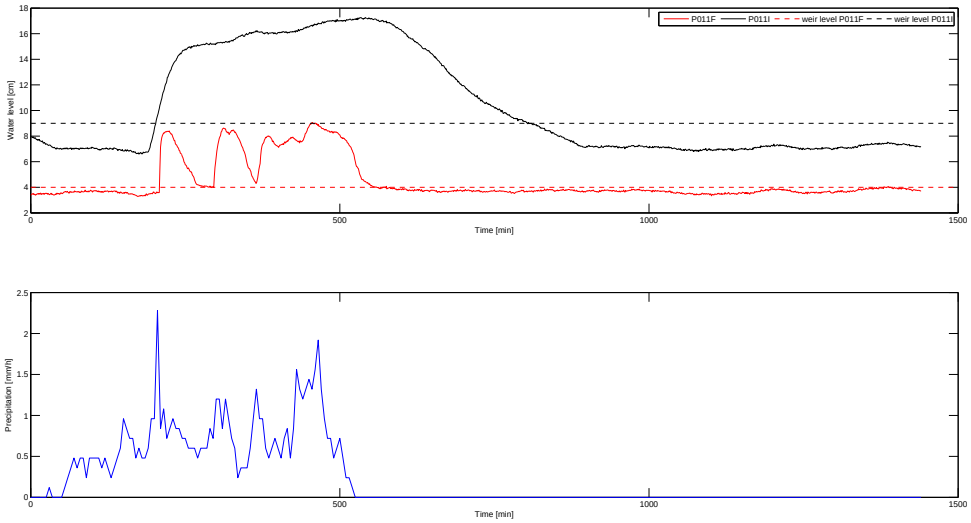

Figure B.11: Event 31 - Water levels and precipitation

Simulation 1

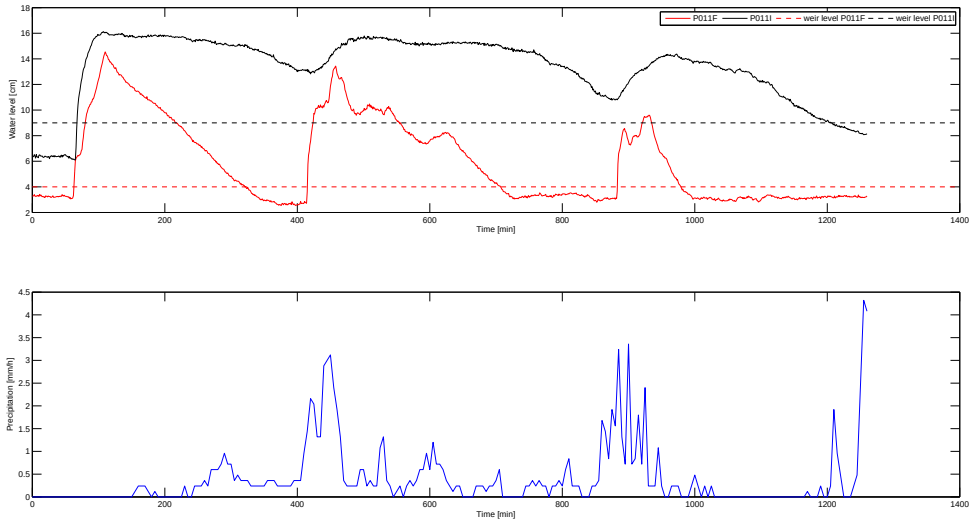

Figure B.12: Simulation 1 - Water levels and precipitation

Simulation 2

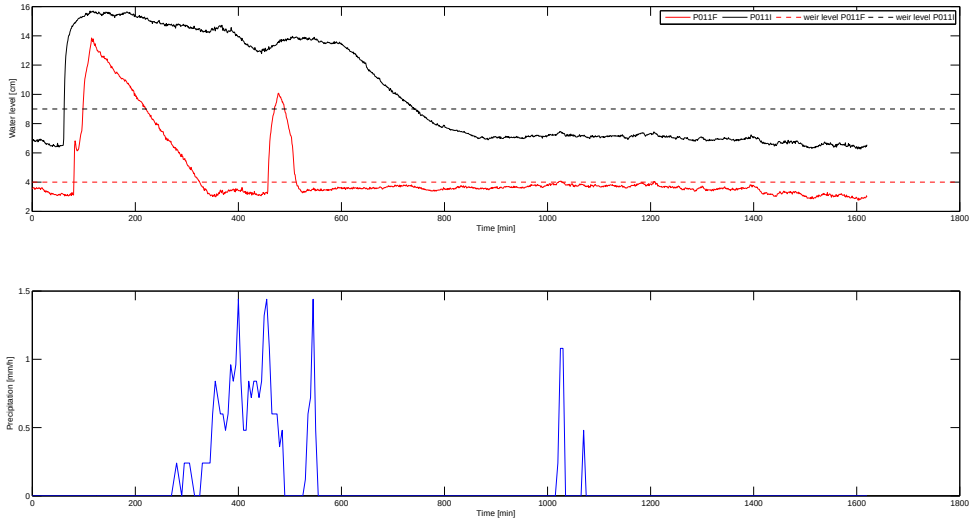

Figure B.13: Simulation 2 - Water levels and precipitation

Simulation 3

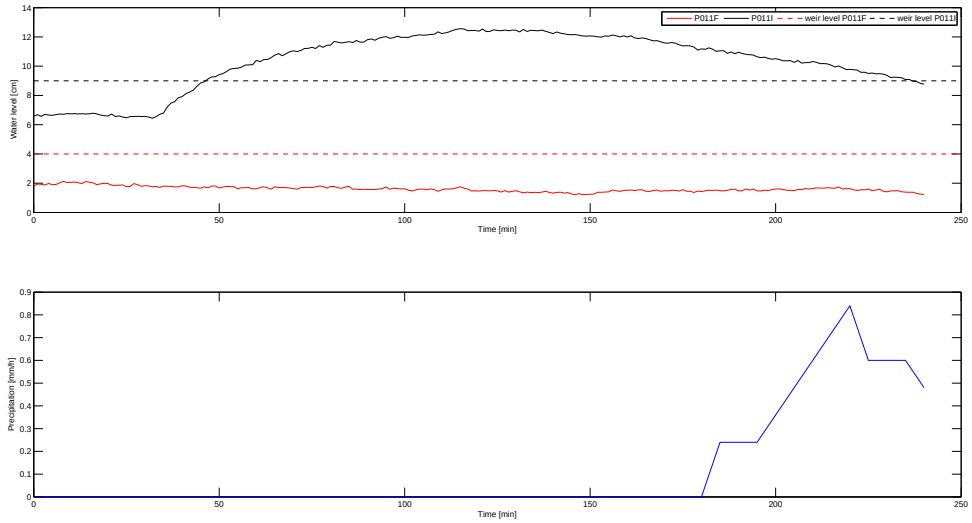

Figure B.14: Simulation 3 - Water levels and precipitation

Simulation 4

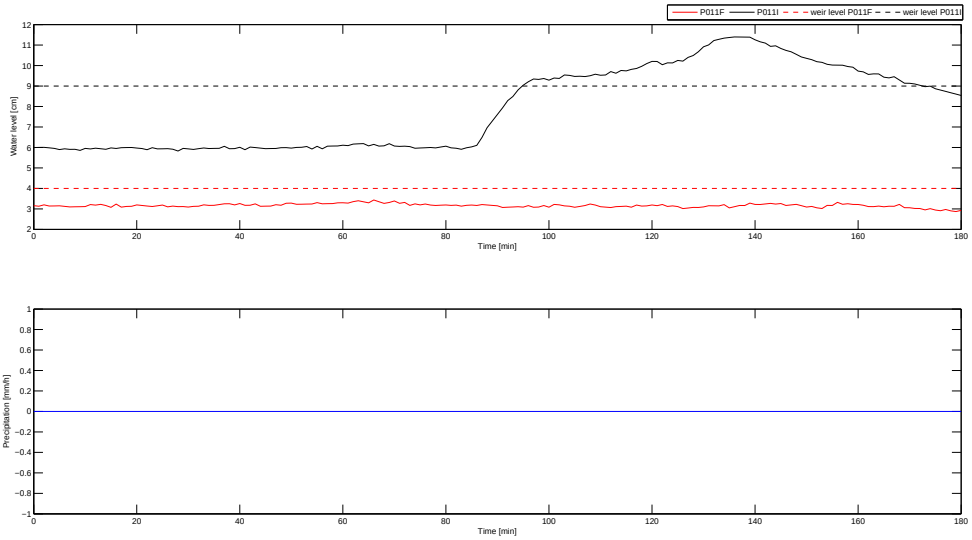

Figure B.15: Simulation 4 - Water levels and precipitation

Simulation 5

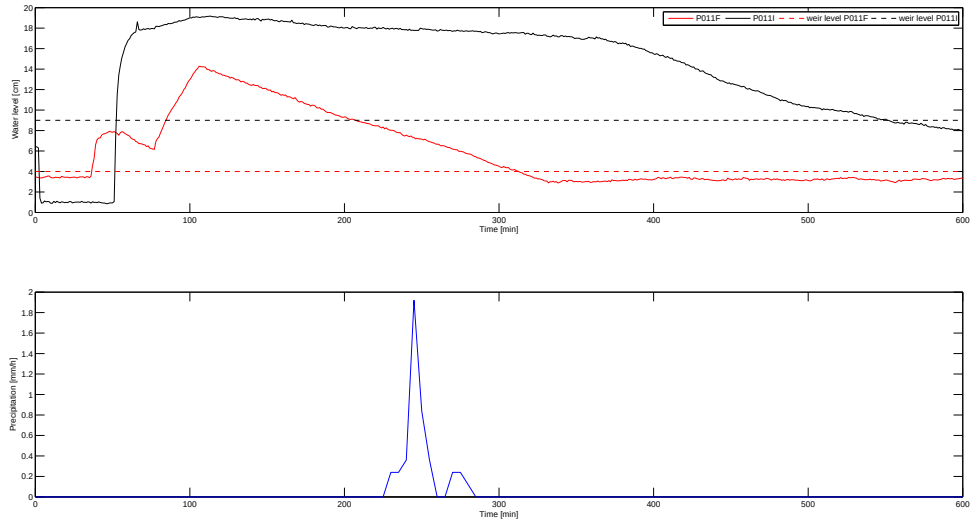

Figure B.16: Simulation 5 - Water levels and precipitation

Simulation 6

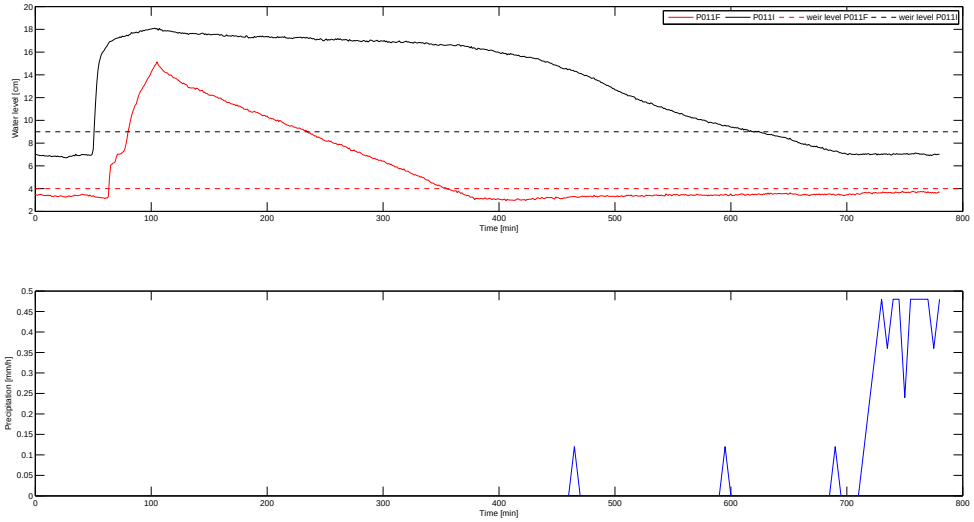

Figure B.17: Simulation 6 - Water levels and precipitation

Simulation 7

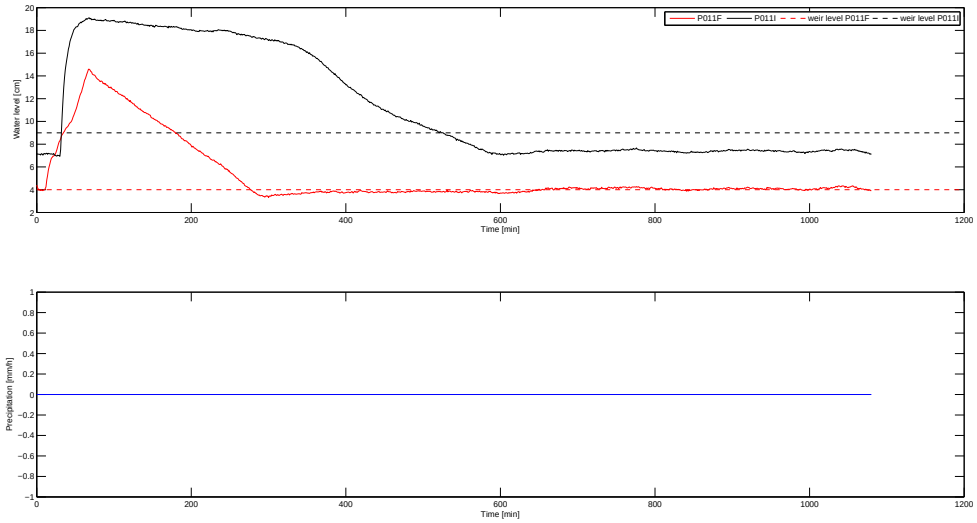

Figure B.18: Simulation 7 - Water levels and precipitation

C

EVENTS

This appendix includes the graphs of the events that were analyzed.

Graphs

Event 21

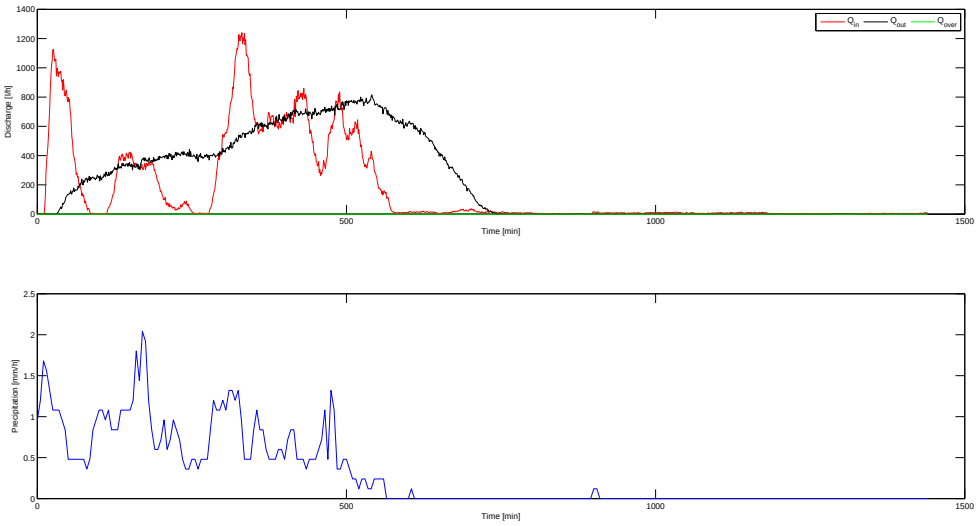

Figure C.1: Event 21 - Discharges and precipitation

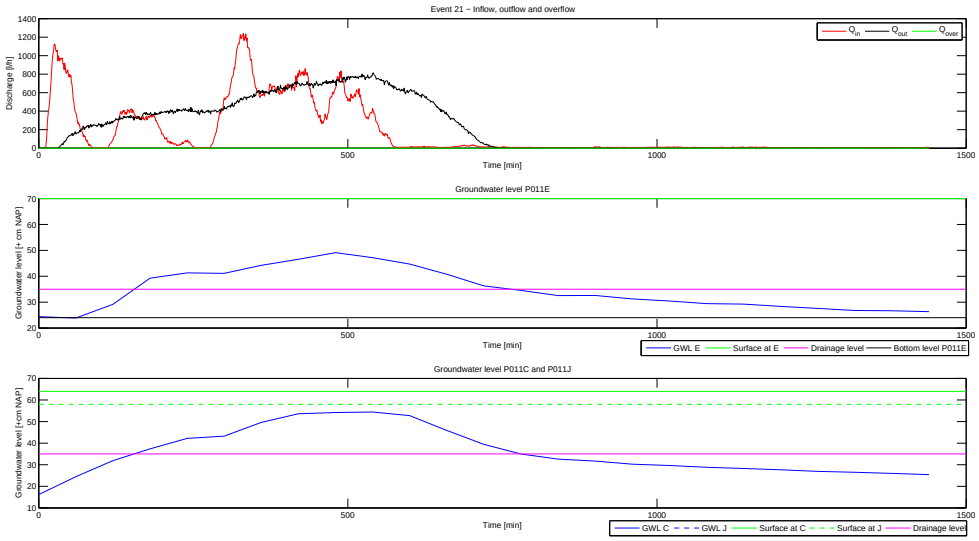

Figure C.2: Event 21 - Discharges and groundwater levels P011E, P011C and P011J

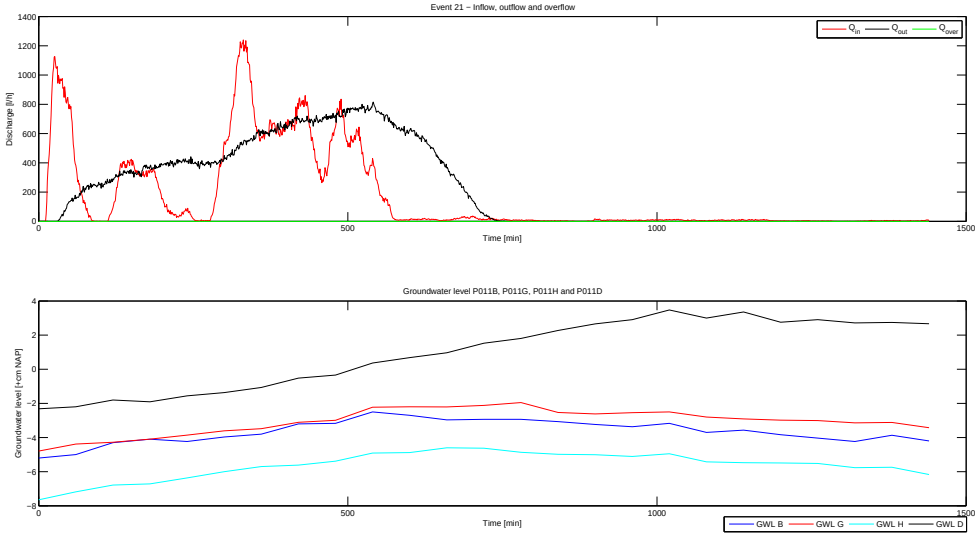

Figure C.3: Event 21 - Discharges and groundwater levels P011B, P011G, P011H and P011D

Event 22

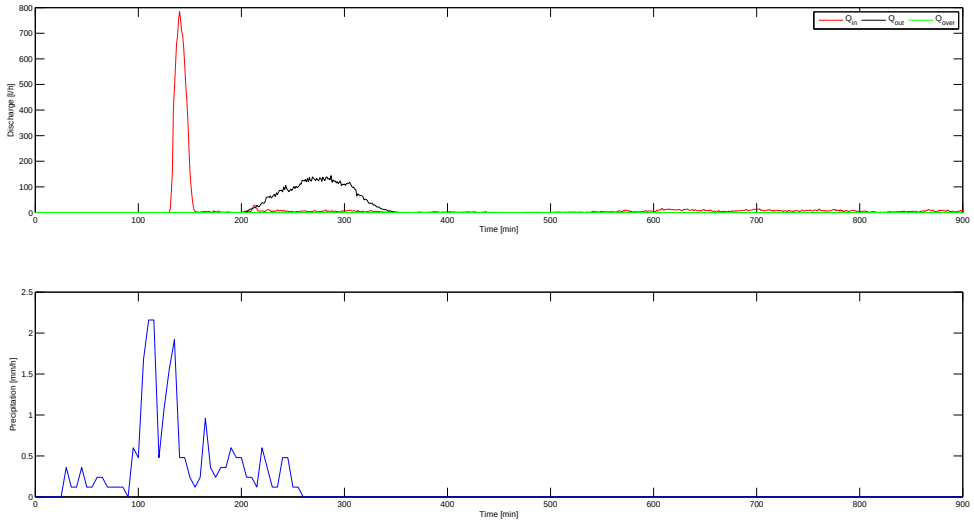

Figure C.4: Event 22 - Discharges and precipitation

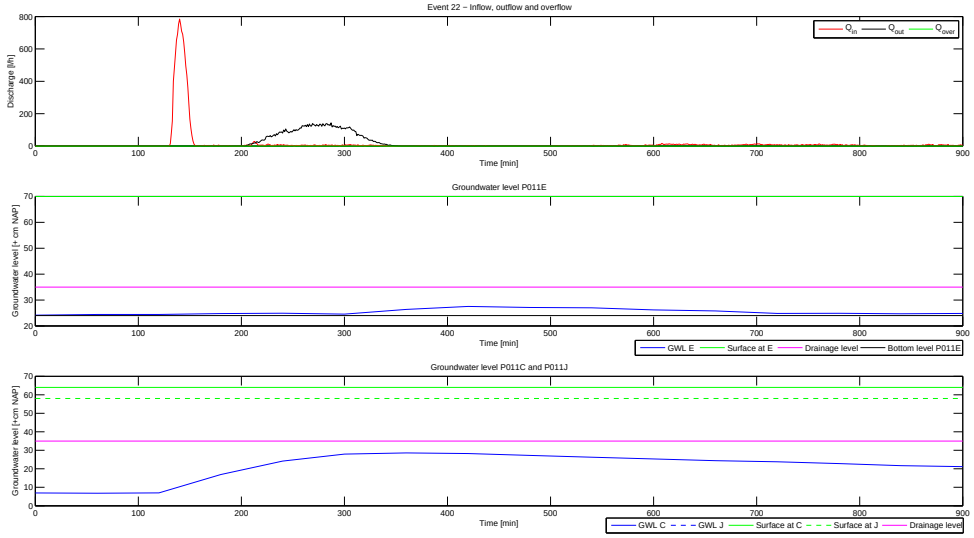

Figure C.5: Event 22 - Discharges and groundwater levels P011E, P011C and P011J

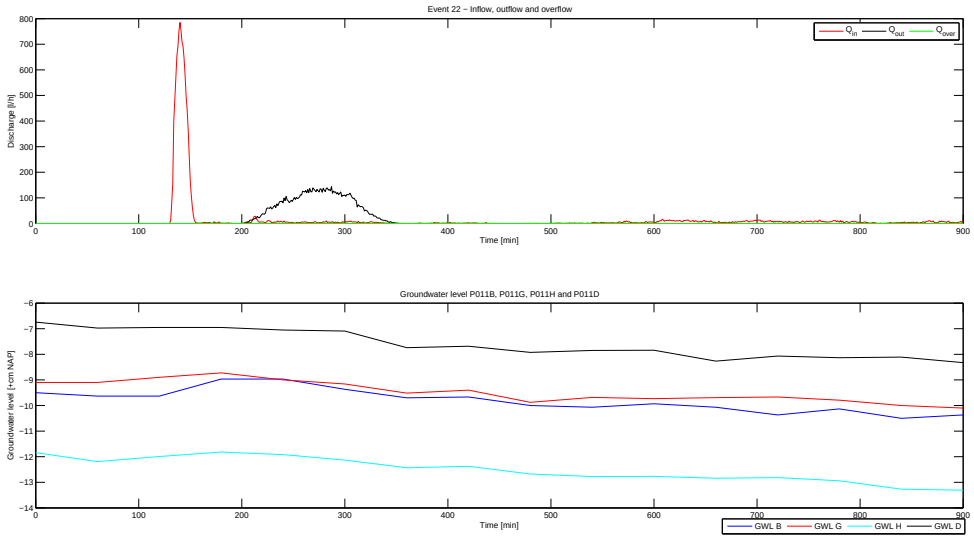

Figure C.6: Event 22 - Discharges and groundwater levels P011B, P011G, P011H and P011D

Event 24

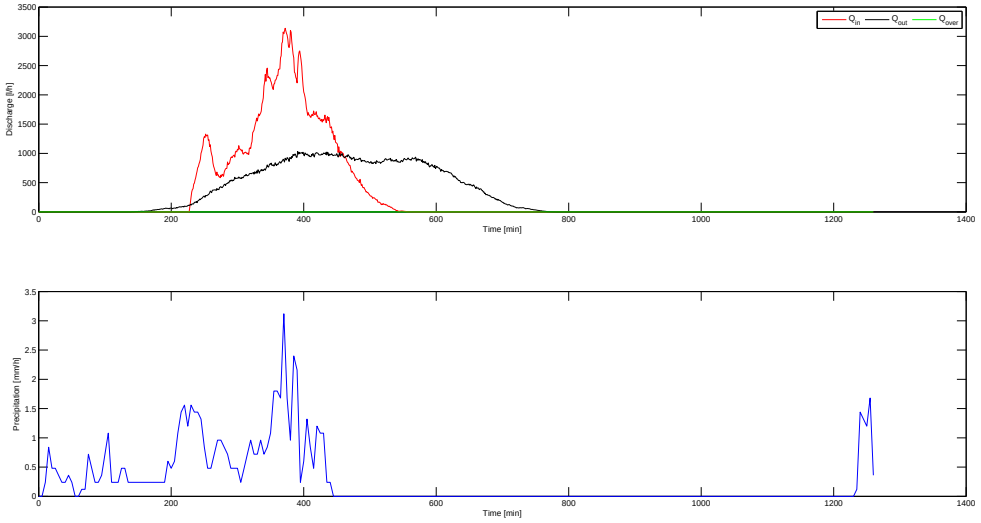

Figure C.7: Event 24 - Discharges and precipitation

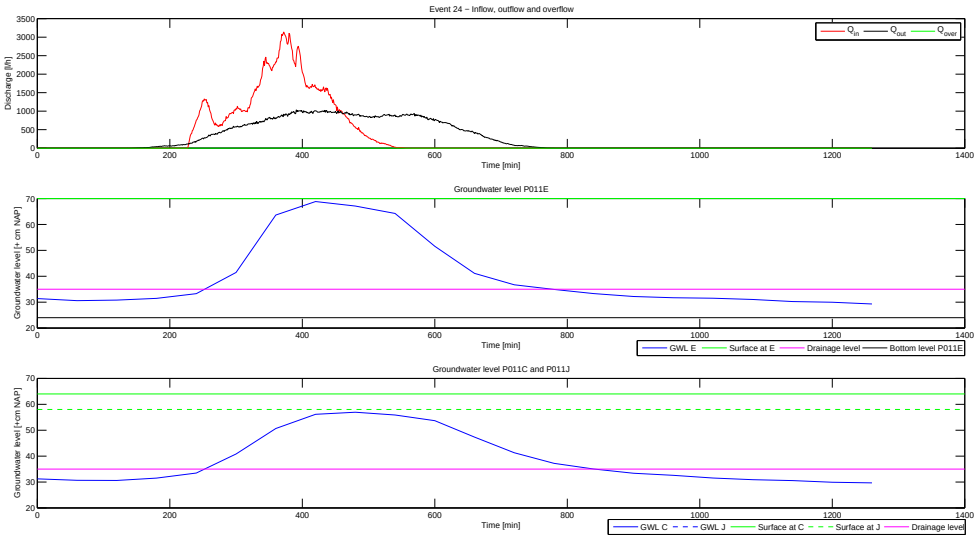

Figure C.8: Event 24 - Discharges and groundwater levels P011E, P011C and P011J

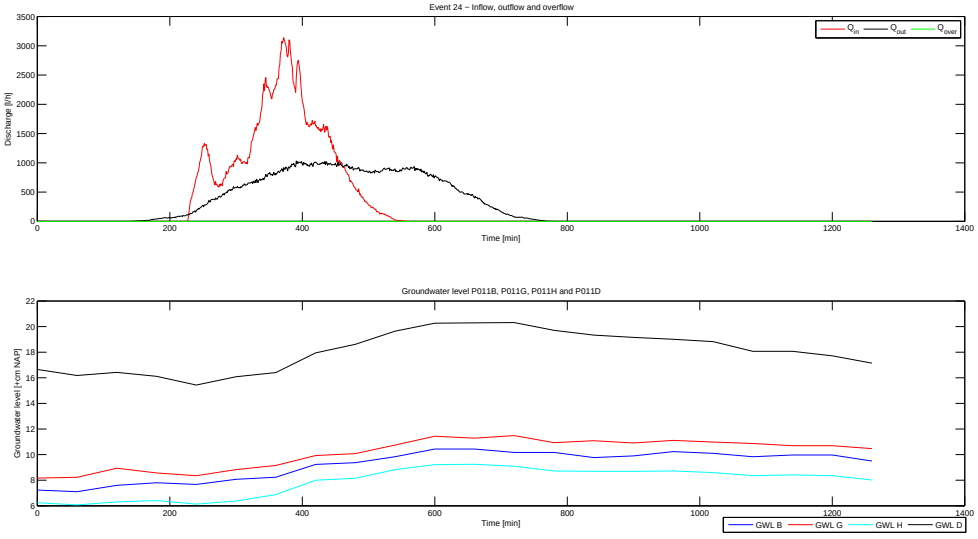

Figure C.9: Event 24 - Discharges and groundwater levels P011B, P011G, P011H and P011D

Event 26

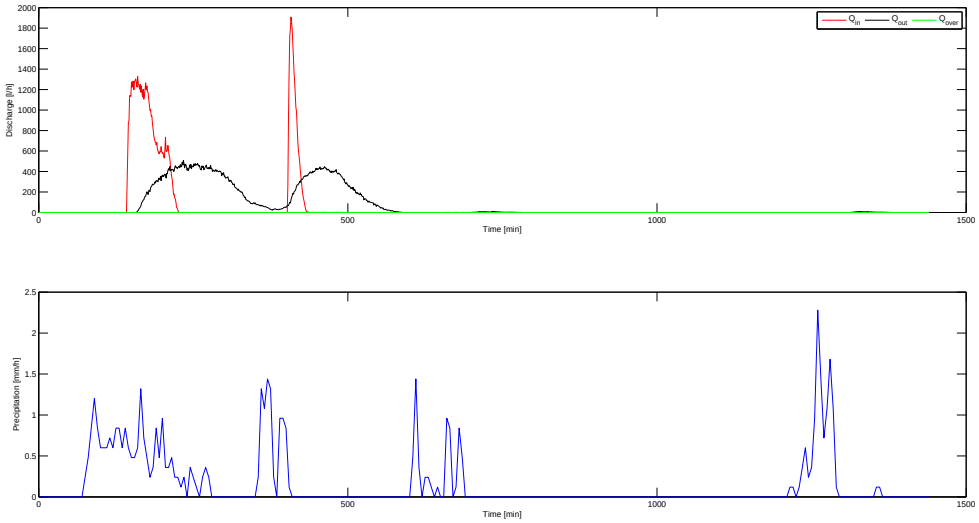

Figure C.10: Event 26 - Discharges and precipitation

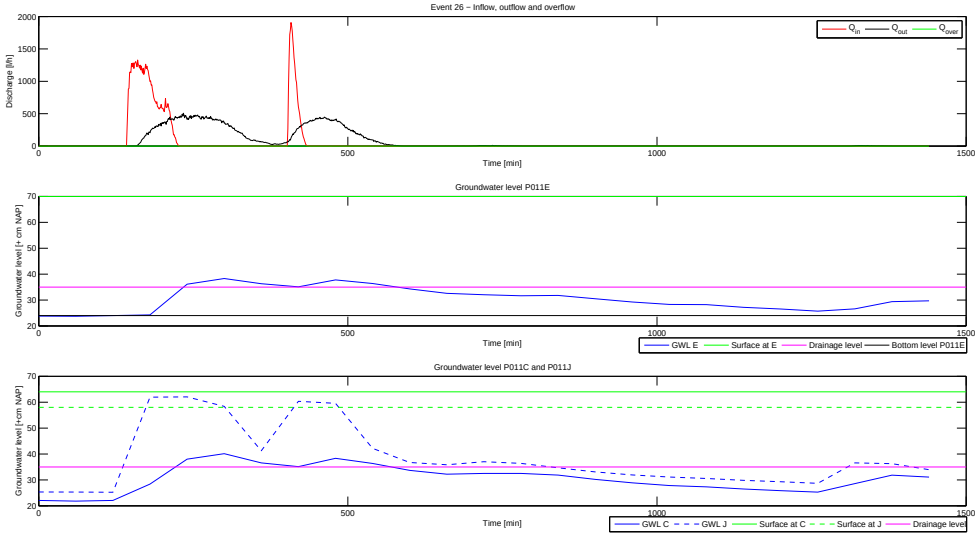

Figure C.11: Event 26 - Discharges and groundwater levels P011E, P011C and P011J

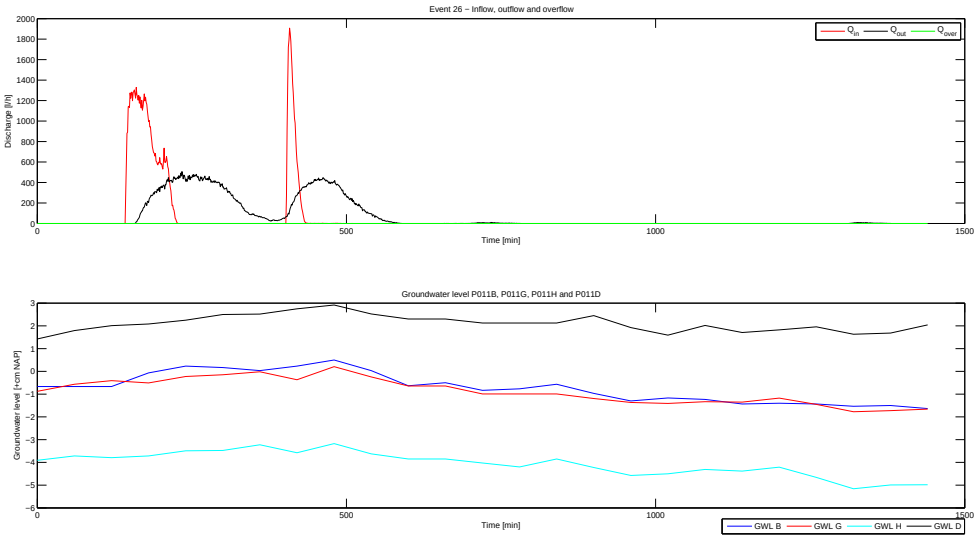

Figure C.12: Event 26 - Discharges and groundwater levels P011B, P011G, P011H and P011D

Event 27

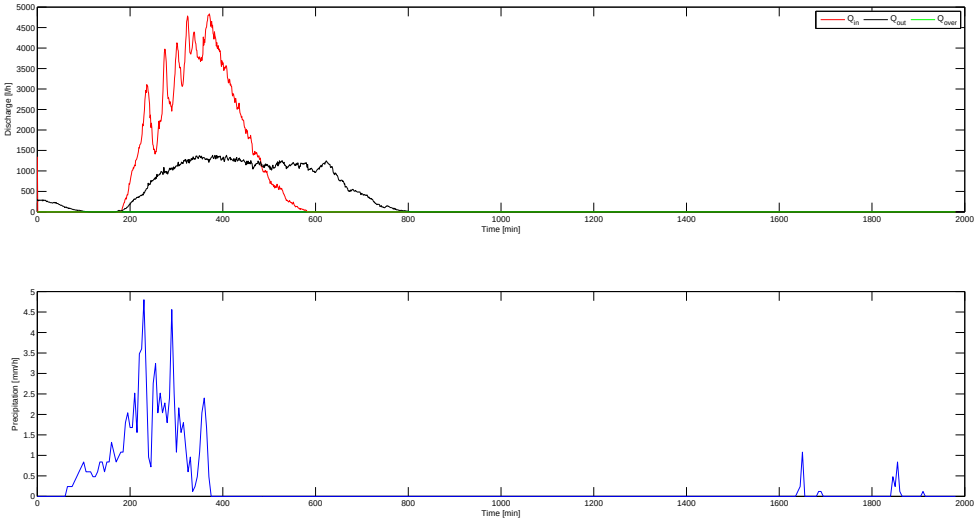

Figure C.13: Event 27 - Discharges and precipitation

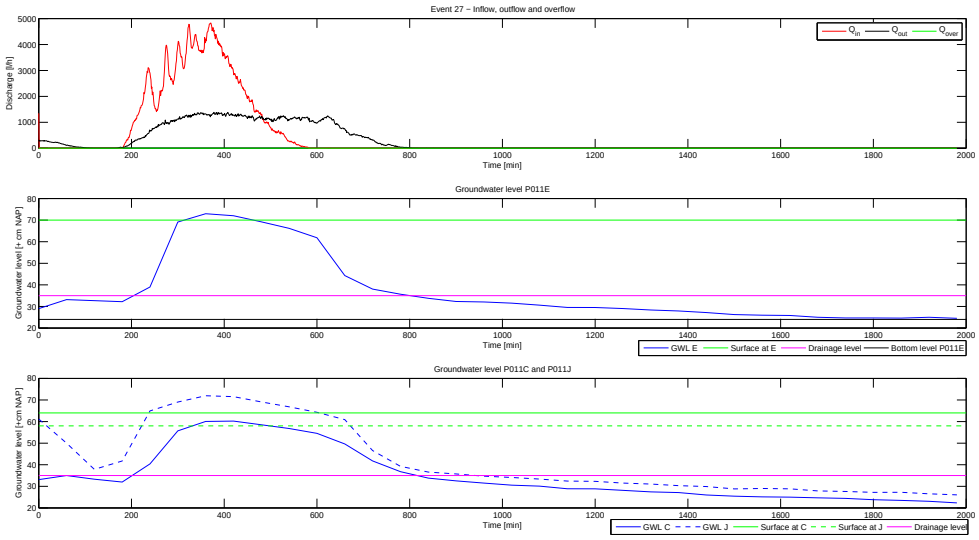

Figure C.14: Event 27 - Discharges and groundwater levels P011E, P011C and P011J

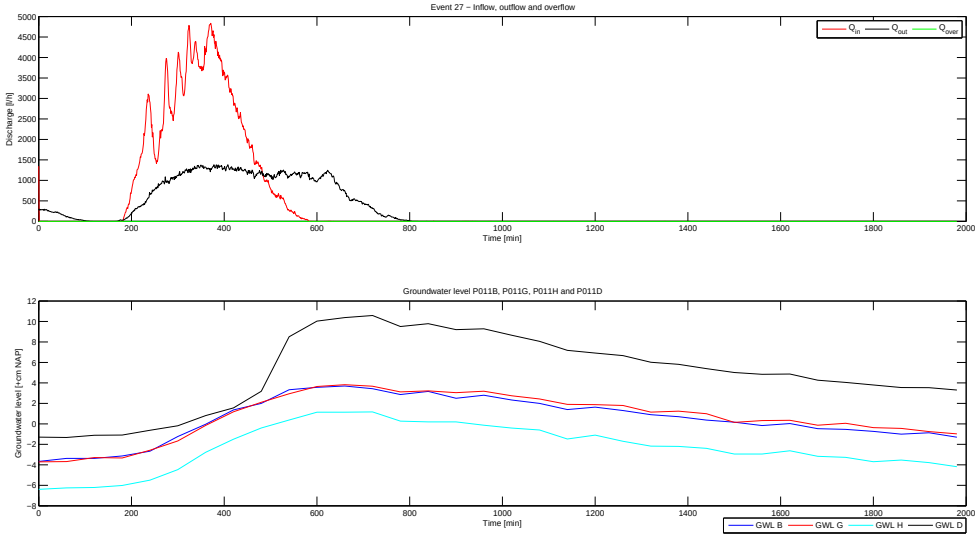

Figure C.15: Event 27 - Discharges and groundwater levels P011B, P011G, P011H and P011D

Event 28

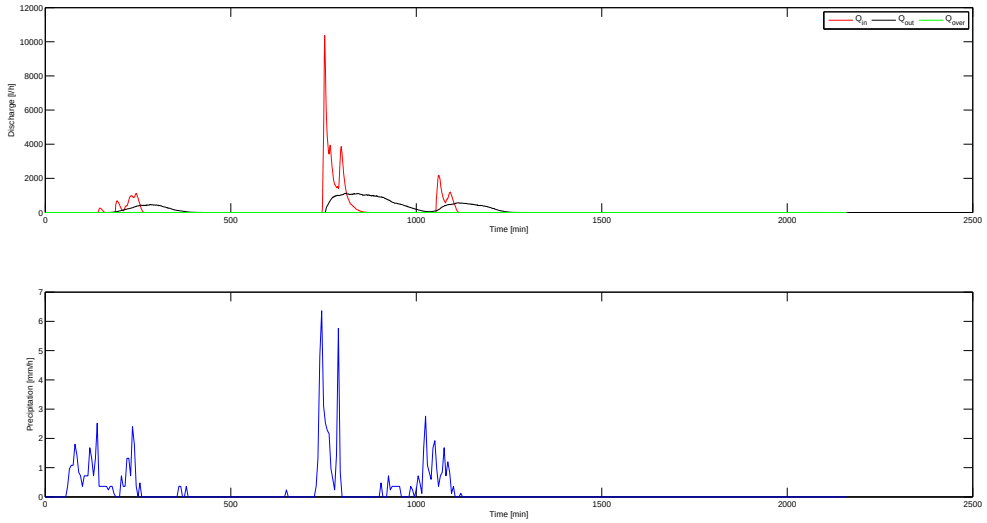

Figure C.16: Event 28 - Discharges and precipitation

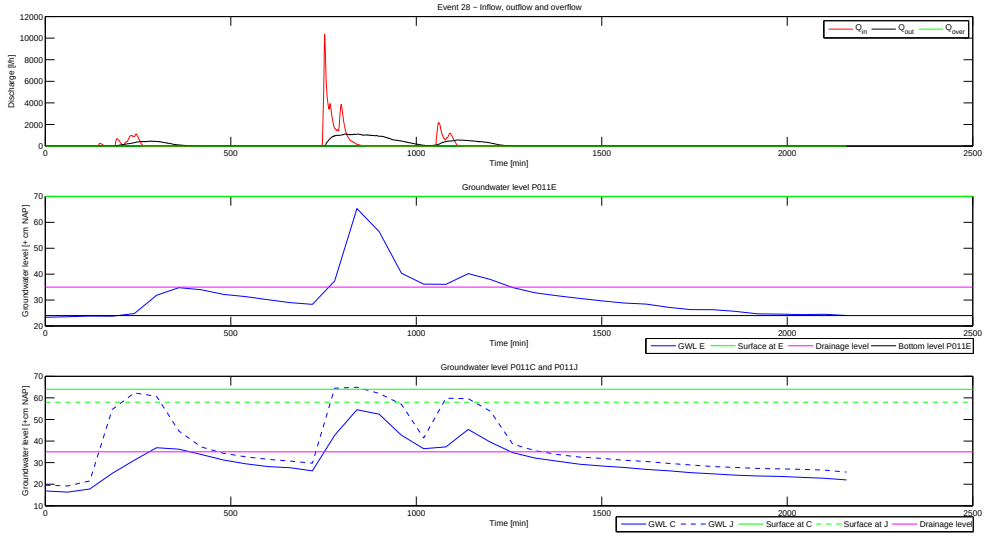

Figure C.17: Event 28 - Discharges and groundwater levels P011E, P011C and P011J

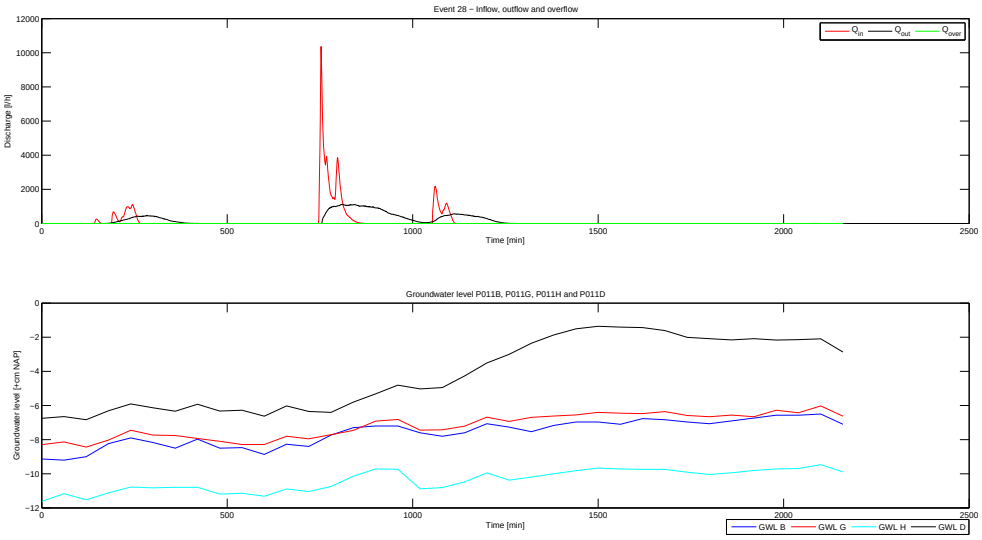

Figure C.18: Event 28 - Discharges and groundwater levels P011B, P011G, P011H and P011D

Event 30

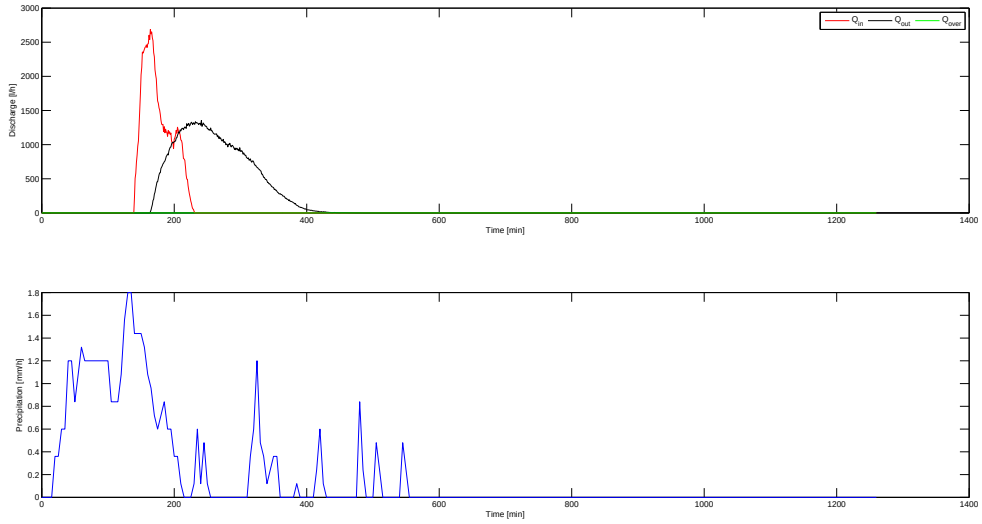

Figure C.19: Event 30 - Discharges and precipitation

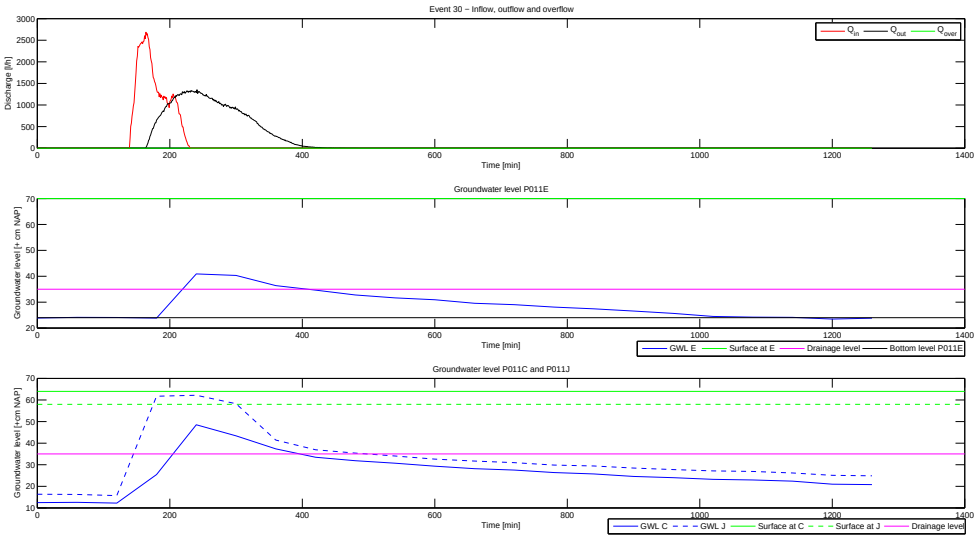

Figure C.20: Event 30 - Discharges and groundwater levels P011E, P011C and P011J

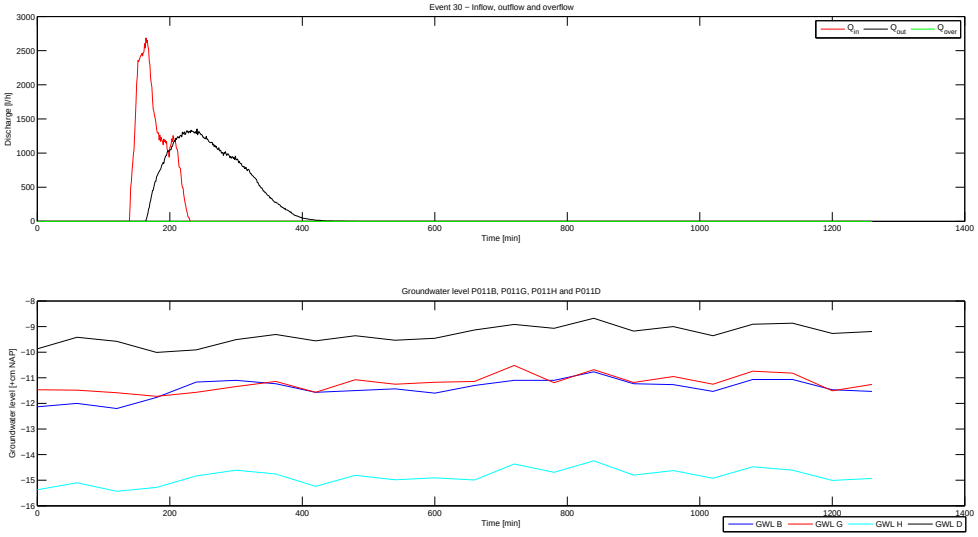

Figure C.21: Event 30 - Discharges and groundwater levels P011B, P011G, P011H and P011D

Simulation 1

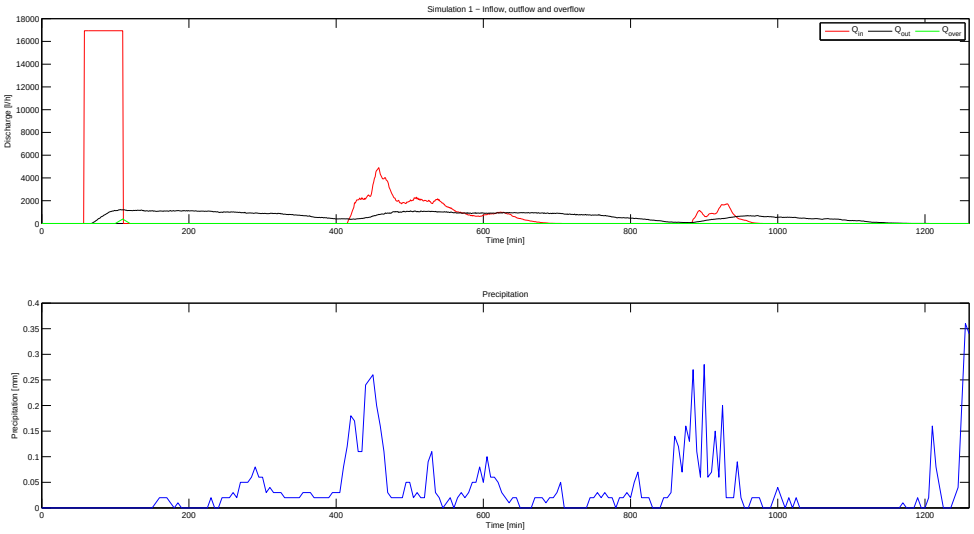

Figure C.22: Simulation 1 - Discharges and precipitation

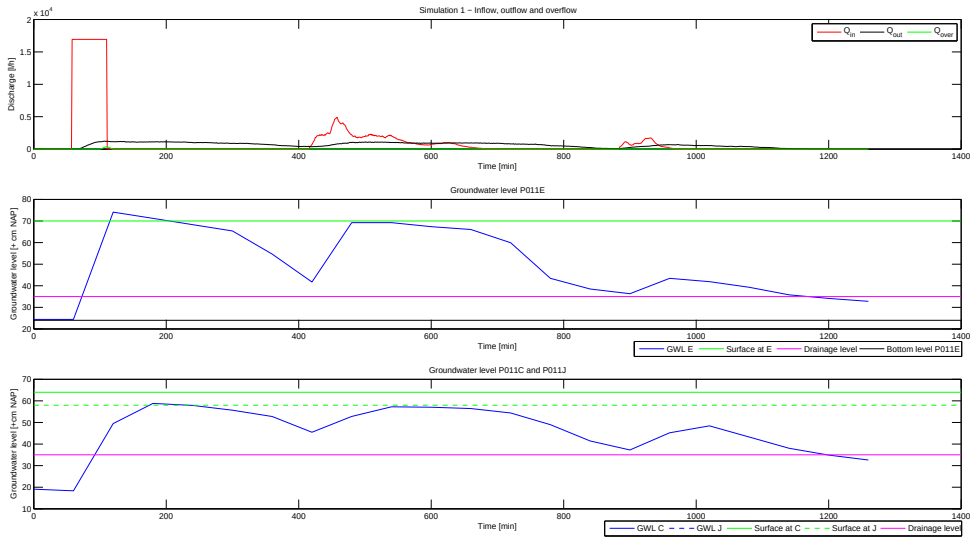

Figure C.23: Simulation 1 - Discharges and groundwater levels P011E, P011C and P011J

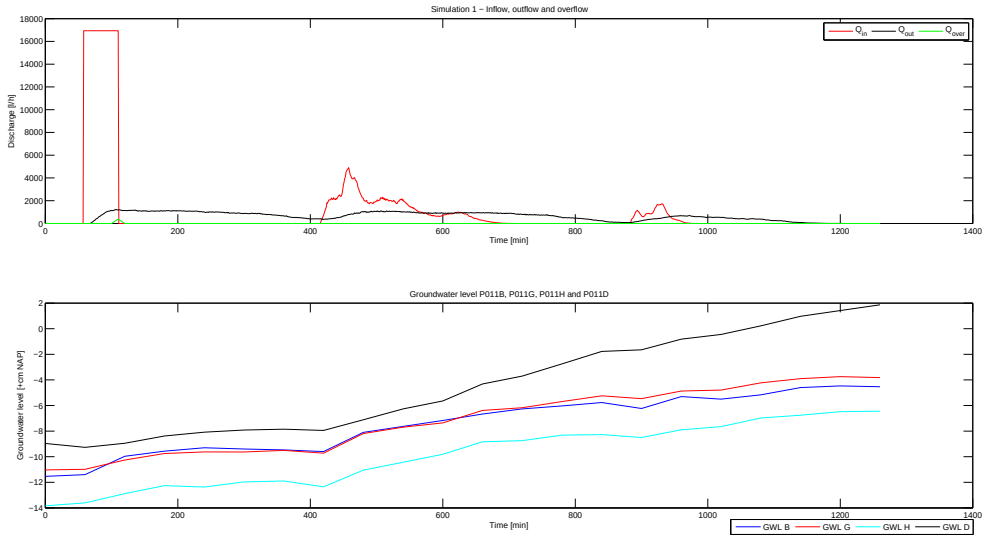

Figure C.24: Simulation 1 - Discharges and groundwater levels P011B, P011G, P011H and P011D

Simulation 2

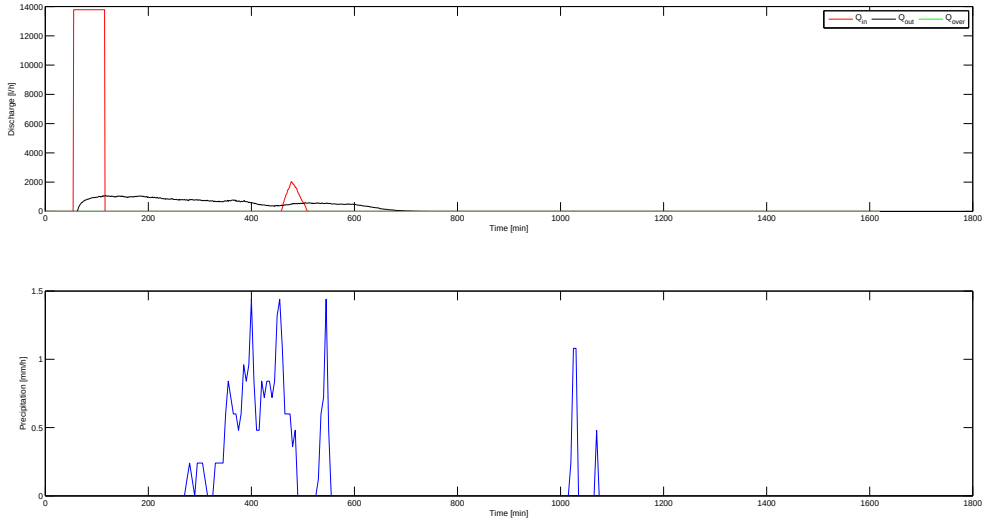

Figure C.25: Simulation 2 - Discharges and precipitation

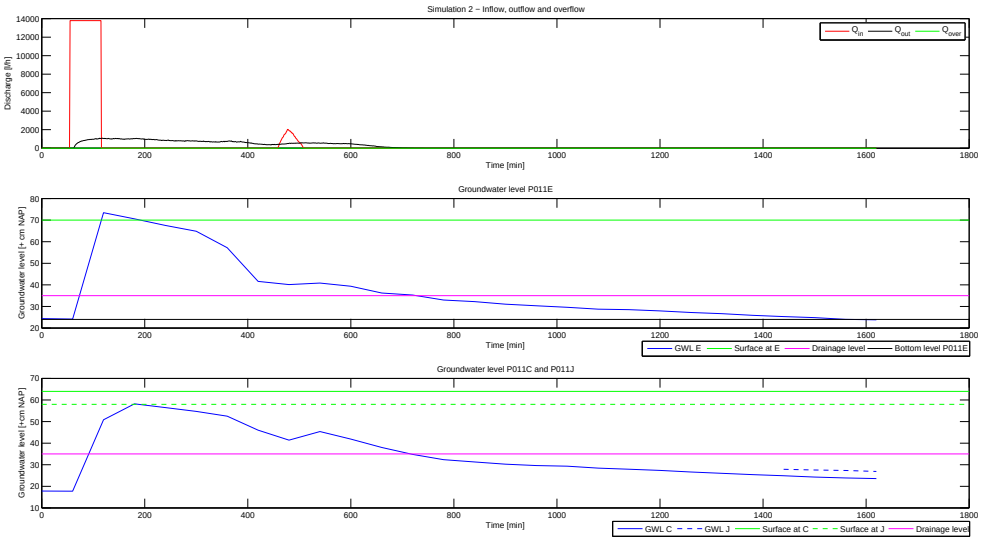

Figure C.26: Simulation 2 - Discharges and groundwater levels P011E, P011C and P011J

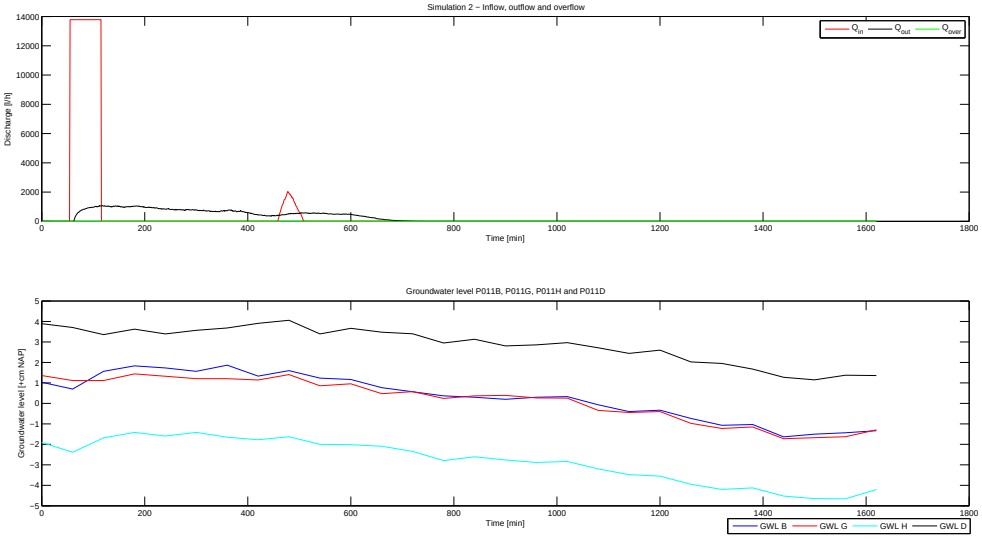

Figure C.27: Simulation 2 - Discharges and groundwater levels P011B, P011G, P011H and P011D

Simulation 3

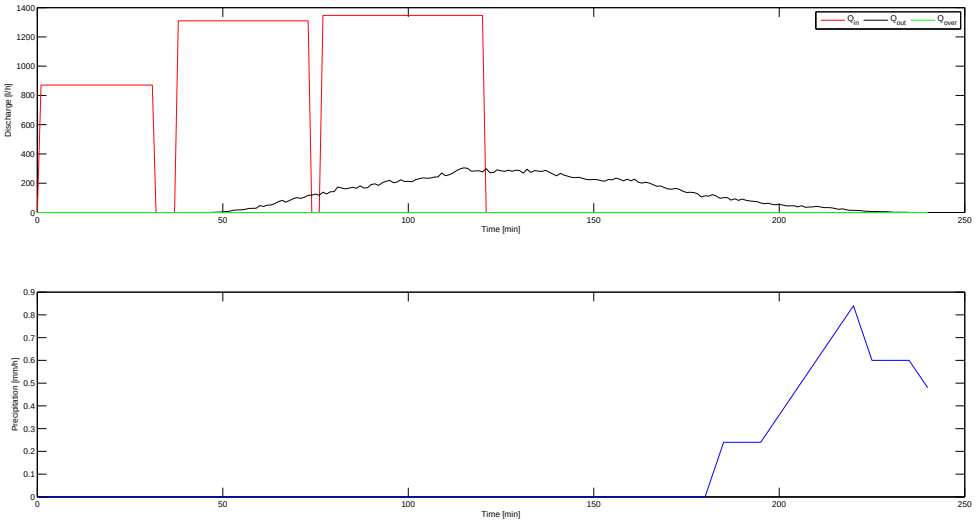

Figure C.28: Simulation 3 - Discharges and precipitation

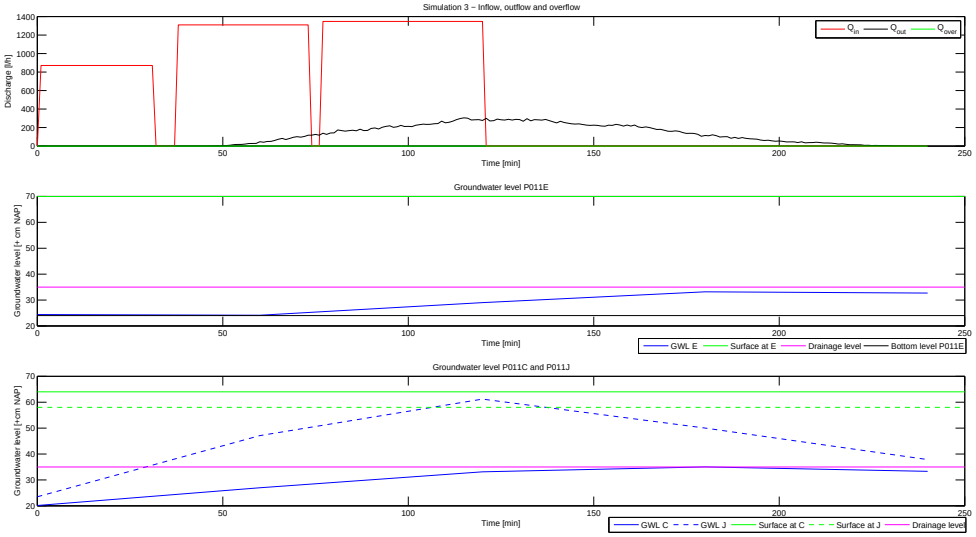

Figure C.29: Simulation 3 - Discharges and groundwater levels P011E, P011C and P011J

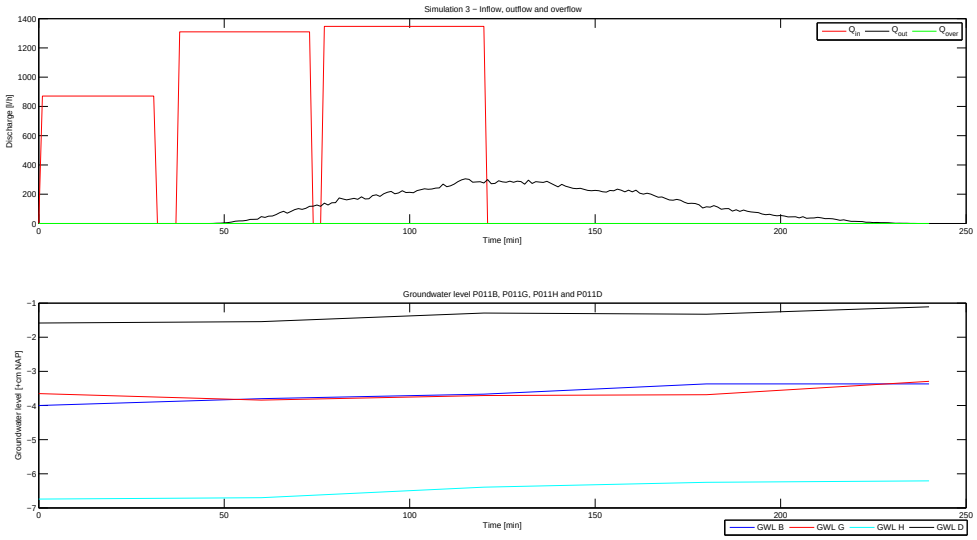

Figure C.30: Simulation 3 - Discharges and groundwater levels P011B, P011G, P011H and P011D

Simulation 4

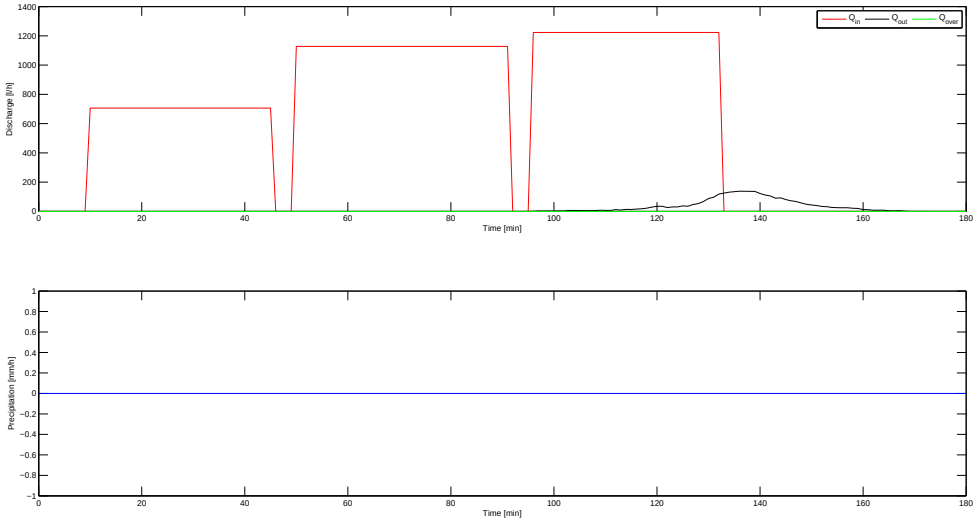

Figure C.31: Simulation 4 - Discharges and precipitation

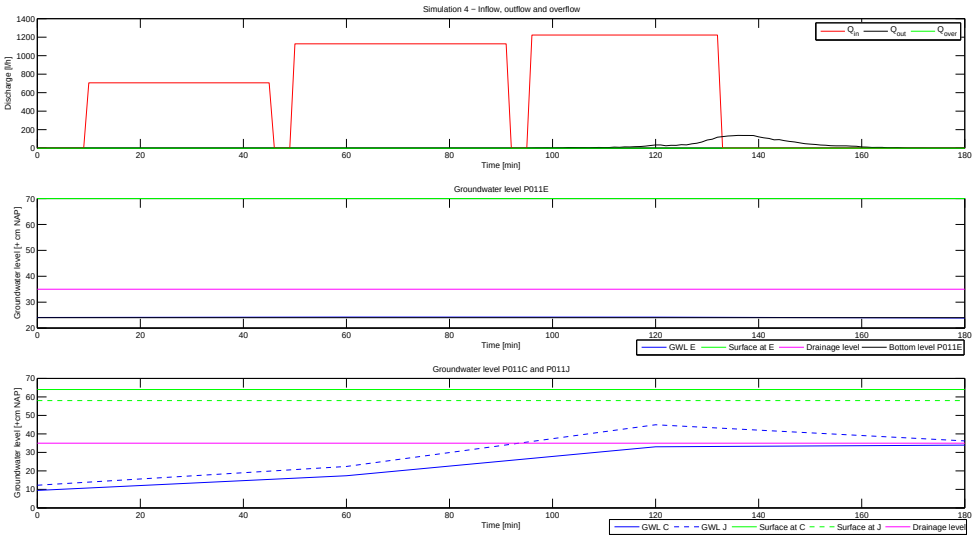

Figure C.32: Simulation 4 - Discharges and groundwater levels P011E, P011C and P011J

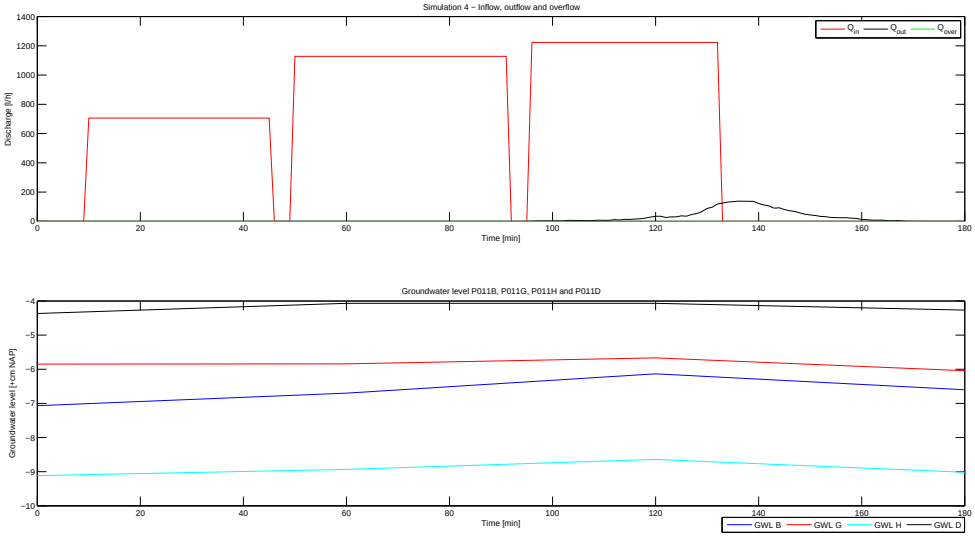

Figure C.33: Simulation 4 - Discharges and groundwater levels P011B, P011G, P011H and P011D

Simulation 5

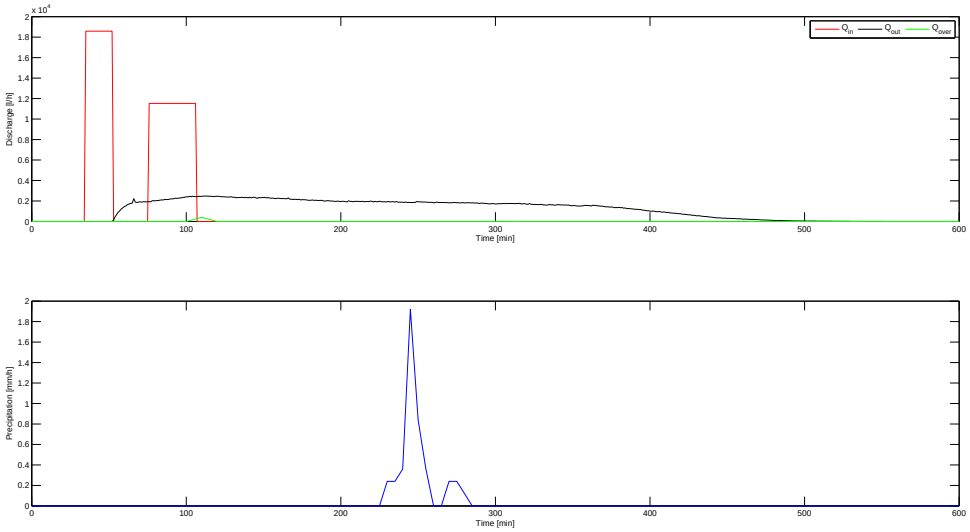

Figure C.34: Simulation 5 - Discharges and precipitation

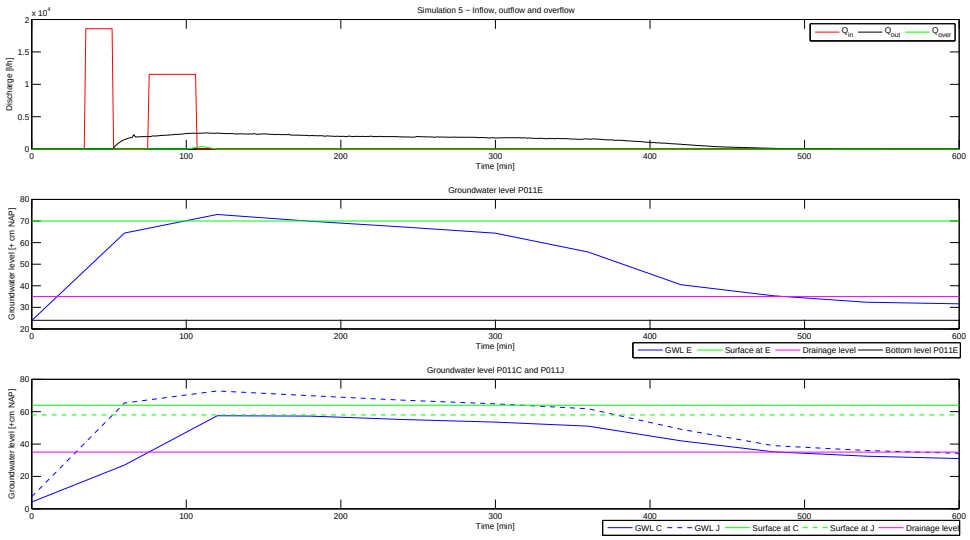

Figure C.35: Simulation 5 - Discharges and groundwater levels P011E, P011C and P011J

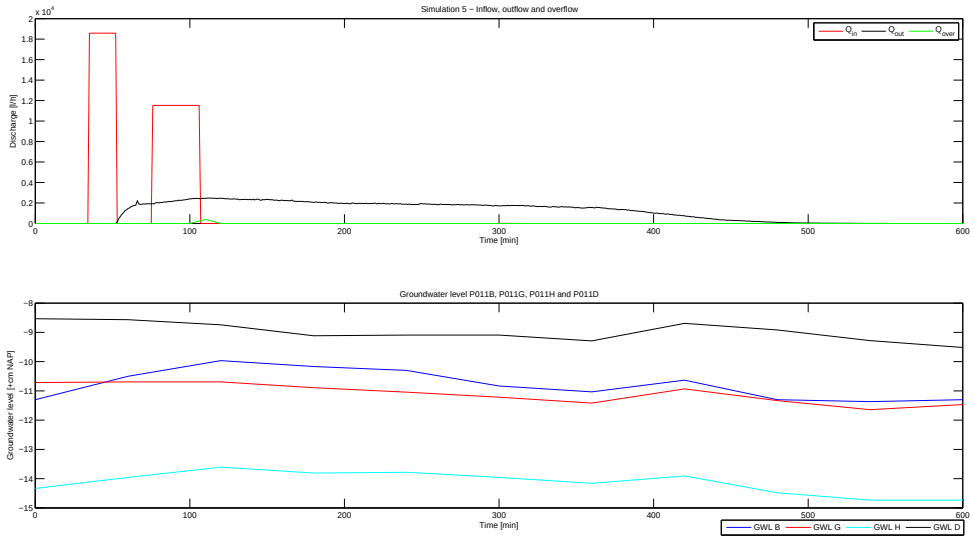

Figure C.36: Simulation 5 - Discharges and groundwater levels P011B, P011G, P011H and P011D

Simulation 6

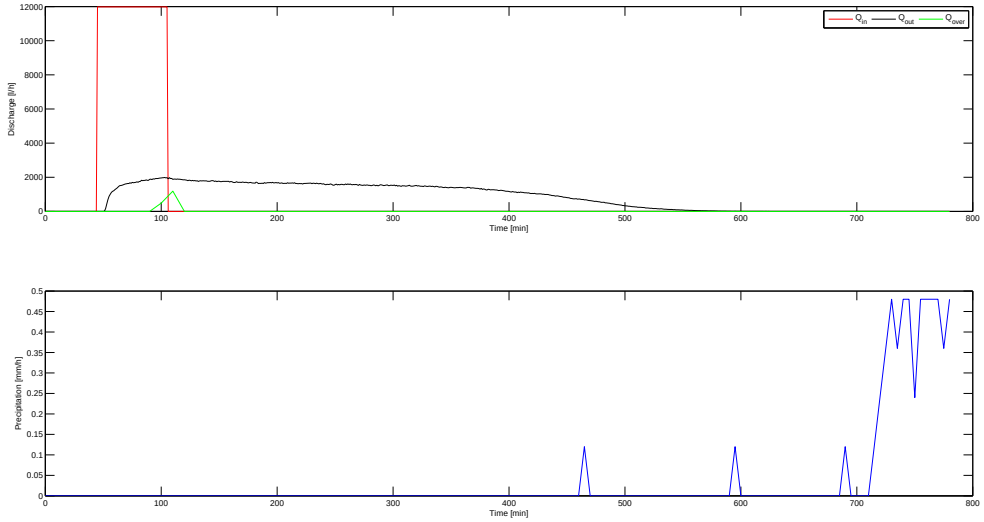

Figure C.37: Simulation 6 - Discharges and precipitation

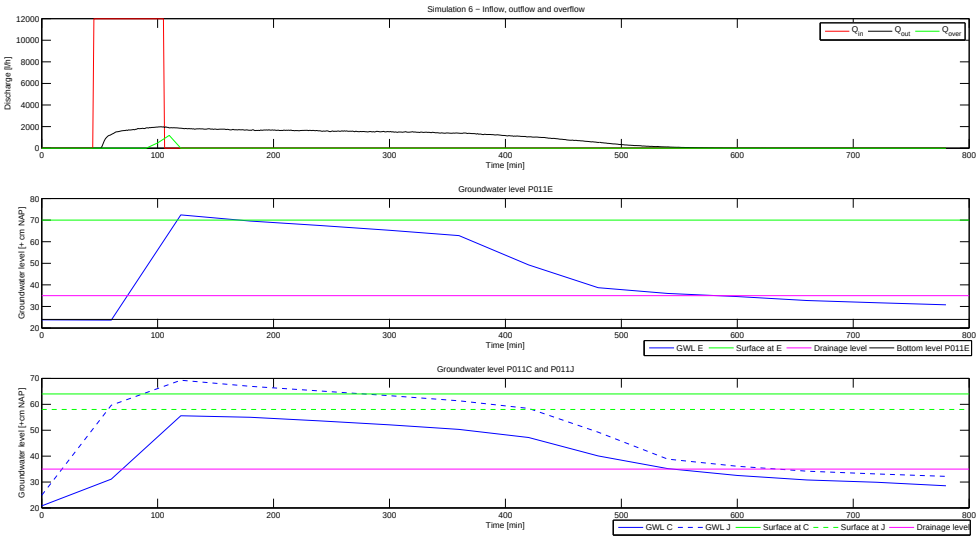

Figure C.38: Simulation 6 - Discharges and groundwater levels P011E, P011C and P011J

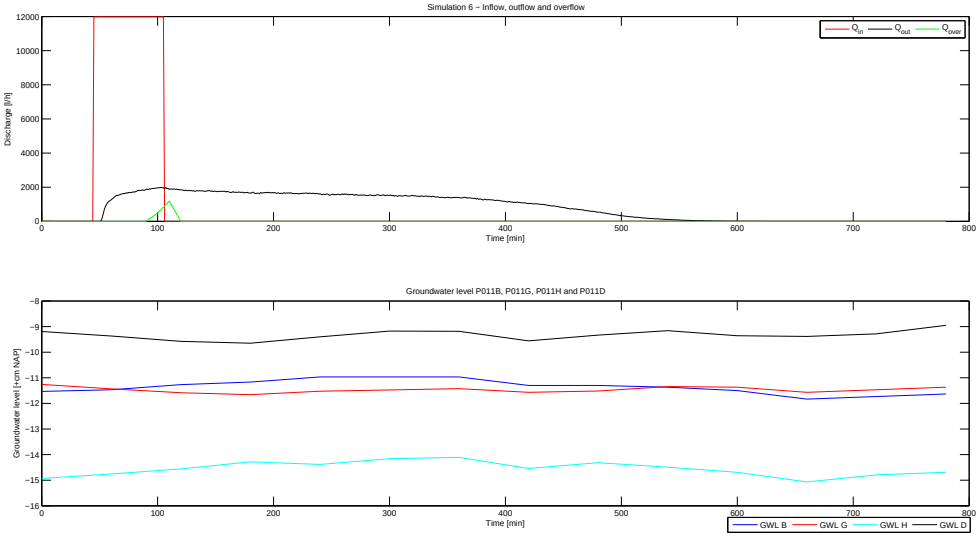

Figure C.39: Simulation 6 - Discharges and groundwater levels P011B, P011G, P011H and P011D

Simulation 7

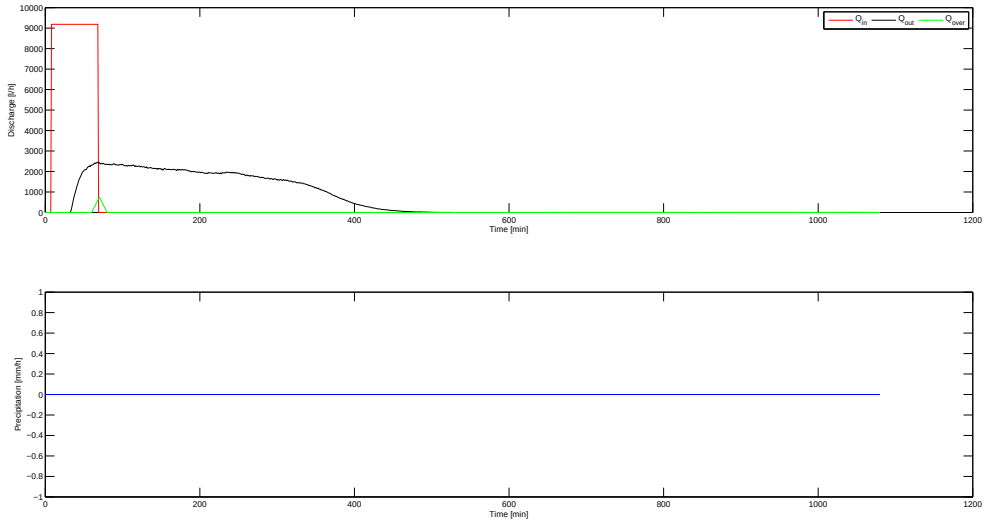

Figure C.40: Simulation 7 - Discharges and precipitation

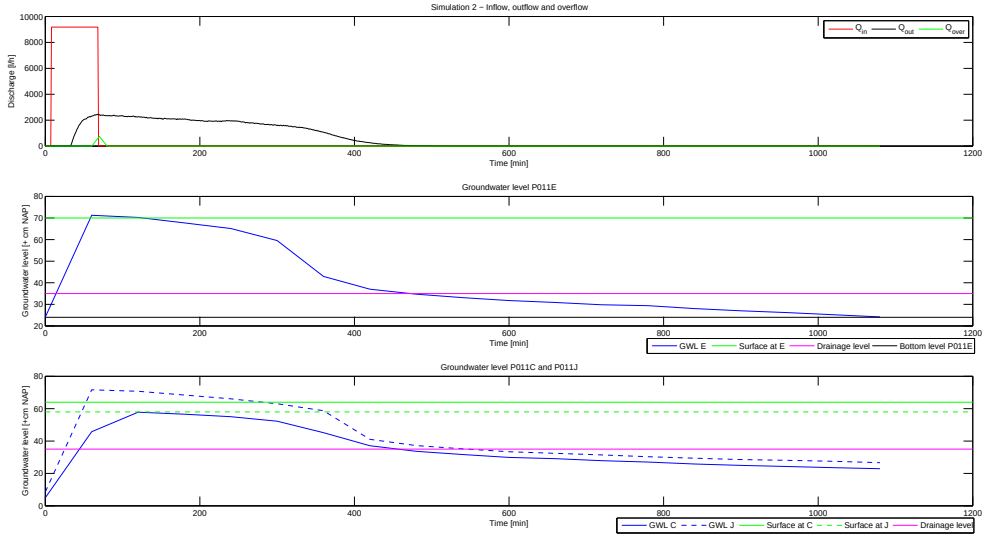

Figure C.41: Simulation 7 - Discharges and groundwater levels P011E, P011C and P011J

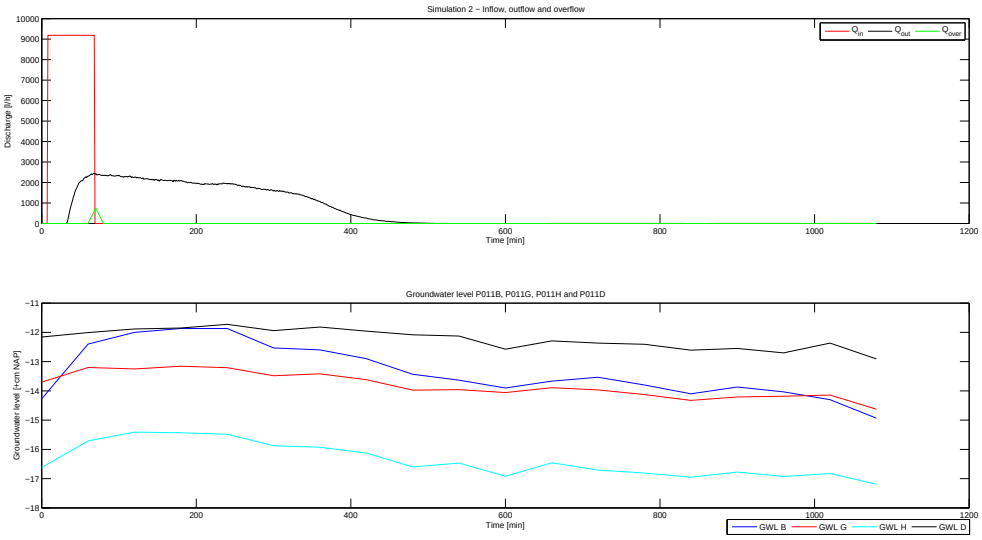

Figure C.42: Simulation 7 - Discharges and groundwater levels P011B, P011G, P011H and P011D